The Roles of Oxidative Stress, Inflammation and Adaptive Immunity in Aortic Stiffening

By

Jing Wu

Dissertation

Submitted to the Faculty of the

Graduate School of Vanderbilt University

in partial fulfillment of the requirements

for the degree of

DOCTOR OF PHILOSOPHY

in

Pharmacology

December, 2014

Nashville, Tennessee

Approved:

David G. Harrison, M.D.

Italo O. Biaggioni, M.D.

Billy G. Hudson, Ph.D.

Sean S. Davies, Ph.D.

Bjorn C. Knollmann, M.D., Ph.D.

To my dear wife, Jing Liu, infinitely supportive and understanding

and

To my lovely daughter, Lexie, sweet and adorable

ACKNOWLEDGEMENTS

I would like to thank my mentor Dr. David G. Harrison for his excellent mentorship. Dr. Harrison has taught me how to maintain a humble attitude, to conduct scientific research with honesty and precision, and to constantly pursue novelty and excellence as a scientist. I will benefit from these not just in my career but also in the rest of my life.

I am grateful to my thesis committee members, Drs. Italo O. Biaggioni, Billy G. Hudson, Sean S. Davies and Bjorn C. Knollmann for their valuable advices and generaous help during the course of my dissertation research.

Many colleagues have helped me over the years. Drs. Meena S. Madhur, Wei Chen, Salim R. Thabet, Daniel W. Trott, Liang Xiao and Hana A. Itani in the laboratory have provided me with assistance and suggestions during my dissertation research. Dr. Mohamed A. Saleh performed intracellular staining of cytokines in spleen T cells for me. Drs. Annet Kirabo, Sean S. Davies and L. Jackson Roberts II provided me with critical insights into isoketal biology. Mr. William Zackert performed the immunohistochemistry staining of isoketals and mass spectrometric analysis for isoketal protein adducts. Mr. Kim R. Montaniel performed immunofluorescence staining and flow cytometry studies on Sca-1^+ cells and circulating fibrocytes during his rotation with Dr. Harrison.I sincerely thank them all.

Drs. Joey V. Barnett, Vsevolod V. Gurevich, Christine L. Konradi and Ms. Karen Gieg in the Department of Pharmacology have always been willing to answer questions and give suggestions on any issue. I appreciate their kindness.

I also thank the Transitional Pathology Shared Resource (TPSR) core and the Epithelial Biology Center at Vanderbilt University for their assistance with imaging and quantification of immunohistochemical staining;the VUMC Hormone Assay and Analytical Services Core (supported by NIH grants DK059637 and DK020593) for the cytokine measurements.

SOURCE OF FUNDING

This work was supported by NIH R01 Grants HL105294, HL039006, HL108701, VITA contract HHSN268201400010C and Program Project Grants P01 HL58000 and GM015431 and a predoctoral fellowship from American Heart Association (13PRE14480008).

TABLE OF CONTENTS

LIST OF TABLES

Table **Page**

LIST OF FIGURES

Figure **Page**

Chapter 1

General Introduction on Aortic Stiffening and Hypertension: the Roles of Oxidative Stress, Inflammation and Adaptive Immunity

Hypertension predisposes to cardiovascular and renal diseases, including stroke, myocardial infarction, heart failure and renal failure. In the United States, 30% of adults suffer from hypertension and another 30% have pre-hypertension that commonly develops into overt hypertension in two years.[1, 2] At age 70, 70% of individuals are hypertensive. Although there are numerous antihypertensive agents available for the treatment of hypertension, only 65% of patients achieve goal blood pressure.[3] Treatment often requires multiple medications, especially in patients with diabetic nephropathy.[4]

Despite extensive research for the past half-century, the etiology of most cases of human hypertension remains undefined. Monogenic hypertension generally involves mutations of transporters in the distal nephron and accounts for less than5% of patients.[5,6] Other correctable causes of hypertension can occur as a consequence of adrenal adenoma, renal artery stenosis or pheochromocytoma, however, these are uncommon. Other cases of hypertension are of unknown etiology and are referred to as "essential".

Traditionally, abnormalities of the resistance arteries with diameter less than 200 μm are believed to increase systemic vascular resistance, which is a common feature of almost all adults with hypertension.. In keeping with this, vasodilators such as calcium channel blockers and nitrates lower blood pressure by vasodilatory effects. Hypertension also changes vascular structure, leading to thickening of vascular wall and loss of capillaries.[7]

1.1 The role of aortic stiffening in hypertension:

In contrast to the traditionally held belief that hypertension is entirely due to the resistance arterioles, large arteries have been recently recognized to play an important role the development of hypertension, particularly systolic hypertension. The thoracic aorta functions as a buffering system that absorbs the force of the ejected blood and blunts blood pressure elevation during systole. During diastole, the blood volume stored by this capacitance function is discharged into the downstream resistance circulation and together with returning waves from the peripheral circulation, maintains diastolic pressure and perfusion. Increase in large artery stiffness increases characteristic aortic impedance, enhances the speed of returned waves from the periphery and is associated with a progressive increase in systolic pressure, a decline in diastolic pressure and an increase in pulse wave velocity (PWV). Apparent arterial pressure pulse is the sum of forward traveling wave and reflected wave and pulse wave velocity is the speed at which it travels down the arterial system. PWV can be measured in humans by a variety of non-invasive methods, including MRI and ultrasound. Arterial stiffening not only contributes to hypertension, but also has significant implications for subsequent morbidity and mortality.

Clinically, aortic stiffening accompanies atherosclerosis, diabetes, obesity, cigarette smoking and autoimmune disease. While aortic stiffening is commonly encountered in hypertension, the causal

relationship between aortic stiffening and blood pressure elevation has been controversial. Abboud and Huston employed a mathematical method to estimate vascular stiffness in humans and concluded that hypertension is not caused by aortic stiffening, but that it is a cause of aortic stiffening.[8] Aatola et al found that elevated childhood blood pressure tracks to adulthood and predicts the development of arterial stiffness. However, in high fat/high sucrose-induced obesity mice, pulse wave velocity increases within 1 month of the initiation of diet while hypertension develops by 5 month.[9] In support of this, recent studies in the Framingham heart cohort demonstrate that higher aortic stiffness, forward wave amplitude and augmentation index precede the development of hypertension at a later time point.[10]

1.2 Molecular characteristics of arterial stiffening: Post mortem analyses have shown that human hypertension is associated with a striking aortic medial fibrosis as indicated by Masson's trichrome blue staning.[11] Atherosclerosis, diabetes, age and renal disease are associated with vascular fibrosis in these subjects. The degree of media fibrosis correlates with pre-mortem pulse pressure and hypertension. In experimental hypertension, hypertension induces vascular fibrosis via the expression of collagen type I, type III and fibronectin.[12] A decrease in elastin content was associated with parameters of arterial stiffness in males but not females in a study of non-human primtes.[13] In keeping with this, mice with elastin haploinsufficiency (Eln+/-) exhibit arterial stiffening and hypertension.[14] Likewise, impaired fetal synthesis of elastin in large arteries is associated with permanent changes in mechanical properties of these vessels and predisposes to hypertension and left ventricular hypertrophy in subjects with low birth weight. Either loss of aortic elastin or elastin fragmentation redistributes circumferential wall stress to less compliant collagen, leading to vascular stiffening.

1.3 The role of oxidative stress in hypertension: The term oxidative stress refers to an imbalance between the production of reactive oxygen species (ROS) and antioxidant defenses.[15] ROS mediate pathological changes in the brain, the kidney and blood vessels associated with the genesis of chronic hypertension. In an initial study, Nakazono and colleagues showed that bolus administration of a modified form of SOD acutely lowered blood pressure in hypertensive rats.[16] Membrane-targeted forms of SOD and SOD mimetics such as tempol lower blood pressure and decrease renovascular resistance in hypertensive animal models.[17] There is ample evidence suggesting that ROS not only contribute to hypertension but that the NADPH oxidase is their major source.[18, 19] Components of this enzyme system are upregulated by hypertensive stimuli, and NADPH oxidase enzyme activity is increased by these same stimuli. Moreover, both angiotensin II-induced hypertension and deoxycorticosterone acetate (DOCA)-salt hypertension are blunted in mice lacking this enzyme.[18-20] Despite the evidence that oxidative stress contributes to hypertension, the mechanisms involved are not well understood.

While scavenging of ROS decreases blood pressure in experimental hypertension, clinical trials with high dose antioxidants have been disappointing. Several large clinical trials have failed to show beneficial effects of either vitamin C or vitamin E supplementation in cancer, cardiovascular disease and neurodegenerative diseases. A recent meta-analysis of 50 randomized trials including almost 300,000 patients confirmed the futility of treatment with a variety of antioxidants in cardiovascular disease.[21] Surprisingly, large doses of beta-carotene, vitamin A and vitamin E have paradoxically worsened cardiovascular outcomes in some studies.[22] The failure of antioxidants in humans might reflect the low rate constant of vitamins such as E and C with superoxide and related ROS, the inability to target subcellular sites where ROS are formed, and the fact that some ROS have beneficial effects in cell signaling and survival.

1.4 The potential role of ROS in aortic stiffening: Oxidative events have been associated with various perturbations of elastin and collagen. Oxidative stress promotes the degradation of elastin fiber components from the extracellular matrix (ECM).[23] This may be due to the activation of matrix metalloproteinases with elastase activity.[24] As an example, oxidative radicals generated by the xanthine/xanthine oxidase complex activate the MMP-2 in coronary smooth muscle cells.[25] In the studies of emphysema, a condition characterized by the fragmentation of elastin fibers, the loss of Cu/Zn superoxide dismutase (SOD) activity due to copper deficiency results in severe emphysema in the Syrian Golden Hamster.[26] In contrast to this, overexpression of Cu/Zn SOD protects from the development of emphysema induced by cigarette smoking or elastase perfusion.[27] Interestingly, the severity of emphysema is associated with parameters of arterial stiffness in patients with chronic obstructive pulmonary disease, suggesting that oxidative stress could affect elastin in both the lung and blood vessels via similar mechanisms.

ROS also affect expression and structure of collagen in the extracellular matrix. Superoxide stimulates production of collagen type I and type III in fetal human fibroblasts and this is prevented by superoxide dismutase.[28] A recent study elegantly demonstrated that hydrogen peroxide (H_2O_2), generated via Nox 4, mediates the differentiation of myofibroblasts and their production of ECM components in response to TGF-β during lung injury.[29] The pro-fibrogenic effects of ROS are abrogated either by pharmacological inhibition of Nox 4 or by its genetic deletion, supporting the concept that ROS produced by NADPH oxidase promotes collagen deposition and lung fibrosis. ROS promote formation of advanced glycation products (AGEs),[30] which react with ECM components especially collagen; and drugs that break AGE-mediated cross-links decrease arterial stiffness in humans and experimental animals.[31, 32] In the setting of oxidative stress, AGE-mediated protein cross-linking may act in concert with increased collagen deposition to promote aortic stiffening during aging.

1.5 The interactions of oxidative stress, inflammation and immunity in hypertension: A variety of mechanical, hormonal and cellular factors common to the hypertensive milieu promote the development of inflammation and in many cases these involve oxidant events. Oxidative stress and inflammation can cause one another. A hallmark of many diseases associated with vascular inflammation, such as aging, atherosclerosis and hypertension, is increased vascular ROS production.[33-35] Studies in experimental animals have implicated ROS formation in inflammation of the vasculature, lung, skin and other tissues. As an example, mechanical stretch activates both endothelial and vascular smooth muscle production of ROS, which in turn can activate pro-inflammatory transcription factors such as NF-κB.[36, 37] This leads to expression of adhesion molecules such as VCAM-1 and ICAM-1 and chemokines such as MCP-1 and RANTES which recruit T cells, macrophages and circulating fibrocytes to blood vessels.[38-40] ROS increase permeability of the vascular endothelium, facilitating the infiltration of these inflammatory cells.[41] The infiltrating inflammatory cells that enter target tissues may promote additional ROS generation, exacerbate oxidant injury and eventually result in fibrotic changes in the heart, kidney and blood vessels.[33, 42]

1.6 T cell-mediated adaptive immunity in hypertension: There is strong evidence that adaptive immunity contributes to hypertension. As an example, Svendson showed that the delayed phase of DOCA-salt hypertension was blunted in thymectomized animals.[43] Pre-eclampsia is associated with an increase in lymphocyte markers and the cytokine profile of natural killer lymphocytes in the uterus.[44] Interestingly, a recent analysis of almost 6000 people with AIDS (with reduced $CD4^+$ cells) showed that the incidence of hypertension was significantly lower than the general population matched non-infected individuals.[45] Treatment with highly active anti-retroviral therapy for 2 years restored the incidence of

hypertension to that of the control population. This finding might reflect a need for functioning helper T cells in the development of hypertension.

During the past several years, we have added significantly to the concept that adaptive immunity plays an important role in hypertension. Studies from my mentor's laboratory have shown that hypertensive stimuli such as angiotensin II, increased salt and aldosterone, catecholamines lead to formation of neoantigens that promote T cell activation.[33, 46, 47] T cells with an effector phenotype infiltrate the vasculature and the kidney and release cytokines such as IL-17A and IFN-γ that, together with the direct effects of these hypertensive stimuli, promote formation of reactive oxygen species (ROS) in these peripheral sites,[33, 39, 48] vasoconstriction and renal sodium retention, ultimately leading to severe hypertension.[49] The deficiency of T lymphocytes or perturbations of IL-17A or IFN-γ signaling blunt angiotensin II-induced hypertension, ameliorate vascular inflammation and target organ damage.[33, 39, 42] In p47phox$^{-/-}$ mice, and in animals treated with antioxidants, hypertensive responses to angiotensin II are markedly blunted.[16, 17, 50] Our recent data indicate that ROS formation is increased in dendritic cells (DCs) and likely plays a role in this pathway.[47] Isoketal accumulation is associated with DC production of IL-6, IL-1β and IL-23 and an increase in costimulatory proteins CD80 and CD86. These activated DCs promote T cell, particularly CD8^{+} T cell, proliferation; production of IFN-γ and IL-17A; and hypertension. Moreover, isoketal scavengers prevented angiotensin II-induced hypertension and these hypertension-associated events.

Chapter 2

Inflammation and Mechanical Stretch Promote Aortic Stiffening in Hypertension Through Activation of p38 MAP Kinase

2.1 Chapter Abstract

Aortic stiffening commonly occurs in hypertension and further elevates systolic pressure. Hypertension is also associated with vascular inflammation and increased mechanical stretch. I sought to determine the role of these factors in aortic stiffening. Chronic angiotensin II infusion caused marked aortic adventitial collagen deposition, as quantified by Masson's trichrome Blue staining and biochemically by hydroxyproline content, in wild-type (WT) but not in Recombination Activation Gene-1 deficient (RAG-1$^{-/-}$) mice. Aortic compliance, defined by ex-vivo measurements of stress-strain curves, was reduced by chronic angiotensin II infusion in WT mice ($p<0.01$) but not in RAG-1$^{-/-}$ mice ($p<0.05$). Adoptive transfer of T cells to RAG-1$^{-/-}$ mice restored aortic collagen deposition and stiffness to values observed in WT mice. Further studies indicated that CD8^{+} and to a lesser extent CD4^{+} T cells contribute to aortic stiffening and collagen deposition. Mice lacking IL-17a were also protected against aortic stiffening. In additional studies, I found that blood pressure normalization, by treatment with hydralazine and hydrochlorothiazide completely prevents angiotensin II-induced vascular T cell infiltration, aortic stiffening and collagen deposition. Finally, I found that mechanical stretch induces expression of collagen 1α1, 3α1 and 5a1 in cultured aortic fibroblasts in a p38 MAP kinase-dependent fashion, and that inhibition of p38 prevented angiotensin II-induced aortic stiffening in vivo. IL-17a also induced collagen 3a1 expression via activation of p38 MAP kinase. Our data suggest a pathway in which inflammation and mechanical stretch lead to vascular inflammation that promotes collagen deposition. The resultant increase in aortic stiffness likely further worsens systolic hypertension and its attendant end-organ damage.

Keywords: Inflammation, mechanical stretch, collagen deposition and aortic stiffening

2.2 Introduction

Normally the capacitance property of the aorta blunts blood pressure elevation during systole and maintains diastolic pressure and tissue perfusion during diastole. Loss of this windkessel function in the proximal aorta causes an increase in systolic pressure, a decline in diastolic pressure and an increase in pulse wave velocity.[51] The augmentation of systolic pressure caused by aortic stiffening increases the incidence of stroke, renal failure and myocardial infarction. Aortic stiffening is associated with aging, insulin resistance, diabetes, atherosclerosis and hypertriglyceridemia.[52-55] Importantly, hypertension per se causes aortic stiffening, leading to progressive elevation of systolic pressure. Thus, aortic stiffening not only contributes to hypertension but also portends cardiovascular morbidity and mortality.[56, 57]

The precise mechanisms underlying aortic stiffening remain undefined. Clinical studies suggest that inflammation and arterial stiffness are related.[58-61] Patients with inflammatory diseases such as lupus erythematosus, rheumatoid arthritis and psoriasis have increased pulse wave velocity.[62-64] Data from our laboratory and others have shown that T cells and T cell-derived cytokines are important in

development of hypertension.[33, 39] We have previously found that Recombination Activation Gene-1 deficient (RAG-1$^{-/-}$) mice develop blunted hypertension in response to angiotensin II, DOCA-salt challenge and norepinephrine.[46] The RAG-1 gene encodes a gene responsible for recombining the variable regions of the T cell receptor and immunoglobulins and in its absence mice fail to develop either B cells or T cells. Adoptive transfer of T cells restores hypertension in RAG-1$^{-/-}$ mice, indicating a critical role of these cells. Recently, deletion of the RAG-1 gene in Dahl Salt-sensitive rats has been shown to lower blood pressure and to reduce renal injury upon salt feeding.[65] Other studies have shown that T cells- derived cytokines also contribute to hypertension, likely by promoting vascular dysfunction and renal injury.[39, 42, 66] One such cytokine is interleukin 17a (IL-17a), which is produced by a subset of pro-inflammatory CD4$^+$ T cells, or T_H17 cells. Mice lacking IL-17a have blunted hypertension and reduced aortic production of ROS following angiotensin II infusion. Recent studies have also shown that administration of IL-17a to mice causes hypertension and reduces endothelium-dependent vasodilatation, at least in part by activating Rho kinase.[67] IL-17a also promotes collagen deposition and contributes to fibrosis in other tissues and conditions.[68-70]

In the present study I sought to examine mechanisms responsible for aortic stiffening in hypertension. In particular I examined the role of adaptive immunity mediated by T cells and their cytokines and the direct effects of mechanical stimulation by blood pressure lowering and by exposing aortic fibroblasts to hypertensive levels of stretch. I identify a novel pathway that promotes striking aortic adventitial collagen deposition and vascular stiffening.

2.3 Materials and methods

Animals: Wild type, Rag-1$^{-/-}$, CD4$^{-/-}$ and CD8$^{-/-}$ mice were obtained from Jackson Laboratories on a C57Bl/6 background. IL-17A-deficient (*IL-17a*$^{-/-}$) mice were produced as previously described. At 3 months of age, these animals were implanted with telemetry units for measurement of blood pressure. One week later osmotic minipumps were implanted subcutaneously for infusion of angiotensin II (490 ng/kg/min) or vehicle for 2 weeks. Blood pressure was recorded for 10 minutes every hour for the duration of the experiments (i.e. three days prior to osmotic minipump implantation and until the end of angiotensin II infusion at Day 14). Hydralazine and hydrochlorothiazide were given in drinking water (320 mg/L and 60 mg/L) to normalize blood pressure at the same time as the 2-week angiotensin II infusion or to reverse established hypertension in the last two weeks of 4-week angiotensin II infusion. In deoxycorticosterone acetate (DOCA)-salt-treated mice, 100 mg deoxycorticosterone acetate pellet were implanted subcutaneously following uninephrectomy. These mice were subsequently maintained on drinking water with 0.9% NaCl for three weeks. P38 MAP kinase inhibitor SB203580 was dissolved in 50% DMSO and administered at 10 mg/kg/day via i.p. injections. At the end of each experiment, mice were sacrificed with CO_2 inhalation and the chest was rapidly opened and the superior vena cava sectioned. A catheter was placed in the left ventricular apex and the animals were perfused at a physiological pressure with Krebs-Hepes buffer until the effluent from the vena cava was cleared of blood. The Institutional Animal Care and Use Committee approved all experimental protocols.

Materials: Antibodies used for flow cytometry included: FITC anti-CD45; PerCP anti-CD45; PE anti-CD3e; FITC anti-CD3e; APC anti-CD3; APC anti-CD4; PerCP anti-CD8a; PE-Cy7 anti-CD8a. These were obtained from Becton Dickinson. Isolation kits for pan-T cells were from either Miltenyi biotech or Invitrogen. RNA isolation kits were purchased from Qiagen. PCR array kits for aortic matrix gene and adhesion molecules were purchased from SABiosciences. Primers for quantitative polymerase chain reactions and reverse transcription kits were obtained from Applied Biosystems, Life Technologies (Grand Island, NY). Rabbit anti-mouse monoclonal antibody for phospho-p38 and p38 were obtained from Cell Signaling (Boston, MA). Secondary goat anti-rabbit antibody was purchased from Bio-Rad (Hercules, CA). SB203580 compound was purchased from Selleckchem (Houston, TX). Seventy-

micron filters for cell separation were obtained from BD Biosciences. All other reagents were obtained in the highest grade possible from Sigma-Aldrich (St. Louis, MO).

Determination of aortic compliance: Using a commercially available system (Danish Myograph Technology, Model 110P) segments of the thoracic aorta were mounted on 0.7 mm cannulas and extended to the in situ length. Vessels were placed in calcium-free buffer to eliminate active tone. Intraluminal pressure was increased in a step-wise fashion while video microscopy was used to follow outer and inner diameter. Diameters were recorded with every increment of 25 mmHg from 0 to 200 mmHg. The maximal intraluminal pressure was 200 mmHg because both the lumen diameter and outer diameter reach a plateau beyond this pressure. Pressure diameter curves were constructed for calculation of vascular compliance, in which the increment of vessel diameter from 0 mmHg was plotted against pressure. The traditional stress-strain relationship was determined as previously described,[71] where a leftward shift indicates aortic stiffening. Circumferential stress (σ) was calculated from the following formula:

Formula 1: $\sigma=(P \times ID)/(2WT)$.

Where P = intraluminal pressure, ID = inner diameter, and WT = wall thickness. Intraluminal pressure was converted from millimeters of mercury to dynes per square centimeter (1 mmHg = 1.334×10^3 dynes/cm^2). Circumferential strain (ε) was calculated from the formula:

Formula 2: $\varepsilon= \Delta OD/OD_0$

Where OD_0 refers to the original outer diameter, defined as diameter at 0 mmHg. ΔOD represents the increase in outer diameter from OD_0 at each pressure level.

Measurement of aortic collagen and elastin: Aortic collagen was visualized by Masson's Trichrome staining. Elastin was visualized by Verhoeff Van Gieson's elastica staining. The effect of angiotensin II-induced hypertension on aortic collagen was determined by measurement of tissue hydroxyproline as described previously[72]. In separate vessels, elastin content was determined as previously described[73, 74], with minor modifications. Briefly, insoluble elastin was separated from all other soluble proteins by hydrolysis in 0.1N NaOH at 90°C for 45 minutes. Both the soluble and insoluble fractions were further digested in 6N HCl at 105°C for 48 hours, neutralized and assayed for ninhydrin content.

T cell adoptive transfer: Pan T cells, $CD4^+$ T cells or $CD8^+$ T cells were isolated using negative selection from spleens of age-matched wild type mice, and 10^7 cells were resuspended in 200 µL of saline and injected by tail vein into RAG-$1^{-/-}$ mice. Three weeks following adoptive transfer, chronic angiotensin II infusion (490 ng/kg/min) was performed for 14 days. Blood pressure, aortic stiffening and collagen deposition were determined in these mice as described above.

Flow cytometry: Following removal, spleens and aortas were rapidly minced and digested using collagenase type XI (125 U/mL), collagenase type I-S (450 U/mL), and hyaluronidase I-S (60 U/mL) in 20 mM Hepes-PBS buffer containing calcium and magnesium for 30 min at 37°C. The tissues were further dispersed using repeated pipetting and the resultant homogenate was passed through a 70-µm sterile filter, yielding single-cell suspensions. The cells were washed with PBS and resuspended in 2 mL 40% Percoll. Two mL of 60% Percoll was then added to the resultant gradient and centrifuged at 2400 RPM for twenty minutes. The uppermost layer of the gradient, containing fat and non-cellular material not removed by the filter was discarded and cells in the lower portion of the gradient was counted and stained for subsequent flow cytometry.

Cell culture: Primary mouse aortic fibroblasts were obtained from Cell Biologics, (Chicago, IL) and low-passage cells were used for cytokine incubation and real-time PCR studies. Briefly, cells were cultured in media provided by the supplier on plates coated with 0.2% gelatin until 90% confluent. The media was changed from 5% to 0.5% FBS for 24 hours prior to experiments. Cells were exposed to 5% or 10% cyclical stretch to mimic mechanical stretch at normotensive and hypertensive conditions using the Flexcell FX-5000^{TM} Tension System (Hillsborough, NC). In additional experiments, p38 MAP kinase inhibitor was added to fibroblasts treated with IL-17a (100 ng/mL) or 10% cyclical stretch.

Real-time PCR: RNA was extracted from freshly harvested aorta or cell culture using Qiagen RNeasy mini kit. PCR array was performed to examine the expression of 84 genes for aortic matrix and adhesion molecules. Additional real-time PCR reactions were performed to examine selected fibrotic genes in cultured fibroblasts, including collagen 1a1, 3a1, 5a1, fibronectin-1, TGF-β, ribosomal 18s and β-actin. Real time quantitative PCR was performed on Applied Bioscience System 7500 Fast.

Western Blot: p38 MAPK was quantified in angiotensin II-treated aortas and mouse fibroblasts stretched with different treatments. Freshly isolated aortas or cultured cells were homogenized in Ripa lysis buffer with proteinease inhibitor and phosphatase inhibitors (Roche). Monoclonal rabbit anti-mouse antibodies were used to detect phosphorylated p38, total p38, β-actin and β-tubulin at a concentration of 1:1000. Polyclonal goat anti-rabbit antibody was used as the secondary antibody (1:4000). Densitometry was performed on Biorad ChemiDoc^{TM} XRS+ imaging system.

Statistical analysis: Data in the manuscript are expressed as the mean ± SEM. Comparisons of blood pressure over time were made using one-way ANOVA for repeated measures, followed by a Student Newman Keuls post hoc test when significance was indicated. Compliance curves and stress-strain curves were also compared using ANOVA for repeated measures. To compare the effect of angiotensin II on parameters other than blood pressure, two-way ANOVA was employed, as indicated. The effects of adoptive transfer of pan T cells or antihypertensive treatment on collagen deposition or aortic inflammation were compared using one-way ANOVA. P values are reported in the figures.

2.4 Results

2.4.1 Effect of angiotensin II-induced hypertension on aortic collagen and elastin content: role of T cells. Two matrix components that predominantly modulate tissue compliance are collagen and elastin. I performed initial studies to determine how hypertension affects these and to understand the role of T cells in this response. Using Masson's Trichrome staining, I observed that collagen is predominantly localized to the adventitia of the aorta of sham infused mice. During angiotensin II infusion, a striking accumulation of collagen in the aortic adventitia occurred. This degree of adventitial collagen deposition was often equivalent to the media (Figure 1A and 1B). By planimetry, adventitial collagen area was increased from 3.8×10^4 μm^2 to 13.6×10^4 μm^2 by angiotensin II treatment. To directly quantify aortic collagen, I measured hydroxyproline content, which was 25 ± 9 ng/μg of total protein in WT mice and was doubled by chronic angiotensin II infusion (Figure 1C). Thus, by both histochemical staining and biochemical analysis, I found that angiotensin II-induced hypertension is associated with a 2-3-fold increase of aortic collagen content, predominantly localized to the adventitia.

I and others have established a role of T cells in hypertension.[15,16] Moreover, the T cell derived cytokine IL-17 contributes to hypertension and has been shown to promote collagen deposition in experimental scleroderma.[17] I therefore examined the role of T cells in aortic stiffening. As in previous studies, I found that the hypertensive response to angiotensin II is blunted in RAG-1$^{-/-}$ mice (Figure 2A and B). In addition, the increase in aortic collagen content caused by angiotensin II, as detected by either Masson's trichrome staining or by hydroxyproline assay, was blunted in RAG-1$^{-/-}$ mice (Figure 1A-C).

Five weeks following adoptive transfer of pan T cells, flow cytometry documented a stable population of these cells in RAG-1$^{-/-}$ mice (Figure 2C). In keeping with our prior studies, T cell adoptive transfer restored the hypertensive response to angiotensin II in RAG-1$^{-/-}$ mice (Figure 2D and 1E). Importantly, adoptive transfer of T cells to RAG-1$^{-/-}$ mice also restored the aortic collagen deposition caused by angiotensin II to levels observed in WT mice (Figure 1A-C). Despite these fibrotic changes in the aorta, I did not observe collagen deposition in the mesenteric arteries of WT or RAG-1$^{-/-}$ mice treated with angiotensin II (Figure 3).

Van Gieson's Elastica staining did not reveal a qualitative difference in elastin between sham or angiotensin II-treat mice or in RAG-1$^{-/-}$ mice (Figure 1A). Angiotensin II-induced hypertension was associated with hypertrophy of medial cells, causing a greater separation of elastin laminae. Biochemical analysis also did not reveal differences in the absolute amount of elastin between sham and angiotensin II-treated WT or RAG-1$^{-/-}$ mice, or an effect of T cell adoptive transfer (Figure 1D). When normalized to total protein, relative elastin levels were decreased by angiotensin II in both mouse strains (Figure 2F), but this could be attributed to the striking increase in total aortic protein associated with angiotensin II-induced aortic hypertrophy (Figure 2G).

2.4.2 Angiotensin II-induced hypertension causes dramatic changes in the expression of the aortic matrix genes: In addition to collagen and elastin, numerous other matrix proteins can influence vascular stiffness. I therefore performed a PCR array to characterize expression of 84 aortic matrix genes related to fibrosis and remodeling. In response to angiotensin II infusion, 17 out 84 genes were significantly upregulated while no genes were down regulated (Table 2). Among these, collagen 1a1 and MMP-2 were upregulated by more than 8 fold and collagen 3a1 by 7 fold. MMP-11, thrombospondin-1, thrombospondin-2 and secreted acidic cysteine rich glycoprotein (Sparc) were upregulated by 4-5 fold. I also found more than 3 fold upregulation for collagen 5a1 and MMP-14. Surprisingly, the potent pro-fibrotic cytokine, TGF-β1, was not altered in angiotensin II-induced hypertension.

2.4.3 Hypertension reduces aortic compliance – role of T cells: Additional studies were performed to measure compliance of isolated segments of the descending thoracic aorta. Chronic angiotensin II infusion caused marked stiffening of the thoracic aorta in WT mice, as evidenced by a downward shift of the compliance curve (Figure 4A) and leftward shift of the stress-strain relationship (Figure 4B). In contrast, in RAG-1$^{-/-}$ mice, chronic angiotensin II infusion had essentially no effect on aortic stiffness. Adoptive transfer of T cells to RAG-1$^{-/-}$ mice restored the increase in aortic stiffening caused by angiotensin II (Figure 4C and 4D). Analysis of the changes in vascular inner and outer diameter showed that these increased in parallel in vessels from sham treated mice as intraluminal pressure was increased. In contrast, following angiotensin II infusion, the increase in outer diameter was constrained in aortas from WT mice, but not in aortas from RAG-1$^{-/-}$ mice (Figure 4E and 4F).

To determine the relative contribution of T cell subtypes, I examined the effect of angiotensin II infusion in CD4$^{-/-}$ and CD8$^{-/-}$ mice. The increase in collagen caused by angiotensin II was blunted in mice lacking either T cell subtype, but was most striking in mice lacking CD8^{+} T cells as evidenced by both Masson's trichrome staining and by hydroxyproline assay (Figure 5A-C). In addition, CD4$^{-/-}$ and CD8$^{-/-}$ mice were both partially protected against the development of aortic stiffening caused by angiotensin II (Figure 5D-5G). In additional studies, I performed adoptive transfer of CD4^{+} T cells or CD8^{+} T cells to RAG-1$^{-/-}$ mice and then infused angiotensin II three weeks later. Neither cell type alone increased aortic stiffness or collagen content significantly (Figure 6). These data indicate that both cell types are required and likely interact to mediate hypertension-related aortic stiffening.

I have previously shown that that mice lacking IL-17a are protected against the development of hypertension, aortic inflammation and angiotensin II-induced vascular oxidative stress.[39] In the present

study, I found that IL-17a$^{-/-}$ mice are also protected against aortic collagen deposition (Figure 7A-C) and aortic stiffening (Figure 7D and E) in response to chronic angiotensin II infusion.

I have previously shown that T cells play a role in models of hypertension other than angiotensin II infusion, including DOCA-salt hypertension and norepinephrine-induced hypertension.[33, 46] To determine if the reduced adventitial collagen deposition and aortic stiffening in RAG-1$^{-/-}$ mice are specific to angiotensin II, I also studied deoxycorticosterone acetate (DOCA)-salt-induced hypertension, which is characterized by low levels of circulating angiotensin II. As shown in Figure 8, while WT mice developed marked collagen deposition and aortic stiffening in response to DOCA-salt challenge, RAG-1$^{-/-}$ mice were protected from these changes. These data suggest that T cells contribute to aortic stiffening in forms of hypertension other than that caused by angiotensin II.

2.4.4 Aortic stiffening is dependent on blood pressure elevation: In clinical studies, aortic stiffening is commonly associated with hypertension; however, the causal relationship remains unclear. To address the possible role of pressure elevation in the genesis of aortic stiffening, I normalized blood pressure in angiotensin II-infused mice by adding hydralazine (320 mg/L) and hydrochlorothiazide (60 mg/L) to the drinking water. As shown in Figure 9A and 9B, concurrent hydralazine and hydrochlorothiazide treatment completely prevented the elevation of blood pressure. This treatment also protected against adventitial collagen deposition (Figure 9C-E). More importantly, the shifts in compliance and stress-strain curves were prevented by this treatment regimen (Figure 9F and 5G). Interestingly, I found that hydralazine and hydrochlorothiazide also abrogated T cell infiltration and inflammation in the aortas of angiotensin II-infused mice (Figure 9H-L). Collectively, these data suggest that aortic stiffening and vascular inflammation are at least in part due to mechanical effects of hypertension.

To determine whether normalization of blood pressure in established hypertension could reverse collagen deposition and aortic stiffening, hydralazine and hydrochlorothiazide treatment was administered from day 15 to day 28 during a 4-week angiotensin II infusion. Although this successfully normalized blood pressure during the last two weeks of angiotensin II infusion, it failed to reverse adventitial collagen deposition and aortic stiffening (Figure 10). These data suggest that hypertension might cause irreversible large vessel fibrosis and remodeling.

2.4.5 Aortic fibroblasts express collagen in response to IL-17a and hypertensive mechanical stretch: The above experiments suggest that both inflammation and mechanical forces contribute to aortic stiffening. To differentiate between the direct effect of mechanical stretch and the inflammatory cytokine IL-17a, I performed additional studies using cell culture. Because I found aortic collagen deposition in hypertension occurs largely in the adventitia, I studied aortic fibroblasts, which represent the predominant cell type of the adventitia. I focused these studies on the collagen subtypes identified in the real-time PCR array. Fibroblasts were exposed to either 5% or 10% stretch, mimicking levels of mechanical stretch observed in the setting of normal and elevated blood pressures, or were exposed to IL-17a (100 ng/mL) for 36 hours. I found that while IL-17a had no effect on the mRNA expression of collagen 1a1, 10% mechanical stretch doubled expression of this subtype beyond that observed with 5% stretch (Table 2). Collagen 3a1 was increased by more than 4-fold by IL-17a and by more than 3-fold in response to 10% stretch. Collagen 5a1 mRNA expression was increased approximately 2-fold by IL-17a and by 10% stretch, but was not further increased by the combination of this cytokine and stretch. The addition of angiotensin II had minimal effect on these responses except for collagen 3a1, where it doubled the effect of 10% stretch. These experiments show that the hypertensive milieu, which includes increased vascular stretch, inflammatory cytokines such as IL-17a and angiotensin II interact to modulate aortic fibroblast collagen production.

2.4.6 Activation of p38 MAPK is required for collagen expression and aortic collagen deposition induced by stretch and inflammation in vitro and in vivo: p38 MAPK has been implicated in the induction of collagen expression and fibrosis in different hypertensive models.[75-78] Interestingly, both 10% stretch and IL-17a at 100 ng/mL induced p38MAP kinase phosphorylation in aortic fibroblasts (Figure 11A-C). Moreover, inhibition of p38 MAP kinase with SB203580 prevented the increase in mRNA for collagens 1a1, 3a1 and 5a1 caused by stretch (Figure 11D-F). In contrast, SB203580 inhibited IL-17a-induced expression of collagen 3a1 but not collagen 5a1 (Figure 11G-I). I also found that angiotensin II-induced hypertension increased p38 MAPK phosphorylation in thoracic aortas, and that this was prevented by the normalization of blood pressure (Figure 12A-C). To gain insight into the role of p38 MAPK in vivo, I treated mice with SB203580 (10 mg/kg/day, i.p.) concurrently with angiotensin II. SB203580 reduced the hypertension caused by angiotensin II (Figure 12D and E). More importantly, SB203580 prevented collagen deposition (Figure 12F-H) and prevented the shift in aortic compliance and stress strain relationships caused by angiotensin II (Figure 12I and J). Of note, inhibition of p38 MAP kinase induced the formation of aneurysm in mice receiving angiotensin II infusion, suggesting collagen deposited in the aortic adventitial in hypertension might protect against destructive changes in the arterial wall (Figure 13). These data show that p38 MAP kinase is responsive to stretch and inflammation, and thus plays a central role in mediating collagen expression in cultured fibroblasts and in inducing aortic stiffness in vivo.

2.5 Discussion

In the present study, I identified novel mechanisms of aortic stiffening associated with hypertension as delineated in the scheme shown in Figure 14. Our data indicate that elevation of blood pressure and the attendent increase in vascular stretch leads to an inflammatory process characterized by infiltration of T cells and activation of p38 MAP kinase. These events lead to a striking deposition of collagen in the aortic adventitia, with scattered amounts of collagen in the media. This is associated with a marked alteration in aortic complaince, characterized by a leftward shift in the stress strain relationship and a downward relationship between aortic distending pressure and diameter. In vivo, this increase in aortic stiffness leads to a loss of the Windkessel or capacitance function of the aorta, increasing systolic pressure and promoting hypertension-related end-organ damage.

Interestingly, I found that T cells and in particular the T cell-derived cytokine IL-17a contribute to aortic stiffening. I have previously shown that mice lacking IL-17a are protected against hypertension.[39] More recently, IL-17 has been shown to increase Rho kinase-mediated phosphorylation of the endothelial nitric oxide synthase, to promote endothelial dysfunction and to elevate blood pressure when administered parenteraly.[67] In keeping with a role of inflammation in collagen deposition, I found that RAG-1$^{-/-}$ mice and IL-17a$^{-/-}$ mice are protected against aortic stiffening and collagen depostion during angiotensin II infusion, and that adoptive transfer of T cells to RAG-1$^{-/-}$ mice restores these abnormalities. I cannot exclude a role of cytokines other than IL-17a. As an example, TNF-α often acts synergistically with IL-17 to promote inflammatory responses. Recent studies showed that the TNF-α antagoinist etanercept reduces pulse wave velocity and aortic stiffness in patients with rheumatoid arthritis.[79, 80] Our laboratory have also found that mice treated with the TNF-α antagonist etanercept and mice lacking IL-17a are protected against these vascular alterations.[33] Thus, it is possible that this and other cytokines act in concert with IL-17 to promote aortic stiffening.

It is likely that both CD4^{+} and CD8^{+} T cells contribute to aortic stiffening, as mice lacking either one alone had an intermediate phenotype. In particular, mice lacking CD8^{+} T cells had a reduction in aortic collagen accumulation caused by angiotensin II. Likewise, adoptive transfer of only CD4^{+} cells or only CD8^{+} T cells to RAG-1$^{-/-}$ mice failed to restore aortic stiffening in response to angiotensin II. While CD8^{+} T cells are generally considered cytotoxic, it is now clear that CD8^{+} T cells produce substantial

amounts of cytokines and contribute to the inflammatory millieu.[81, 82] In preliminary studies, I have found that angiotensin II infusion induces IL-17a production in several T cell subtypes in vivo.

Our data also indicate that the mechanical effect of increased blood pressure also contributes to aortic stiffening. Prevention of hypertension with hydralazine and hydrochlorothiazide prevented collagen deposition and the increase in aortic stiffness caused by chronic angiotensin II infusion. These data do not separate mechanical effects from inflammation, because blood pressure lowering also prevented aortic leukocyte iniltration. In keeping with this finding, there are numerous mechanisms by which mechanical stretch could affect vascular inflammation. As examples, increased cyclical strain, similar to that observed in hypertension, activates the NADPH oxidase and NF-κB, increases expression intracellular adhesion molecule-1 (ICAM1), and enhances adhesion of monocytes to the endothelium.[83,84]

Substantial research has focused on the role of TGF-β in tissue fibrosis and collagen deposition. In several preliminary studies, I found that mRNA for TGF-β1 is not increased in aortas from angiotensin II-treated mice nor in cultured fibroblasts exposed to stretch. This does not exclude the possibility that TGF-β activity is increased at a post-translational level in response to hypertension. Latent TGF-β is processed to its active form by components of the inflammatory milieu, including matrix metalloproteinases, reactive oxygen species, thrombospondin-1 and integrins.[85,86]Related to this, our array analysis of the genes affected by hypertension provides insight. This analysis showed that hypertension led to a 9-fold increase in MMP-2 and a 5-fold increase in thrombospondin-1. These could contribute to post-translational activation of latent TGF-β in the absence of changes in its expression.

In an effort to separate the direct effects of stretch and inflammation, I exposed cultured murine aortic fibrobasts to either cyclical stetch or IL-17a. I selected fibroblasts because these represent the predominant cell in the adventital region where collagen deposition occurs. Our data indicate that both of these stimuli induce mRNA of various collagen subtypes, all of which could contribute to aortic stiffening. Our data also indicate that p38 MAPK likely plays an important role in collagen expression both in cultured fibroblasts and in vivo. Several studies has shown that inhibition of p38 blocks the pro-fibrotic effects of mechanical stretch both in vitro and in vivo. Park et al have shown that inhibition of p38 MAPK reduces cardiac and renal fibrosis in double transgenic rats harboring the human renin and angiotensinogen genes.[76] Similarly p38 inhibition decreases cyclical stretch-induced collagen expression in isolated smooth muscle cells from WKY and SHR rats.[78] Of note, p38 MAPK has been shown to bypass TGF-β signaling by transactivation of Smad-2/3 in mouse models of Marfan's Syndrome and systemic inhibition of p38 blocks these effects. In addition, increased activation of p38 MAPK due to loss of MAPK phosphatase-1 activity induces expression of microRNA-21 (miR-21),[87] a critical regulator of TGF-β signaling involved in renal and myocaridal fibrosis.[88,89,90] MiR-21 inhibits Smad-7 and augments TGF-β signalling, enhancing its pro-fibrotic effects.[91] Interestingly, miR-21 also contributes to renal fibrosis by regulating MMP9/TIMP-1. Thus, p38 MAPK plays a pivital role in the interaction between vascular inflammation and mechanical stretch.

It is important to differentiate the causal relationship bewteen aortic stiffening and hypertension in vivo. Recent data from the Framingham study indicate that increases in pulse wave velocity precede the development of overt hypertension in the general population.[92] Our study does not refute this, but suggests that once hypertension is initiated, aortic stiffening is markedly exagerated. In keeping with this, in mice subjected to transverse aortic constriction, adventitial collagen deposition is observed proximal to the constriction, where pressures are elevated, but not distal to the constriction where pressures are normal.[93] No matter the cause, stiffening of the proximal aorta leads to the loss of windkessel effect, further elevating systolic blood pressure. Therefore, in the long run, aortic stiffening

and hypertension likely promote one another in a feed-forward fashion, ultimately leading to progressive elevations in systolic blood pressure.

In the present study, the absolute amount of elastin present in the aorta was not affected by angiotensin II infusion, while the relative amount of elastin, expressed as a percent of total protein was reduced by about 50%. This relative loss of elastin might also contribute to the reduced aortic compliance observed in angiotensin II-induced hypertension. Loss of aortic elastin leads to aortic stiffening and hypertension in mice that are haploinsufficient for the elastin gene.[14] It is also possible that while total elastin is not changed, elastin damage might occur in the setting of angiotensin II-induced hypertension. Of note, MMP3, which was increased by 2.5 fold by angiotensin II infusion in our gene array analysis, has elastase activity, and could contribute to elastin fragmentation in hypertension.

The striking deposition of collagen in the adventitial layer might not only promote vascular stiffness, but could also increase compression of vascular smooth muscle cells during systole. Our in vitro studies showed that when intraluminal pressure is increased in a normal aorta, there is relatively equal expansion of both the lumen and the outer vascular media, thus preserving medial thickness. In contrast, increasing intraluminal pressure in aortas from angiotensin II-treated mice led to an increase in the lumen that was substantially greater than that of the outer media, leading to comparession of the media. This could lead to a condition in which vascular smooth muscle cells undergo cyclic compression during each cardiac cycle. The impact of this on vascular smooth muscle function remains to be defined.

In summary, this study provides new insight into mechansims of aortic stiffening in hypertension as depicted in Figure 14. An important component of this process is a striking deposition of collagen in the adventitia. Our data indicate that aortic stiffening is mediated by both mechanical factors assoicated with elevated pressures and by T cells and their release of inflammatory cytokines. The p38 MAP kinase likely plays an important signalling role in response to these stimuli. Adventitial collagen deposition and aortic stiffening can not only be considered a form of end-organ damage in hypertension but can also further elevate systolic pressure, leading to progression of this disease.

Chapter 3

Vascular Oxidative Stress Promotes Immune Activation and Aortic Stiffening in Hypertension

3.1 Chapter Abstract

T cells and interleukin 17A contribute to aortic stiffening, an important cause of systolic hypertension. Isoketals are lipid oxidation products that modify proteins to become immunogenic. I hypothesized that chronic vascular oxidative stress promotes T cell activation, aortic stiffening and hypertension via formation of isoketal-adducts. Mice with excessive vascular production of reactive oxygen species ($tg^{sm/p22phox}$ mice and mice with targeted deletion of the extracellular superoxide dismutase) develop vascular collagen deposition, aortic stiffening and hypertension with age. T cells of $tg^{sm/p22phox}$ mice produce high levels of IL-17A and IFN-γ. Crossing $tg^{sm/p22phox}$ mice with lymphocyte-deficient mice eliminated vascular inflammation, aortic stiffening and hypertension and adoptive transfer of T cells restored these processes. Isoketal-protein adducts were increased in aortas, dendritic cells and macrophages of $Tg^{sm/p22phox}$ mice. Autologous pulsing with $tg^{sm/p22phox}$ aortic homogenates promoted DCs of $tg^{sm/p22phox}$ mice to stimulate T cell proliferation and production of IFN-γ, IL-17A and TNF-α. Scavenging with tempol or 2-hydroxybenzylamine (2-HOBA) normalized blood pressure and prevented vascular inflammation, aortic stiffening and hypertension. Scavenging superoxide or isoketals also reduced formation of isoketals, and prevented DC and T cell activation. These results define a novel pathway linking vascular disease to immune activation. The resultant vascular inflammation promotes collagen deposition, aortic stiffening and age-related hypertension. Isoketal scavenging may prove useful in preventing these processes.

Keywords: Oxidative stress, inflammation, collagen deposition and aortic stiffening

3.2 Introduction

The normal aorta expands to accommodate a portion of the ejected blood during cardiac contraction, and then recoils during cardiac relaxation. This capacitance or “Windkessel” function of the aorta reduces systolic pressure and maintains diastolic pressure and perfusion to the periphery. In several conditions, including aging, autoimmune diseases, cigarette smoking, diabetes, obesity and hypertension per se, the aorta stiffens, leading to loss of the Windkessel function and systolic hypertension. Pulse wave velocity, a surrogate measure of aortic stiffness, predicts untoward outcomes in aged and hypertensive humans.[57, 94] A recent analysis of the Framingham population indicated that aortic stiffening is a precursor of hypertension.[10]

A potential common feature of the many conditions associated with aortic stiffening is vascular oxidant stress. Clinically, plasma levels of myeloperoxidase and F_2-isoprostanes, markers of oxidation, correlate with arterial stiffening in humans.[95] Studies in experimental animals have implicated reactive oxygen species (ROS) in fibrotic changes in the blood vessel, lung, skin and other tissues.[26, 96] In addition to oxidative events, chronic inflammation is associated with of arterial stiffness in humans.[62, 64, 80] Patients with systemic lupus erythematosus, rheumatoid arthritis and psoriasis exhibit increased aortic stiffness, and TNF-a antagonists improve parameters of aortic stiffness in patients with rheumatoid arthritis.[97, 98] I have shown that hypertension is associated with infiltration of immune cells

into the peri-adventitial fat and activation of T cells that release pro-inflammatory cytokines such as IL-17A, IFN-γ and TNF-α.[33, 39] IL-17A induces collagen synthesis in fibroblasts via activation of p38 MAP kinase.[99] IFN-γ also promotes hypertension-related fibrosis in the heart, arteries and the kidney.[42]

A potential mechanism linking oxidative injury to immune activation and inflammation relates to oxidative modification of self-proteins. In particular, isoketals, alternatively referred to as isolevuglandins or γ-ketoaldehydes, are formed from fatty acid oxidation and undergo a pyrrolation reaction with protein lysines.[100] Pyrrole modified proteins become auto-antigens and can illicit antibody formation.[101] Our laboratory has recently shown that hypertension is associated with accumulation of isoketal-adducted proteins within dendritic cells (DCs). These adducts markedly enhance DC expression of the co-stimulatory molecules CD80 and CD86 and enhance DC production of IL-6, IL-23 and IL1b.[47] Moreover, DCs modified in this fashion robustly drive T cell activation and can prime hypertension when adoptively transferred to naïve mice. In this study, I found that hypertension stimulates DC production of reactive oxygen species, suggesting that lipid oxidation leading to isoketal formation was occurring inside the DC. Whether or not DCs can acquire oxidatively modified proteins produced by other cells remains undefined. Such a process could link oxidative injury in other cells to immune activation, and might explain how oxidative stress leads to vascular inflammation and ultimately aortic stiffening. In the present studies, I employed mice with chronic vascular oxidative stress to define a novel pathway which links oxidative damage to immune activation via formation of immunoreactive isoketal protein-adducts, vascular inflammation, aortic stiffening and hypertension. These experiments provide new insight into how diverse conditions diminish aortic compliance and ultimately cause hypertension. These findings also provide potential therapeutic options for treatment or prevention of aortic stiffening.

3.3 Materials and methods

Animals: The Institutional Animal Care and Use Committee at Vanderbilt approved all experimental protocols. Male wild type and $tg^{sm/p22phox}$ mice were studied at 3, 6 and 9 months of age. For measurement of blood pressure, 6 mice at each age were implanted with telemetry units. Ten days later, blood pressure was recorded for 10 minutes every hour for three days. In additional (n = 6) $tg^{sm/p22phox}$ mice, tempol or 2-hydroxybenzylamine was administered in the drinking water from 4 to 9 months of age. In some experiments, 3 month-old $tg^{sm/p22phox}$ mice x RAG-$1^{-/-}$ mice underwent adoptive transfer of T cells as described previously.[33, 99, 102] Nine month-old $tg^{sm/p22phox}$ mice x RAG-$1^{-/-}$ mice, with or without T cell reconstitution, were used for blood pressure and vascular stiffness measurements. $SOD3^{loxp/loxp}$ x $tg^{sm/p22phox}$ mice and $SOD3^{loxp/loxp}$ x Cre-/- mice are treated with tamoxifen (3 mg/20 kg, dissolved in corn oil) via 5 consecutive intraperitoneal injections at 3 month of age and are studied at 9 month of age.[103]

Ex vivo measurement of aortic stiffness: For studies of vascular stiffness, the descending thoracic aorta was mounted on cannulas at the in situ length in calcium-free buffer.[71] Intraluminal pressure was increased in a step-wise fashion while video microscopy was used to follow outer and inner diameter. Diameters were recorded with every increment of 25 mmHg from 0 to 200 mmHg. Stress-strain relationships were calculated as described by Baumbach et al.[71]

Measurement of aortic collagen: Aortic collagen was visualized by Masson's trichrome staining as described previously, with minor modifications.[99] Isolated thoracic aortas were digested in 6 N HCl at 105 ˚C for 48 hours before hydroxyproline was quantified.[72-74]

Flow cytometry: Single cell suspensions were prepared from aortas as previously described.[99, 102] Briefly, the entire aorta with surrounding perivascular fat was minced with fine scissors and digested with 1 mg/mL collagenase A, 1 mg/ml collagenase B, and 100 ug/ml DNAase I in phenol-free RPMI 1640 medium with 5% FBS for 30 min at 37°C, with intermittent agitation. Fc receptors were blocked with CD16/CD32 for 20 min at 4°C (BDbiosciences, clone 2.4G2) prior to the staining of surface markers. The antibodies used were: Amcyan anti-CD45, PE anti-F4/80, Pacific Blue anti-CD19, APC-Cy7 anti-CD3e, APC anti-CD4 and PE-Cy7 anti-CD8a. 1 x 10^6 cells were incubated with 1.5 µl of each antibody in 100 µl of FACS buffer for 35 minutes. The cells were then washed twice with FACS buffer and immediately analyzed on a FACSCanto flow cytometer with DIVA software (Becton Dickinson). Dead cells were eliminated from analysis using 7-AAD (BD Phermingen). For each experiment, we performed flow minus one (FMO) controls for each fluorophore to establish gates. Data analysis was performed using FlowJo software (Tree Star, Inc.).

Intracellular staining of spleen cells: 1 x 10^6 spleen cells were resuspended in RPMI medium supplemented with 5% FBS and stimulated with ionomycin and phorbol myristate acetate and brefeldin A at 37°C for 5 hrs. Dead cells were excluded from analysis with a fixable Violet dead cell stain. The following surface antibodies were employed for staining T cells: BV510 anti-CD45, PerCP-Cy5.5 anti-CD3 antibody, PE-Cy7 anti-CD8, APC-H7 anti-CD4. Intracellular staining was then performed with the Cytofix/Cytoperm™ Plus fixation/permeabilization solution kit (BDbiosciences) using PE anti-IL17A and FITC anti-IFN-γ antibodies (eBioscience). In some experiments, macrophages, dendritic cells and monocytes were gated using APC anti-CD11b, PE anti-MerTK, APC-Cy anti-CD11c, PerCP-Cy5.5 MHC II/I-A b, PE-Cy anti-CD64, Amcyan anti-F4/80, Alexa Fluor 700 anti-Ly-6C as previously described.[104]A single-chain antibody, D11 ScFv, was conjugated to Alexa Fluor 488 for the detection of isoketals in these cells.

Measurement of isoketals: Six-micron sections were obtained from paraffin-embedded aortas and stained with D11 ScFv as previously described.[47, 105] Isoketals in mouse aortas were also measured as the isoketal-lysyl-lactam adducts using mass spectrometric analysis as previously described.[47, 100]

T cell proliferation assay: Aorta homogenates were obtained from WT mice, $tg^{sm/p22phox}$ mice or $tg^{sm/p22phox}$ mice chronically treated with tempol or 2-HOBA. Protein concentrations were determined in these samples using Bradford assay. CD11c+ DCs were isolated from total splenocytes of WT mice using a magnetic cell sorter and a commercially available kit (Miltenyi Biotec). This is an acceptable method to isolate essentially all DCs from mouse splenocytes. One million DCs were exposed to 100 mg aortic protein for 2 hours in RPMI 1640 with 10% FBS, 5% penicillin/streptomycin/fungizone and 5% Sodium pyruvate. These DCs were washed twice before being co-cultured for 7 days with pan T cells pre-labeled with CFSE. T cells were obtained from 9 month-old WT mice or $tg^{sm/p22phox}$ mice that either been untreated or had been chronically treated with tempol or 2-HOBA in the drinking water. Various combinations of aorta homogenate and T cells were employed as described in Figure 9A and B. These cells were subjected to flow cytometry analysis and cytokines in the culture medium were measured by luminex.

Statistical analysis: Data in the manuscript are expressed as the mean ± SEM. Comparisons of blood pressure over time and aortic mechanics were made using one-way ANOVA for repeated measures, followed by a Bonferroni post hoc test when significance was indicated. To compare the effect of treatments on various mouse strains, two-way ANOVA was employed. All other comparisons were made using one-way ANOVA. P values are reported in the figures.

3.4 Results

3.4.1 Chronic vascular oxidative stress induces aortic stiffening and hypertension: As an initial approach to detecting aortic collagen, I studied $tg^{sm/p22phox}$ mice. These animals have smooth muscle targeted overexpression of $p22^{phox}$, a docking subunit of all NADPH oxidase catalytic subunits.[106] This leads to an increase in vascular Nox1 and an approximately 2-fold increase in vascular superoxide and hydrogen peroxide production. Masson's trichrome staining revealed minimal collagen staining in the aorta of wild-type (WT) mice at either 3, 6 or 9 months of age (Figure 15A-B). In contrast, aortic adventitial collagen content was increased in the $tg^{sm/p22phox}$ mice at 6 and 9 months of age. Hydroxyproline analysis confirmed that aortic collagen content was increased by about 2-fold at 6 and 9 months of age in $tg^{sm/p22phox}$ mice (Figure 15C).

Mechanical properties of the aortas of WT and $tg^{sm/p22phox}$ mice were studied in a pressurized vessel apparatus. Aortas from WT mice at 3, 6 and 9 months of age demonstrated identical responses to increasing pressure (Figure 15D). Aortas from 3 month-old $tg^{sm/p22phox}$ mice were similar to those of WT mice, but at 6 and 9 month of age, aortas of these mice demonstrated depressed pressure-diameter relationships. This was reflected by a leftward shift in the stress-strain curves (Figure 15E), indicating increased stiffness of the aortas of $Tg^{smp22phox}$ mice at 6 and 9 month of age.

Although aortic stiffening developed at 6 month of age in $tg^{sm/p22phox}$ mice, their blood pressure was normal at that age. At 9 months however, the $tg^{sm/p22phox}$ mice developed moderate hypertension, while WT mice remained normotensive (Figure 15F and 15G). Thus, in $tg^{sm/p22phox}$ mice, age-related aortic stiffening precedes the elevation of blood pressure, mimicking the relationship between these events in humans.

The effects of oxidative stress on aortic stiffening and age-related hypertension were confirmed in mice with vascular smooth muscle targeted deletion of the extracellular superoxide dismutase ($SOD3^{loxp/loxp}$ x $tg^{smmhc/Cre}$ mice), another model of vascular oxidative stress.[48] At 9 month of age, these mice exhibited increased aortic adventitial collagen deposition compared to age-matched WT mice (Figure 16A and B). This was associated with development of aortic stiffening (Figure 16C and D) and elevation of blood pressure (Figure 16E and F). Collectively, these data support a role of vascular ROS in promoting vascular fibrosis, aortic stiffening and age-related hypertension.

3.4.2 Oxidative stress-induced vascular inflammation contributes to age-related hypertension: We and others have previously demonstrated that vascular inflammation contributes to the development of hypertension and aortic stiffening.[33, 39, 42, 65, 99] I therefore sought to determine if chronic oxidative stress promotes vascular inflammation in $tg^{sm/p22phox}$ mice. Flow cytometry of single cell suspensions revealed that total leukocytes, monocyte/macrophages, B cells, total T cells and $CD4^+$ and $CD8^+$ T cell subsets were all increased in aortas of 6 and 9 month old $tg^{sm/p22phox}$ mice compared to similarly aged WT mice (Figure 17A-N). Immunohistochemistry (IHC) using anti-CD3 indicated that T lymphocyte were predominantly located in the adventitia and perivascular fat of thoracic aortas in $Tg^{smp22phox}$ mice at 6 and 9 month of age, compared to age-matched WT mice (Figure 17P).

3.4.3 T lymphocytes are required for oxidative stress-induced collagen deposition, aortic stiffening and hypertension. Because T cells contribute to hypertension in other models, I crossed $tg^{sm/p22phox}$ mice with mice lacking Recombination Activation Gene-1 ($Rag\text{-}1^{-/-}$ mice), to generate $tg^{sm/p22phox}$ mice x $Rag\text{-}1^{-/-}$ mice. Unlike $tg^{sm/p22phox}$ mice, $tg^{sm/p22phox}$ mice x $RAG\text{-}1^{-/-}$ mice did not develop collagen deposition (Figure 18A-C), aortic stiffening (Figure 18D-E) or hypertension (Figure 18F-G). To further examine a role of T cells in aortic stiffening and hypertension in response to vascular oxidative stress, I adoptively transferred 2 X 10^7 T cells to $tg^{sm/p22phox}$ x $Rag\text{-}1^{-/-}$ mice at 3 months of age and allowed them to survive until 9 months of age. Adoptive transfer of T cells restored collagen deposition, aortic stiffening and blood pressure elevation in the $tg^{sm/p22phox}$ x $RAG\text{-}1^{-/-}$ mice, supporting an essential

role of T cells in the development of aortic fibrosis and hypertension induced by chronic vascular oxidative stress.

3.4.4 Isoketals accumulate in the aorta and antigen presenting cells of $Tg^{smp22phox}$ mice: Because isoketal-adducted proteins can act as auto-antigens and stimulate inflammatory responses,[47, 101] I sought to determine if chronic vascular oxidant stress promotes their formation. Immunohistochemical staining using the single chain antibody D-11, revealed abundant isoketal protein adducts in aortas of 9 month-old $tg^{smp22phox}$ mice, but not WT mice (Figure 19A). Treatment of mice from 4 to 9 months of age with either the superoxide dismutase (SOD) mimetic tempol or the isoketal scavenging agent 2-hydroxybenzylamine (2-HOBA) eliminated isoketal staining in the $tg^{sm/p22phox}$ mouse vessels.

To further confirm the presence of isoketal-protein adducts in these vessels of $tg^{sm/p22phox}$ mice, I employed mass spectrometry in collaboration with Drs. L. Jackson Roberts and Sean S. Davies in the Department of Pharmacology at Vanderbilt University. Thoracic aortic homogenates of 9 month-old WT, $tg^{smp22phox}$ mice and $tg^{smp22phox}$ mice either untreated or treated with tempol or 2-HOBA, were homogenized and analyzed by liquid chromatography/mass spectrometry (LC/MS). Isoketals were identified as isoketal-lysine-lactam adducts in these measurements (Figure 19B). Aortic isoketal content was increased in $Tg^{smp22phox}$ mice compared to WT mice, and this was prevented by treatment with either tempol or 2-HOBA. These data confirm that vascular oxidative stress induces formation of isoketals and that this can be prevented by treatment with either tempol or 2-HOBA.

In additional experiments, I found that isoketals also accumulate in the antigen presenting cells (APCs) of $tg^{sm/p22phox}$ mice. Using a gating strategy recently described [104], macrophages were identified as $CD64^{+}MerTK^{+}$, and dendritic cells were selected from the remaining cells as $CD11c^{+}$ and major histocompatibility complex class II (MHC II)$^{+}$ cells (Figure 20). Monocytes were identified as $CD11b^{+}CD64^{+}F4/80^{low}SSC^{low}$ cells. Virtually all monocytes were Ly-$6C^{+}$ and most expressed MHC II. Intracellular staining for isoketals, using D11 conjugated to Alexa Fluor 488 revealed that DCs, macrophages and to a smaller extent, monocytes of $tg^{sm/p22phox}$ mice accumulate isoketal-protein adducts while cells of WT animals do not (Figure 19C-H). This was prevented by chronic treatment with either tempol or 2-HOBA.

3.4.5 Scavenging of ROS prevents vascular inflammation, aortic stiffening and hypertension in $tg^{smp22phox}$ mice. To determine if scavenging superoxide or isoketals prevents vascular oxidative stress-induced aortic stiffening and hypertension I employed telemetry. Chronic treatment with either tempol or 2-HOBA prevented aortic fibrosis in $Tg^{smp22phox}$ mice at 6 and 9 months of age (Figure 21A-C). Similarly, tempol and 2-HOBA prevented the development of aortic stiffening and age-related hypertension (Figure 21D-G), underscoring the importance of vascular ROS this disease. These data support a role of vascular ROS in promoting vascular fibrosis, aortic stiffening and age-related hypertension.

To determine if the protective effects of antioxidants were due to reduced vascular inflammation, I performed flow cytometry on the aortas of $tg^{sm/p22phox}$ mice treated with vehicle, tempol or 2-HOBA from 4 to 9 months of age. Interestingly, tempol and 2-HOBA also markedly reduced the aortic infiltration of leukocytes (Figure 22A-C). The infiltrating $CD45^{+}$ total leukocytes, $F4/80^{+}$ monocyte/macrophages, $CD19^{+}$ B cells, $CD3^{+}$ total T cells and $CD4^{+}$ and $CD8^{+}$ T cell subsets were significantly reduced by either of these treatments (Figure 22D-I).

3.4.6 Vascular oxidative stress promotes cytokine production by splenic T cells. We and others have previously shown that IL-17A and IFN-γ contribute to hypertension,[39, 42, 107] and that IL-17A plays a critical role in aortic stiffening. I therefore sought to determine if T cells of mice with vascular oxidative stress produce IL-17A and IFN-γ. Splenic T cells from 9 months old WT and $tg^{sm/p22phox}$ mice were analyzed by flow cytometry using intracellular staining for the cytokines (Figure 23A). While WT T cells

produced minimal amounts of IL-17A, 5% of $CD4^+$ T cells and 10% of double negative ($CD3^+/CD4^-/CD8^-$) T cells of $Tg^{smp22phox}$ mice produced this cytokine (Figure 23B-C and J-K). Likewise, IFN-γ-producing cells were doubled in all three subsets of T lymphocytes in $tg^{sm/p22phox}$ mice compared to WT (Figure 23F-G and M-O). Treatment with tempol or 2-HOBA normalized T cell production of IL-17A and IFN-γ in $tg^{sm/p22phox}$ mice. These data suggest that vascular oxidative stress activates T cells and promotes their pro-inflammatory cytokine production.

3.4.7 Protein homogenates of $tg^{sm/p22phox}$ mouse vessels are immunogenic: Our laboratory have shown that isoketal-protein adducts promote maturation and activation of dendritic cells in angiotensin II-induced hypertension, and that these activated DCs can drive proliferation of T cells from angiotensin II-treated mice.[47] To determine if proteins from the aortas of $tg^{sm/p22phox}$ mice are immunogenic, I prepared aortic homogenates from WT and $tg^{sm/p22phox}$ mice at 9 months of age. These were used to pulse naïve DCs from WT mice for 2 hours and were then washed from the cells. As depicted in Figure 24A, the DCs were then co-cultured with $1x10^7$ T cells isolated from the spleen of either WT or $tg^{sm/p22phox}$ mice and pre-labeled with CFSE at a ratio of 1:10. Aortic homogenates of $tg^{sm/p22phox}$ mice, but not WT mice, supported survival of $CD3^+$ (Figure 24B and F), $CD4^+$ and $CD8^+$ T cells (Figure 24C and G) when presented to T cells by DCs. DCs pulsed with $tg^{sm/p22phox}$ aortic homogenates also induced proliferation of $CD4^+$ (Figure 24D and H) and to a lesser extent $CD8^+$ T cells (Figure 24E and J), and increased the release of IL17A/F, IFN-γ and TNF-α into the medium (Table 3). Chronic treatment of $tg^{sm/p22phox}$ mice with tempol or 2-HOBA reduced the immunogenicity of their aortic protein, as indicated by the diminished survival, proliferation and cytokine production of T cells in this assay (Figure 24B-J and Table 3). Interestingly, T cells isolated from $tg^{sm/p22phox}$ mice, but not those from WT mice, survived and proliferated in response to the stimulation of immunogenic protein homogenate, suggesting that pre-exposure to isoketal-adducted antigens in vivo primed these cells for clonal expansion upon a second challenge.

To determine if dendritic cells were functionally activated in these conditions, I also evaluated the polarizing cytokines released into the medium. When DCs exposed to $tg^{sm/p22phox}$ mice aorta homogenate were co-cultured with T cells isolated from $tg^{sm/p22phox}$ mice, there was a marked increase of GM-CSF, IL-1α, IL-1β, IL-6 and TGF-β1 and TGF-β3 (Table 3). These increases were blunted when DCs were primed with aortic homogenates from $tg^{sm/p22phox}$ mice chronically treated with tempol and 2-HOBA, suggesting that antioxidant treatment reduced the immunogenicity of the vascular protein in these mice. Interestingly, $tg^{sm/p22phox}$ mice aorta homogenate failed to induce DCs to produce these cytokines if they were co-cultured with unresponsive WT T cells, suggesting that interactions with isoketal-primed T cells promote DC activation. Other cytokines, such as IL-2, IL-12(p40), IL-12(p70), IL-21, IL-23 and TGF-β2 were either undetectable or not differentially produced across treatment groups. Collectively, these data suggest that vascular oxidative stress and the formation of isoketals induce DC activation, T cell proliferation and cytokine production.

3.5 Discussion

Aortic stiffening accompanies several common conditions including aging, hypertension, atherosclerosis, overt diabetes, obesity and cigarette smoking.[52, 53, 95, 108] While aortic stiffening promotes systolic hypertension and predisposes to cardiovascular events, the precise mechanisms underlying its cause remain poorly understood. Our present study defines a new pathway in which vascular oxidative stress promotes formation of immunogenic isoketal protein adducts. These act as autoantigens that are presented to T lymphocytes by antigen presenting cells, leading to T cell activation. These activated T cells then infiltrate into the aortic periadventitial region and release cytokines that induce collagen deposition, leading to aortic stiffening and hypertension (Figure 25).

A recent analysis of the Framingham population revealed that aortic stiffening precedes the development of overt hypertension.[10] In this regard, the $tg^{sm/p22phox}$ mouse mimics this sequence of events. At 6 months, aortic compliance was reduced in these animals prior to development of hypertension. At 9 months, these mice developed modest elevations of blood pressure, while WT mice remained normotensive at this time. I also observed aortic stiffening and hypertension in 9 month-old mice with targeted vascular smooth muscle deletion of SOD3. Our laboratory has previously shown that these mice have increased vascular superoxide production but are normotensive at 3 months.[103] Taken together, data from these two models suggest that mice with chronic vascular oxidative stress recapitulate age related aortic stiffening and hypertension in humans, and suggest that chronic vascular oxidative stress might contribute to the human disease.

In addition to oxidative events, aging is associated with the formation of advanced glycation end-products (AGEs), which are generated from a reaction of sugars with proteins that accumulate in tissues with aging in the settings of insulin resistance and hypertension.[30, 109] Like isoketals, AGEs also adduct lysine residues and crosslink matrix proteins, including collagen.[110, 111] Of note, there is substantial interplay between AGEs and ROS. In human endothelial cells, ROS induced by high glucose stimulates the expression of receptors for AGEs (RAGEs) and RAGE ligands including S100 calgranulins and high mobility group box 1.[31] Drugs like ALT-711, a nonenzymatic breaker of AGE-mediated cross-links, decrease arterial stiffness, improve endothelial function and slightly lower systolic blood pressure in humans and experimental animals.[30, 32] It is likely that AGE deposition acts synergistically with the increase in collagen deposition to enhance arterial stiffening during aging. Of note, our laboratoey have previously shown that AGE-modified proteins do not share the immunogenicity of isoketal modifications.[47]

Studies by our laboratory and others have implicated a role of T cell-derived cytokines in the development of tissue fibrosis and target organ damage in hypertension.[33, 39, 42, 66, 99] In the present study, I found that vascular oxidative stress induces production of IL-17 by spleen T cells. Moreover, DCs primed with aortic homogenates from $tg^{sm/p22phox}$ mice markedly activated T cells from this same strain, but not WT mice. This activation profile included not only proliferation but also robust production of IL-17A, TNF-a and IFN-γ. These observations support a pathway in which vascular oxidative stress leads to formation of isoketal-protein adducts that are taken up by DCs that in turn can activate T cells. Of note, I have previously shown that IL-17A induces fibroblast production of collagen via activation of p38 MAP Kinase. Similarly, Valente et al have shown that IL-17A stimulates mouse cardiac fibroblast migration and proliferation via a p38 MAP kinase pathway.[112] IFN-γ also mediates cardiac inflammation and fibrosis in angiotensin II-infused WT mice and IFN-γ receptor deficient mice are protected from these changes.[42] Similarly, TNF-α has been implicated in angiotensin II-induced hypertension and TNF-α antagonist treatment improves parameters of aortic compliance in humans with autoimmune disease.[33, 97]Thus, the milieu of Th1/Th17 cytokines stimulated by isoketal-adducted proteins likely promotes age-related aortic stiffening and hypertension.

It is of interest to note that approximately 7×10^4 $CD4^+$ cells persisted in the CFSE assay following stimulation of 10^7 T cells with DCs that had been pulsed with aortic homogenates. Given that these cells divided approximately 3 to 4 times (figure 24D), it is likely that they were derived from approximately 7×10^3 original T cells. Thus, approximately 0.01% of total T cells from the $tg^{sm/p22phox}$ mice seem capable of responding to antigens in their own aortic homogenates. These findings are in keeping with our recent observation that an oligoclonal population of T cells respond to angiotensin II-induced hypertension.[113] The fact that WT T cells did not respond to DCs pulsed with $tg^{sm/p22phox}$ aortic proteins suggests that these animals have not accumulated memory cells capable of this response, while $tg^{sm/p22phox}$ mice possess such cells. In accord with this conclusion, our laboratory recently showed that mice with angiotensin II-induced hypertension possess memory T cells capable of responding to isoketal-adducted proteins.[47]

Related to the above considerations, a striking finding in the current study is the marked production of cytokines, including IL-1β, IL-6, TGF-β1 and GM-CSF, by DCs primed with $tg^{sm/p22phox}$ aortic homogenates when exposed to T cells from $tg^{sm/p22phox}$ mice. This finding suggests that not only do DCs stimulate T cell proliferation and cytokine production, but also that T cells with T cell receptors that respond to isoketal adducts can reciprocally activate DCs. One such signal might involve co-stimulatory engagement of DC B7 ligands by T cell CD28, which our laboratory have previously shown to be critical for hypertension and T cell activation in this disease.[102] In this regard, Orabona et al have shown that CD28 can stimulate DCs to produce IL-6, IFN-γ and to a lesser extent IL-23 in a B7 and p38 MAP kinase-dependent fashion.[114]

Macrophages and monocytes may also function as antigen presenting cells and have the capability of triggering adaptive immune responses in addition to professional DCs.[104] In the present study, I found an increase of total $F4/80^+$ cells in the aorta of $tg^{sm/p22phox}$ mice with aging. In addition, I found that splenic macrophages and monocytes of $tg^{sm/p22phox}$ mice accumulate isoketals. We have previously shown that monocyte/macrophage like cells do not increase expression of the B7 ligands, CD80 and CD86 in concert with their acquisition of isoketal adducts as robustly as DCs, suggesting that they might not be as effective in T cell stimulation.[47]

Despite the plethora of studies implicating ROS in diseases such as atherosclerosis, hypertension and diabetes, several large clinical trials using either vitamin E or combinations of antioxidants have failed to show any decrease in cardiovascular morbidity or mortality,[21, 115] and high doses of vitamin E have paradoxically been associated with increased cardiovascular event rates,[22] perhaps because ROS can have important signaling functions that modulate vascular tone, cell growth and survival,[116-118] and are critical for innate immunity. It has been previously shown that these higher concentrations of vitamin E are required to suppress plasma F2 isoprostanes, which are formed in the same pathway as isoketals.[119] It is therefore possible that agents such as 2-HOBA, which directly scavenge isoketals with a high rate constant and do not interfere with other ROS, will prove beneficial in treatment of disorders such as hypertension and aortic stiffening.

Chapter 4

Aortic Sca-1$^+$ Cells and Circulating Fibrocytes Promote Angiotensin II-induced Aortic Stiffening

4.1 Chapter Abstract

Aortic stiffening precedes hypertension and correlates with end-organ damage in the brain, heart and kidney. An important cause of aortic stiffening is adventitial collagen deposition, which impairs the capacitance function of large arteries. The sources of fibrosis in this condition are poorly defined. In the present study, I found that adventitial Sca-1$^+$ progenitor cells proliferate and acquire a fibroblast-like phenotype in hypertension as determined by flow cytometry and immunofluorescence studies. CD31$^-$ Sca-1$^+$ cells isolated from angiotensin II-infused mice have upregulated expression of collagen 1a1, 3a1, 5a1 and fibronectin-1 compared to those from sham treated mice. CD31$^+$ endothelial cells and CD31$^-$Sca-1$^-$ cells also expressed collagen and fibronectin-1 in response to angiotensin II infusion. Collagen I$^+$CD45$^+$ circulating fibrocytes were identified in the peripheral blood and were increased in the aortas of hypertensive mice. In WT mice transplanted with bone marrow from tg$^{CAG-EGFP}$ mice, hypertension caused EGFP$^+$Col I$^+$CD45$^+$ cells to infiltrate the aortic adventitia where they co-localized with areas of collagen deposition. 45% of total Col I$^+$ cells in the aorta were EGFP$^+$ and therefore are derived from the bone marrow. The remaining 54% were EGFP$^-$, representing vascular resident fibroblasts. In conclusion, fibroblast-like cells derive from Sca-1$^+$ progenitors and infiltrating circulating fibrocytes are the two major contributors of arterial fibrosis in hypertension.

Key words: Sca-1$^+$ progenitors, circulating fibrocytes and collagen deposition

4.2 Introduction

Hypertension induces a striking deposition of collagen in the aortic adventitia. This fibrotic process results in loss of the “Windkessel function” of the proximal aorta and leads to systolic hypertension and target organ damage. Resident fibroblasts have been traditionally been thought to be a major source of tissue fibrosis in wound healing, atherosclerosis and vascular fibrosis. I have previously shown that T cell cytokine IL-17A and increased mechanical stretch, which are commonly encountered in hypertension, drive expression of multiple collagen subtypes in primary mouse aortic fibroblasts. This is mediated by activation of the p38 MAP kinase and inhibition of this enzyme prevents collagen deposition both in vitro and in vivo.[99] Hypertensive stimuli such as reactive oxygen species also activate fibroblasts, promoting fibrinogenesis and tissue remodeling.[28, 29]

Stem cell antigen-1 (Sca-1, alternatively known as lymphocyte antigen 6 complex, locus A or Ly-6A) positive progenitor cells reside in the vascular adventitia, which is a major site of collagen deposition in hypertension.[99, 120] These pluripotent cells emerge during embryogenesis, persist into adulthood and represent roughly 20% of aortic adventitial cells.[121, 122] In mouse aortas, they express several hematopoietic stem cell (HSC) markers, including Lin, c-kit and CD34.[123, 124] Sca-1 cells are maintained by sonic hedgehog signaling (Shh) in the aortic adventitia, and in Shh-/- mice these cells are either absent or diminished in number.[121] In healthy arteries of adult mice, Sca-1$^+$ progenitors maintain endothelial and smooth muscles cells and generate vascular-like branching structures when cultured on

matrigel.[124] However, under disease conditions such as atherosclerosis and vascular injury, these cells have the capacity to differentiate into mesenchymal phenotype and might contribute to tissue fibrosis.[122]

Circulating fibrocytes are considered a specialized population of leukocytes that express collagen I and CD45.[38, 125-127] These cells migrate to inflamed or injured tissues via chemotactic ligand-receptor interactions, and have been shown to play a role in wound healing and fibrosis of the heart, lung and kidney.[38, 125-127] Once recruited to sites of inflammation, fibrocytes secrete additional chemokines that attract more fibrocytes and other leukocytes, including T cells, macrophages and dendritic cells.[38, 128, 129] Fibrocytes also promote tissue remodeling by depositing fibrotic proteins including collagen. In addition, by secreting TGF-beta1, they may also induce transformation of endothelial cells to a fibroblast-like phenotype, a phenomenon known as endothelial to mesenchymal transition.[38, 130]

Thus, collagen-forming cells of the vessel can include resident fibroblasts, endothelial to mesenchymal transition, Sca-1 cells and recruitment of circulating fibrocytes. It is unclear however whether and how these different populations are involved the pathogenesis of aortic stiffening in hypertension. In the present study, I found that adventitial Sca-1^+ progenitor cells acquire a collagen I-producing phenotype in hypertension, potentially contributing to collagen deposition and aortic stiffening. I also found that collagen I^+CD45^+ circulating fibrocytes infiltrate the large vessels and further promote arterial fibrosis in hypertension. These findings provide a new paradigm to support the roles of vascular and bone marrow origins of fibroblasts in response to vascular injury and inflammation.

4.3 Methods

Animals: C57Bl/6, $tg^{Ly\text{-}6A/EGFP}$ and $tg^{CAG\text{-}EGFP}$ mice were obtained from Jackson Laboratories at 12 weeks of age. Hypertension was induced by infusion of angiotensin II (490 ng/kg/min) via osmotic minipumps for two weeks in WT and $tg^{Ly\text{-}6A/EGFP}$ and 4 weeks in mice receiving bone marrow transplantation. The Institutional Animal Care and Use Committee at Vanderbilt approved all experimental protocols.

Bone marrow transplantation (BMT): Two weeks prior to BMT, 12 week old WT mice were transferred to sterile cages and fed sterile chow and acidified water (pH 2.0) containing 1 mg/ml of sulfamethazine-Na^+ (Sigma) and 0.2 mg/ml of trimethoprim (Sigma) for prophylaxis. On the day of BMT, mice were lethally irradiated with a dose of 10 Gy 4 hours prior to BMT via a ^{137}Cs irradiator (J. L. Shepherd and Associates, Glendale, CA). Bone marrow cells (2 x 10^7 cells) were obtained from femurs and tibias of $tg^{CAG\text{-}EGFP}$ mouse mice and were injected by the tail vein of recipient mice. The mice were then housed for 6 weeks to allow engraftment of the bone marrow. Successful engraftment was confirmed upon sacrifice by flow cytometry of peripheral blood mononuclear cells for EGFP expression.

Flow cytometry: Single cell suspensions were prepared from aortas as previously described.[99, 102] Briefly, the entire aorta with surrounding perivascular fat was minced with fine scissors and digested with 1 mg/mL collagenase A, 1 mg/ml collagenase B, and 100 ug/ml DNAase I in phenol-free RPMI 1640 medium with 5% FBS for 30 min at 37°C, with intermittent agitation. Fc receptors were blocked with anti-mouse CD16/CD32 for 20 min at 4°C (BDbiosciences, clone 2.4G2) prior to the staining of surface markers. The antibodies used were: PerCP-Cy5 anti-CD45; PE anti-CD34; APC anti-CD34, APC-Cy7 anti-Sca-1/Ly-6A; PE-Cy7 anti-c-kit/CD117; Amcyan anti-CD31. All aortic cells were incubated with 1.5 µl of each antibody in 100 µl of FACS buffer for 35 minutes. The cells were then washed twice with FACS buffer and immediately analyzed on a FACSCanto flow cytometer with DIVA software (Becton Dickinson). Dead cells were excluded from analysis with a fixable Violet dead cell stain. Intracellular staining was then performed with the Cytofix/Cytoperm™ Plus fixation/permeabilization solution kit (BDbiosciences) using a mouse monoclonal antibody (Abcam)

conjugated to Alexa Fluor 488 or 647 (Molecular Probes). For each experiment, I performed flow minus one (FMO) controls for each fluorophore to establish gates. Data analysis was performed using FlowJo software (Tree Star, Inc.).

Immunohistochemistry (IHC) and immunofluorescence: Aortic collagen was visualized by Masson's Trichrome staining as previously described.[99] Immunofluorescence staining was performed on fix-perfused mouse aortas embedded in OCT. Six micron sections were sliced in a serial sequence. Samples were permeabilized with Triton X-100 (Sigma-Aldrich). Antigen blocking was performed with 10% donkey serum (Abcam) prior to incubation with primary antibodies. These include monoclonal rat anti-Sca-1, mouse anti-collagen, polyclonal goat anti-EGFP and rabbit anti-Fsp-1 antibodies. Donkey polyclonal antibodies conjugated to Alexa Fluor 488, 555 or 647 were used for binding 1st antibodies. DAPI (Invitrogen) was added in the last wash following incubation with secondary antibodies. All slides were mounted with Prolong Anti-fade media (Life Technologies).

Statistical analysis: Data are expressed as the mean ± SEM. Student's t tests were used to compare the effects of sham and angiotensin II. Two-way ANOVA was used to analyze the effect of angiotensin II infusion on the gene expression of aortic cells as well as the density of circulating fibrocytes followed by a Bonferroni post hoc test when significance was indicated. P values are reported in the figures.

4.4 Results

4.4.1 Aortic Sca-1$^+$ cells develop fibroblast-like phenotype in hypertension. Using multicolor flow cytometry, I first examined the effect of chronic angiotensin II-induced hypertension on the presence of collagen-forming cells within the aorta. Sca-1$^+$ cells were identified after excluding CD31$^+$ endothelial cells which also express the Sca-1 marker (Figure 26A-D). Hypertension was associated with a 2.6-fold increase of CD31$^-$Sca1$^+$ progenitor cells (Figure 25D and I) compared to sham-infused mice. Interestingly, a small fraction of these progenitors produced collagen I at baseline, and these were more than doubled with hypertension (Figure 26F, H and J), suggesting hypertension promoted differentiation of these progenitors into a fibroblast-like phenotype. Of note, I observed a 4-fold increase of CD31$^+$Col I$^+$ cells in these experiments, suggesting that endothelial to mesenchymal transition contributes to vascular fibrosis in hypertension (Figure 26E and K). CD31$^-$Sca-1$^-$Col I$^+$ cells were also increased in the aortas of angiotensin II-infused mice (Figure 26G and L).

I have previously found that multiple collagen subtypes, fibronectin-1 and other matrix proteins are increased in aortas of hypertensive mice. To determine the relative contribution of various cell populations to arterial fibrosis, I isolated CD31$^+$, CD31-Sca-1$^+$ and CD31$^-$Sca-1$^-$ cell fractions from mouse aortas using magnet-activated cell sorting (Figure 27A). In response to angiotensin II infusion, collagen 1a1, 3a1 and 5a1 were upregulated by 2-fold and fibronectin-1 by 4-fold in CD31$^+$ cells, again supporting the notion that endothelial to mesenchymal transition contributes to arterial fibrosis in hypertension (Figure 27B-E). These collagen subtypes were also upregulated by 3-5 fold and fibronectin-1 by 2-fold in the CD31$^-$Sca-1$^+$ cells. Similarly, the CD31$^-$Sca-1$^-$ cells markedly expressed collagen 1a1 and fibronectin-1 in response to hypertension, confirming a direct role of these cells in collagen deposition and aortic stiffening.

In order to determine whether Sca-1$^+$ progenitor cells differentiate into fibroblasts, I co-stained for Sca-1 and collagen I on frozen sections of mouse aortas. To identify Sca-1+ cells in the aorta, I employed transgenic mice expressing a Sca-1-EGFP construct (tg$^{Ly\text{-}6A/EGFP}$). These hemizygous tg$^{Ly\text{-}6A/EGFP}$ mice express EGFP in all adult hematopoietic stem cells and the expression of EGFP generally corresponds to Sca-1.[131] As shown in Figure 27F and G, I observed a striking increase of total Sca-1$^+$ cells in the aortic adventitia with hypertension compared to sham treated mice. Of note, these cells were closely

associated with the region of adventitial collagen deposition and some of them were observed to be actively producing collagen I, as indicated by the yellow co-localization. The number of Sca-1$^+$Col I$^+$ cells was increased 3-fold with hypertension (Figure 27G). Collectively, these data indicate that Sca1$^+$ cells develop a fibroblast-like phenotype and contribute to collagen deposition in aortic stiffening and hypertension.

4.4.2 Adventitial Sca-1$^+$ cells proliferate during aortic stiffening. To determine whether the increase of Sca-1$^+$ cells in the aortic adventitial was due to proliferation, I co-stained for Ki-67. As shown in Figure 28A, Ki-67 was undetectable in the aortic adventitial of sham-infused mice; in contrast, hypertension caused a marked increase of Ki-67$^+$ cells that co-localize with Sca-1$^+$ cells. Immunohistochemistry of serial sections of these aortas indicated that most of the Ki-67$^+$ cells were embedded in the adventitial collagen layer (Figure 28B-D). These data suggest that Sca-1$^+$ cells proliferate as they differentiate into collagen-producing cells in aortic stiffening.

4.4.3 Bone marrow-derived circulating fibrocytes are recruited to aortic adventitia in hypertension. Fibrocytes expressing markers of leukocytes and mesenchymal cells circulate in the peripheral blood and migrate to injured tissues in response to chemokines.[38] To determine if these cells contribute to aortic stiffening in hypertension, I identified all collagen I-producing cells in the peripheral blood mononuclear cells (PBMCs) and aorta using flow cytometry (Figure 29A). Col I$^+$ cells were CD34$^-$ CD31$^-$ and almost all expressed CD45. Very few of these cells expressed Sca-1 (less than 10%) or c-kit (1.5%). Circulating Col I$^+$ cells and Col I$^+$CD45$^+$ cells are found at similar density in the peripheral blood of sham and angiotensin II-infused mice (Figure 29B, C and E), suggesting that these fibrocytes are maintained at a constant rate. Of note, hypertension is associated with a roughly 3-fold increase of Col I$^+$CD45$^+$ cells in the aorta, which may have been recruited from the circulation. These cells are also reminiscent of the CD31$^-$Sca-1$^-$Col I$^+$ cells shown in Figure 26.

Because hypertension is associated with increased expression of chemokines in the vascular cells, I sought to determine whether these circulating fibrocytes migrate to aortic adventitia during the onset of hypertension. Using bone marrow transplantation, I tracked cells derived from the marrow (Figure 30A). Flow cytometry analysis of PBMCs indicated that roughly 90% of circulating CD45$^+$ leukocytes were EGFP$^+$ in these mice, suggesting that the transplanted bone marrow was successfully engrafted in the recipients and was functional in hematopoiesis (Figure 30B). These mice also developed similar degrees of aortic stiffening in response to angiotensin II compared to WT mice (Figure 30B). Therefore, the bone marrow transplantation (BMT) procedure does not affect the pathogenesis of aortic stiffening in hypertension.

I then co-stained for EGFP and fibroblast specific protein 1 (Fsp-1, also known as S100A4) on frozen sections of these transplanted mice (Figure 30C). There are very few EGFP$^+$ cells in the adventitial region of sham-treated mice. In contrast, hypertension caused a 4-fold increase in recruitment of bone marrow-derived cells to the aortic adventitia (Figure 30C and E). The fibroblast marker, Fsp-1, was markedly increased in hypertension (Figure 30C and F). The number of cells positive for both EGFP and Fsp-1 were increased by 5-fold (Figure 30G), indicating these fibroblast-like cells are bone marrow-derived. In addition, only 10% of EGFP$^+$ cells were found to be Fsp-1 positive in sham mice, but this number increased to 40% with hypertension (Figure 30H), suggesting differentiation of these cells into fibroblast-like phenotype.

I also examined collagen I-immunoreactivity to determine if these cells contribute to aortic fibrosis (Figure 30D). While there was minimal collagen (red) in sham treated mice, collagen immunoreactivity was markedly increased by chronic angiotensin II infusion. The location of the collagen deposition corresponded to Masson's trichrome blue staining previously observed in normotensive and hypertensive animals.[99] Of note, most of the bone marrow derived cells were found in this collagen layer. EGFP$^+$Col I$^+$ cells were detected by yellow co-localization, and represented 45% of total EGFP$^+$

cells. Taken together, these data support a role of bone marrow derived cells in the development of vascular fibrosis associated with aortic stiffening.

4.4.4 Aortic Col I$^+$ cells are derived equally from resident vascular sources and the bone marrow. I also determined the relative contribution of bone marrow-derived fibrocytes to resident fibroblasts within aortas of BMT mice infused with angiotensin II. I found that 45% of collagen I-producing cells were EGFP$^+$ and therefore are derived from the bone marrow (Figure 31A and B). Most of Col I$^+$EGFP$^+$ cells were CD45$^+$ (Figure 31A), suggesting they are recruited from circulating fibrocytes. Roughly 55% of all collagen I-producing cells were EGFP negative, representing resident vascular cells that are not derived from the marrow (Figure 31A and B). In Col I$^+$EGFP$^-$ cells, 54.3% were CD31$^-$Sca-1$^-$, 40.8% were CD31$^-$Sca-1$^+$ and 4.5% were CD31$^+$Sca-1$^+$ (Figure 31A and C), representing the relative contribution of fibroblast-like cells originated from vascular sources.

4.5 Discussion

The present study demonstrates that there are at two major sources of tissue fibrosis that contribute to aortic stiffening in hypertension. Resident Sca-1$^+$ progenitor cells differentiate into fibroblast-like cells in response to hypertensive stimuli and contribute to collagen deposition. In addition, bone marrow derived fibrocytes accumulate in the aortic adventitia and elaborate collagen (Figure 31D). Although these are two distinct sources of collagen, they contribute equally to arterial fibrosis in hypertension.

Vascular resident Sca-1 cells are embryonically derived and continue to reside in the adventitia. Sca-1 is expressed in all embryonic and adult mouse hematopoietic stem cells.[131, 132] Sca-1$^+$c-kit$^+$CD41$^+$ hematopoietic cells first emerge from the endothelium of dorsal aorta at embryonic date 10.5.[132] Adventitial Sca-1$^+$ cells appear in the perivascular space between the ascending aorta and the pulmonary trunk between E15.5 and E18.5 and persist in this position until afterbirth.[121] Adventitial Sca-1$^+$ cell emerge well after development of the tunica media, and likely represent embryonic hematopoietic stem cells that have arrived by the vasa vasorum.[121] These cells remain in the vascular adventitia thereafter and expand in number during postnatal growth.[121] It is noteworthy, however, that Sca-1$^+$Lineage$^-$ progenitor cells also exist in the peripheral blood of adult mice.[123, 133] In adult mice, whether there is exchange between the vascular resident progenitor cells and bone marrow-derived circulating progenitors remains controversial.[134, 135]

In adult heart and blood vessels, resident Sca-1$^+$ progenitor cells can differentiate into multiple lineages, including cardiomyocytes, endothelial and smooth muscle cells.[121-124] There is evidence that these cells contribute to atherosclerotic lesions.[122] In keeping with a role of these progenitors in vascular remodeling, I found that Sca-1$^+$ cells in the aortic adventitial increase in number and promote arterial fibrosis by producing collagen subtypes and fibronectin-1 in response to hypertension. Likewise, others have shown Sca-1 expressing cells acquire a fibroblast-llike phenotype and demonstrate enhanced expression of connective tissue growth factor (CTGF) and fibronectin, contributing to fibrosis in aged murine skeletal muscle.[136]

Circulating fibrocytes are recruited to injured tissue via chemoattactant molecules. One such signal is CCL-21, which recruits CCR7-expressing circulating fibrocytes to the injured kidney in unilateral ureter obstruction-induced renal fibrosis.[38]I and others have previously shown that hypertension causes leukocyte infiltration in the peri-adventitial adipose tissue and this infiltration is associated with an increase in intercellular adhesion molecule-1 (ICAM-1) and RANTES in the aorta. Furthermore, hypertension is also associated with increased T cell production of IL-17A and TNF-α.[33] These cytokines synergistically upregulate the expression of multiple chemokines in human aortic smooth muscle cells,[39] which may attract the migration of circulating fibrocytes to blood vessels in hypertension.

In support of this, I found increased the recruitment of these cells to the aortic adventitia of hypertensive mice where they actively synthesize collagen.

Endothelial to mesenchymal transition contributes to tissue fibrosis in various tissues including the lung, heart, kidney and blood vessels.[130, 137-140] In pressure-overload induced cardiac fibrosis, a condition closely related to hypertension, $CD31^+$ endothelial cells become $vimentin^+$ and express collagen I, III and fibronectin 28 days after surgery. Similarly, endothelial-originated fibroblasts express Fsp-1, α-smooth muscle actin (α-SMA) and collagen I, and contribute to unilateral ureter obstruction-induced renal fibrosis. TGF-β1 is a potent signal that induces endothelial to mesenchymal transition and inhibition of TGF-β pathway prevents these changes.[130, 137, 138] Interestingly, inflammatory molecules associated with hypertension, such as IFN-γ, TNF-α and IL-1β, can also promote endothelial to mesenchymal transition by suppressing expression of fibroblast growth factor receptor (FGFR), an inhibitor of TGF-β/TGF-βR1 signaling.[141] In the current study, I found $CD31^+$ cells isolated from the in the aorta of hypertensive mice moderately expressed collagen 1a1, 3a1, 5a1 and fibronectin-1, confirming a role of endothelial to mesenchymal transition in aortic stiffening.

Of note, various sources of fibroblasts do not contribute equally to tissue fibrosis. LeBleu et al have gracefully demonstrated that tissue-resident (50%) and bone marrow-derived (35%) fibroblasts represent 85% of total myofibroblasts to unilateral ureter obstruction-induced fibrosis, while those derived from endothelial (10%) or epithelial cells (5%) account for the rest. In line with this, I found that 45% of collagen I-producing cells in the aortas of hypertensive mice were derived from the bone marrow, while 54% derived from the vascular sources. Only 4.5% of Col I^+EGFP^- aortic cells were $CD31^+$ (data not shown), suggesting that the contribution of endothelial to mesenchymal transition in aortic stiffening is limited. There are also temporal differences in the recruitment of these cells. As the first responders to tissue injury and inflammation, resident fibroblasts first become active in synthesizing collagen.[142] As tissue injury and inflammation persist, bone marrow-derived fibrocytes may be recruited to further promote fibrosis. In severer situations, endothelial, epithelial and even pericytes subsequently transform into fibroblast-like cells.[142] With the loss of functional cells, these events additively lead to irreversible tissue fibrosis and organ damage.

Chapter 5

Conclusions

My dissertation research investigated the roles oxidative stress, inflammation and adaptive immunity in the pathogenesis of aortic stiffening in hypertension. My studies revealed a previously undefined pathway in which hypertensive stimuli, including angiotensin II, salt, and reactive oxygen species promote the activation of T cells and other components of the adaptive immunity via, at least in part, the formation of immunogenic isoketal-protein addcuts. DC-T cell crosstalk amplifies the effect of oxidative damage and initiates specific inflammatory responses. These involve the engagement of specific leukocytes populations that infiltrate the vasculature. Vascular inflammation is a critical stage during the onset of aortic stiffening, in which inflammatory cytokines such as IL-17A, IFN-γ and TNF-α may directly trigger the activation of arterial fibroblasts leading collagen production. Other cellular components such as Sca-1+ progenitors and circulating fibrocytes likely also participate in these fibrotic changes, ultimately leading to aortic stiffening and worsened hypertension (Figure 32).

Kirabo et al has shown that hypertensive stimuli, such as angiotensin II or salt overload lead to neoantigen formation, in part by ROS formed in dendritic cells.[47] This promotes activation of T cells, in particular $CD8^+$ T cells, likely via isoketals presented by MHC I complexes. Class I complexes are loaded in the endoplasmic reticulum with peptides largely derived from self-proteins that have been degraded in the proteasome of all nucleated cells. When presented on the cell surface these send a protective "self" signal to immune cells such as Natural Killer (NK) cells, such that healthy cells will be ignored. Viral proteins in the cytoplasm can be loaded in MHC I. Likewise, oxidized proteins and peptides can be presented on MHC I, increasing immunogenicity.[143]There is also a phenomenon known as cross presentation or priming, in which exogenous proteins are taken up by phagocytosis, degraded in the phagosome and presented in class I complexes. My findings in the $tg^{smp22phox}$ mice add to this paradigm. In this model of chronic vascular oxidative stress, isoketals are formed by ROS generated in the vascular smooth muscle cells; however, these preferentially promoted the activation of $CD4^+$ T cells when presented by dendritic cells. In keeping with the concept $CD4^+$ and $CD8^+$ T cells have very different modes of activation and function; $CD4^+$ cells are activated by antigens presented in type II major histocompatibility complexes (MHC II) on professional antigen presenting cells such as dendritic cells and mononuclear phagocytes. Antigens presented by MHC II complex are generally derived from extracellular proteins. The fact that more $CD4^+$ cells than $CD8^+$ cells proliferate when co-cultured with DCs pulsed with aorta homogenates from $tg^{smp22phox}$ mice supports the concept that isoketals are presented by MHC II peptides in this context. Therefore, isoketals formed both inside and outside of dendritic cells can cause T cell activation and vascular inflammation in hypertension.

Tissue fibrosis is often the consequence of chronic inflammatory responses. Chemokines made by inflammatory cells might recruit bone marrow derived fibrocytes, which are a major source of tissue fibrosis.[38, 142] In support of this, Xia et al have showed that CXCL16 is expressed in the kidney in angiotensin II-infused mice in an NF-κB dependent manner.[144] CXCL16 deficiency suppressed bone marrow-derived fibroblast accumulation and myofibroblast activation and reduced expression of extracellular matrix proteins in the kidneys of angiotensin II-treated mice. In addition, WT mice engrafted with $CXCR6^{-/-}$ bone marrow displayed fewer bone marrow-derived fibrocytes in the kidney after angiotensin II treatment compared to WT mice engrafted with $CXCR6^{+/+}$ bone marrow.[125] Similarly, CCL21 recruits circulating fibrocytes to the kidney by binding to CCR7 expressed on these cells and blocking this interaction reduces renal fibrosis.[38] Hypertension causes infiltration of T cells to aortic adventitial.[33, 99] Activated T cells secrete proinflammatory cytokines, including IFN-γ, IL-17A and TNF-α,

which in turn increase expression of chemokines that recruit bone marrow derived fibrocytes, promote vascular fibrosis and ultimately lead to aortic stiffening and severe hypertension.[33, 39, 47, 49]

Aortic stiffening is both a cause and consequence of hypertension. Previous studies have established that aortic stiffening precedes hypertension both in experimental hypertension and epidemiological studies.[9, 10] My findings in the $Tg^{smp22phox}$ mice add to this literature and support the concept that stiffening of large capacitance arteries predispose to hypertension. My studies also support the concept that large arteries are targets of hypertensive end-organ damage. This is supported by the fact that normalization of blood pressure prevents the development of aortic stiffening and mechanical stretch alone induced the expression of collagen genes in cultured aortic fibroblasts. In human hypertension, it is likely that aortic stiffening and hypertension promote one another in a feed-forward fashion. On one hand, aortic stiffening causes loss of the "Windkessel" function of capacitance arteries, particularly the thoracic aorta, leading to elevation of the systolic blood pressure and rapid transmission of the stoke volume to the periphery. One the other, increased mechanical stretch associated with hypertension causes activation of vascular fibroblasts, resulting in aortic fibrosis characterized by the formation of a collagen "rind" in the adventitial region (Figure 32). This circumferential collagen deposition reduces vascular compliance and causes aortic stiffening.

Fibrosis is an end-stage pathological change in many forms of tissue damage in the heart, lung and kidney. However, arterial fibrosis may not just a detrimental consequence of prolonged hypertension, the adventitial collagen deposition might actually be protective against the aneurysm development. In support of this notion, a recent study demonstrated that systemic neutralization TGF-β enhances development of angiotensin II-induced aneurysm formation in mice and markedly increases mortality due to aortic rupture.[145] In keeping with this, mice in which IL-17 production is reduced by overexpression of suppression of cytokine secretion 3 (SOCS3) are markedly prone to developed aneurysms[146] In my study, inhibition of p38 MAPK reduced adventitial collagen deposition and aortic stiffening but also promoted aneurysm formation. Furthermore, transglutaminase type 2-mediated ECM crosslinking also protects against the development of abdominal aortic aneurysm via the stabilization of extracellular matrix in post mortem analysis of human subjects.[147] Therefore, aortic stiffening may represent a protective mechanism to prevent aortic aneurysm formation in the setting of hypertension.

Table 1 Effect of hypertension on the expression of aortic ECM gene and adhesion molecules

Symbol	Extracellular Matrix Gene	Sham $2^{(-\Delta\Delta Ct)}$	Angiotensin II $2^{(-\Delta\Delta Ct)}$	Fold Increase
Mmp2	Matrix metallopeptidase 2	0.21±0.04	1.88±0.12*	8.85
Col1a1	Collagen, type I, alpha 1	1.10±0.60	9.40±2.73*	8.56
Col3a1	Collagen, type III, alpha 1	6.19±2.14	42.92±3.77**	6.93
Thbs1	Thrombospondin 1	0.19±0.03	0.93±0.12**	4.88
Thbs2	Thrombospondin 2	0.08±0.03	0.39±0.06**	4.81
Sparc	Secreted acidic cysteine rich glycoprotein	1.79±0.79	8.08±0.96**	4.51
Mmp11	Matrix metallopeptidase 11	0.0004±0.0001	0.0015±0.0005*	4.24
Mmp14	Matrix metallopeptidase 14	0.03±0.01	0.11±0.02**	3.89
Col5a1	Collagen, type V, alpha 1	0.30±0.13	0.99±0.22*	3.34
Adamts2	A disintegrin-like and metallopeptidase with thrombospondin type 1 motif, 2	0.47±0.12	1.32±0.14**	2.83
Itgam	Integrin alpha M	0.013±0.004	0.036±0.011*	2.83
Fbln1	Fibulin 1	0.05±0.01	0.14±0.03*	2.81
Timp1	Tissue inhibitor of metalloproteinase 1	0.0001±0.00002	0.0003±0.00003*	2.46
Mmp3	Matrix metallopeptidase 3	0.07±0.02	0.18±0.02**	2.45
Itga2	Integrin alpha 2	0.003±0.001	0.006±0.001*	2.34
Fn1	Fibronectin 1	1.33±0.48	2.79±0.57*	2.10
Timp2	Tissue inhibitor of metalloproteinase 2	0.74±0.16	1.54±0.12*	2.08
Adamts5	A disintegrin-like and metallopeptidase (reprolysin type) with thrombospondin type 1 motif, 5 (aggrecanase-2)	0.017±0.004	0.023±0.004	N.A.
Adamts8	A disintegrin-like and metallopeptidase (reprolysin type) with thrombospondin type 1 motif, 8	0.060±0.020	0.049±0.018	N.A.
Ctnna1	Catenin (cadherin associated protein), alpha 1	0.37±0.06	0.38±0.04	N.A.
Ctnna2	Catenin (cadherin associated protein), alpha 2	0.015±0.0093	0.0003±0.0095	N.A.
Ctnnb1	Catenin (cadherin associated protein), beta 1	0.31±0.07	0.33±0.06	N.A.
Cd44	CD44 antigen	0.09±0.01	0.17±0.01	N.A.
Cdh1	Cadherin 1	0.0014±0.0008	0.0010±0.0005	N.A.
Cdh2	Cadherin 2	0.026±0.012	0.042±0.012	N.A.
Cdh3	Cadherin 3	<0.0001	<0.0001	N.A.
Cdh4	Cadherin 4	0.0005±0.0002	0.0003±0.0002	N.A.
Cntn1	Contactin 1	0.014±0.001	0.001±0.001	N.A.
Col2a1	Collagen, type II, alpha 1	0.0002±0.0001	0.0149±0.0001	N.A.
Col4a1	Collagen, type IV, alpha 1	0.70±0.27	1.11±0.28	N.A.

Symbol	Extracellular Matrix Gene	Sham $2^{(-\Delta\Delta Ct)}$	Angiotensin II $2^{(-\Delta\Delta Ct)}$	Fold Increase
Col4a2	Collagen, type IV, alpha 2	0.87±0.27	1.31±0.26	N.A.
Col4a3	Collagen, type IV, alpha 3	0.006±0.003	0.008±0.002	N.A.
Col6a1	Collagen, type VI, alpha 1	0.55±0.21	1.17±0.19	N.A.
Vcan	Versican	0.05±0.02	0.07±0.02	N.A.
Ctgf	Connective tissue growth factor	6.65±2.91	6.81±3.05	N.A.
Ecm1	Extracellular matrix protein 1	0.21±0.07	0.28±0.05	N.A.
Emilin1	Elastin microfibril interfacer 1	0.16±0.06	0.17±0.06	N.A.
Entpd1	Ectonucleoside triphosphate diphosphohydrolase 1	0.19±0.08	0.09±0.07	N.A.
Hapln1	Hyaluronan and proteoglycan link protein 1	0.004±0.002	0.002±0.002	N.A.
Hc	Hemolytic complement	0.0004±0.0003	0.0003±0.0001	N.A.
Icam1	Intercellular adhesion molecule 1	0.029±0.006	0.036±0.004	N.A.
Itga3	Integrin alpha 3	0.05±0.02	0.03±0.02	N.A.
Itga4	Integrin alpha 4	0.12±0.07	0.12±0.07	N.A.
Itga5	Integrin alpha 5 (fibronectin receptor alpha)	0.13±0.06	0.11±0.06	N.A.
Itgae	Integrin alpha E, epithelial-associated	0.002±0.002	0.001±0.001	N.A.
Itgal	Integrin alpha L	0.011±0.010	0.004±0.001	N.A.
Itgav	Integrin alpha V	0.23±0.05	0.24±0.05	N.A.
Itgax	Integrin alpha X	0.004±0.002	0.007±0.002	N.A.
Itgb1	Integrin beta 1 (fibronectin receptor beta)	1.80±0.53	1.65±0.50	N.A.
Itgb2	Integrin beta 2	0.04±0.02	0.06±0.01	N.A.
Itgb3	Integrin beta 3	0.11±0.03	0.05±0.03	N.A.
Itgb4	Integrin beta 4	0.0015±0.0011	0.0005±0.0002	N.A.
Lama1	Laminin, alpha 1	0.0001±0.0001	<0.0001	N.A.
Lama2	Laminin, alpha 2	0.022±0.006	0.041±0.004	N.A.
Lama3	Laminin, alpha 3	0.0031±0.0004	0.0037±0.0004	N.A.
Lamb2	Laminin, beta 2	0.40±0.14	0.54±0.11	N.A.
Lamb3	Laminin, beta 3	0.0004±0.0001	0.0008±0.0002	N.A.
Lamc1	Laminin, gamma 1	0.07±0.02	0.13±0.03	N.A.
Mmp1a	Matrix metallopeptidase 1a	<0.0001	<0.0001	N.A.
Mmp7	Matrix metallopeptidase 7	0.0001±0.0001	<0.0001	N.A.
Mmp8	Matrix metallopeptidase 8	0.0001±0.004	<0.0001	N.A.
Mmp9	Matrix metallopeptidase 9	0.009±0.006	0.003±0.006	N.A.
Mmp10	Matrix metallopeptidase 10	<0.0001	<0.0001	N.A.
Mmp12	Matrix metallopeptidase 12	<0.0001	<0.0001	N.A.
Mmp13	Matrix metallopeptidase 13	0.0008±0.0002	0.0029±0.0006	N.A.
Mmp15	Matrix metallopeptidase 15	0.009±0.004	0.008±0.003	N.A.
Ncam1	Neural cell adhesion molecule 1	0.19±0.06	0.07±0.07	N.A.
Ncam2	Neural cell adhesion molecule 2	0.0003±0.0001	0.0002±0.0002	N.A.

Symbol	Extracellular Matrix Gene	Sham $2^{\wedge(-\Delta\Delta Ct)}$	Angiotensin II $2^{\wedge(-\Delta\Delta Ct)}$	Fold Increase
Pecam1	Platelet/endothelial cell adhesion molecule 1	0.35±0.08	0.27±0.06	N.A.
Postn	Periostin, osteoblast specific factor	0.74±0.37	1.00±0.32	N.A.
Sele	Selectin, endothelial cell	0.0022±0.0004	0.0048±0.0005	N.A.
Sell	Selectin, lymphocyte	0.052±0.050	0.004±0.001	N.A.
Selp	Selectin, platelet	0.04±0.01	0.04±0.01	N.A.
Sgce	Sarcoglycan, epsilon	0.05±0.01	0.05±0.01	N.A.
Spock1	Sparc/osteonectin, cwcv and kazal-like domains proteoglycan 1	0.0019±0.0001	0.0011±0.0010	N.A.
Spp1	Secreted phosphoprotein 1	0.01±0.01	0.20±0.04	N.A.
Syt1	Synaptotagmin I	0.034±0.020	0.001±0.019	N.A.
Tgfbi	Transforming growth factor, beta induced	0.79±0.23	1.04±0.17	N.A.
Thbs3	Thrombospondin 3	0.04±0.01	0.07±0.02	N.A.
Timp3	Tissue inhibitor of metalloproteinase 3	0.03±0.01	0.03±0.01	N.A.
Tnc	Tenascin C	0.05±0.02	0.12±0.02	N.A.
Vcam1	Vascular cell adhesion molecule 1	0.033±0.006	0.073±0.004	N.A.
Vtn	Vitronectin	0.02±0.01	0.02±0.01	N.A.

Mice received either sham or angiotensin II treatment for 2 weeks. RNA was extracted from freshly isolated thoracic aorta after mice sacrifice. Matrix gene PCR array was performed to screen 84 aortic structural genes. 17 out 84 genes were upregulated in hypertension. Fold increase stands for the extent of gene upregulation compared to sham-treated mice based on ΔΔCt values. Data expressed as mean±SEM; *, $p<0.05$; $p<0.01$ vs. sham.

Table 2 Effects of IL-17a, angiotensin II and mechanical stretch on collagen expression by mouse aortic fibroblasts

Treatment				Angiotensin II (100 nM)		
	Col 1a1	Col 3a1	Col 5a1	Col 1a1	Col 3a1	Col 5a1
Control	1.00±0.05	1.00±0.34	1.00±0.12	1.03±0.02	1.59±0.08	1.24±0.25
IL-17a (100 ng/mL)	1.20±0.07	4.63±0.66 **	1.89±0.10 *	1.12±0.12	4.28±0.33 **	1.74±0.20
5% Stretch	1.33±0.25	1.98±0.20	1.39±0.21	NA	NA	NA
10% Stretch	2.24±0.24 **	3.40±0.53 ** #	2.45±0.37 **	2.80±0.34 **	7.50±1.43 **	2.68±0.62 **
IL-17a (100 ng/mL) + 10% Stretch	2.16±0.13 **	3.67±0.41 **	2.32±0.43 **	NA	NA	NA

Primary mouse aortic fibroblasts were exposed to 5% or 10% cyclic stretch or exposed to IL-17a (100 ng/mL) in the presence or absence of angiotensin II (100 nM) for 36 hours. Relative quantity of mRNA was calculated based on the ΔΔCt value normalized to control. Data are expressed as mean ± SE. The effects of IL17a and mechanical stretch are analyzed with one-way ANOVA, while the effect of angiotensin II by two-way ANOVA (n=3-6), * $p<0.05$, ** $p<0.01$ vs. control; # $p<0.05$ vs. angiotensin II. NA, not assessed. ECM, extracellular matrix.

Table 3 Vascular oxidative stress-induced dendritic cell activation and cytokine production

Cytokine (pg/ml)	WT *	WT *	$Tg^{sm/p22phox}$ *	$Tg^{sm/p22phox}$ *	$Tg^{sm/p22phox}$ + Tempol *	$Tg^{sm/p22phox}$ + 2-HOBA *
	WT **	$Tg^{sm/p22phox}$ **	WT **	$Tg^{sm/p22phox}$ **	$Tg^{sm/p22phox}$ **	$Tg^{sm/p22phox}$ **
GM-CSF	12.99±1.42$^{\#\#}$	8.24±2.18$^{\#\#}$	23.47±11.17$^{\#\#}$	1450.50±620.01	45.04±28.71$^{\#\#}$	73.80±58.52$^{\#\#}$
IL-1α	10.27±4.23$^{\#}$	5.17±1.71$^{\#}$	23.15±10.99	44.43±9.48	19.46±9.40	14.40±3.35
IL-1β	7.33±2.58$^{\#\#}$	5.51±1.97$^{\#\#}$	12.51±4.59$^{\#\#}$	52.03±8.80	14.96±3.14$^{\#\#}$	17.41±11.26$^{\#\#}$
IL-2	5.60±1.48	16.92±5.42	4.70±1.25	8.26±2.41	14.01±6.02	15.16±5.17
IL-6	20.63±9.43$^{\#\#}$	28.64±12.70$^{\#\#}$	39.10±17.35$^{\#\#}$	1461.00±439.78	122.42±76.91$^{\#\#}$	215.62±126.10$^{\#\#}$
IL-12(p40)	3.20±0.00	3.20±0.00	15.89±12.69	4.03±0.51	6.66±2.77	3.20±0.00
IL-12(p70)	3.20±0.00	3.20±0.00	5.25±2.06	3.20±0.00	3.55±0.44	3.20±0.00
IL-21	Undetectable	Undetectable	Undetectable	Undetectable	Undetectable	Undetectable
IL-23	Undetectable	Undetectable	Undetectable	Undetectable	Undetectable	Undetectable
TGF-β1	598.25±89.60$^{\#\#}$	779.67±79.89	733.25±50.09$^{\#}$	1078.00±121.93	807.20±56.93	860.60±75.65
TGF-β2	Undetectable	Undetectable	Undetectable	Undetectable	Undetectable	Undetectable
TGF-β3	194.25±5.92	184.33±5.589$^{\#\#}$	189.00±1.68$^{\#}$	218.00±10.19	188.20±4.859$^{\#\#}$	190.00±3.54$^{\#}$
IL-17A	20.06±2.27$^{\#\#}$	288.02±223.47$^{\#}$	30.24±11.86$^{\#\#}$	4433.50±1871.88	219.88±153.60$^{\#\#}$	298.38±197.49$^{\#\#}$
IL-17F	4.23±0.00$^{\#\#}$	49.49±39.19$^{\#\#}$	15.80±11.57$^{\#\#}$	920.00±111.09	155.62±124.28$^{\#\#}$	142.70±88.87$^{\#\#}$
IFN-γ	3.20±0.00$^{\#\#}$	38.47±30.54$^{\#\#}$	4.87±1.17$^{\#\#}$	3848.25±2662.32	50.53±52.53$^{\#\#}$	110.15±72.34$^{\#\#}$
TNF-α	7.66±2.54$^{\#\#}$	10.69±5.07$^{\#\#}$	13.26±5.14$^{\#\#}$	83.45±8.10	21.73±5.57$^{\#\#}$	23.58±8.08$^{\#\#}$

T cells from either 9 month-old WT or $Tg^{sm/p22phox}$ mice were stimulated with DCs pulsed by aorta homogenate of WT mice, $Tg^{smp22phox}$ mice and $Tg^{smp22phox}$ mice treated with tempol or 2-HOBA. Cytokines released into the culture medium were measured by a Luminex assay (n=6). IFN-γ was normalized by logarithmic transformation prior to one-way ANOVA. * Sources of aorta homogenate; ** Sources of T cells. $^{\#}$ $p<0.05$, $^{\#\#}$ $p<0.01$ vs. $Tg^{sm/p22phox}$ mice.

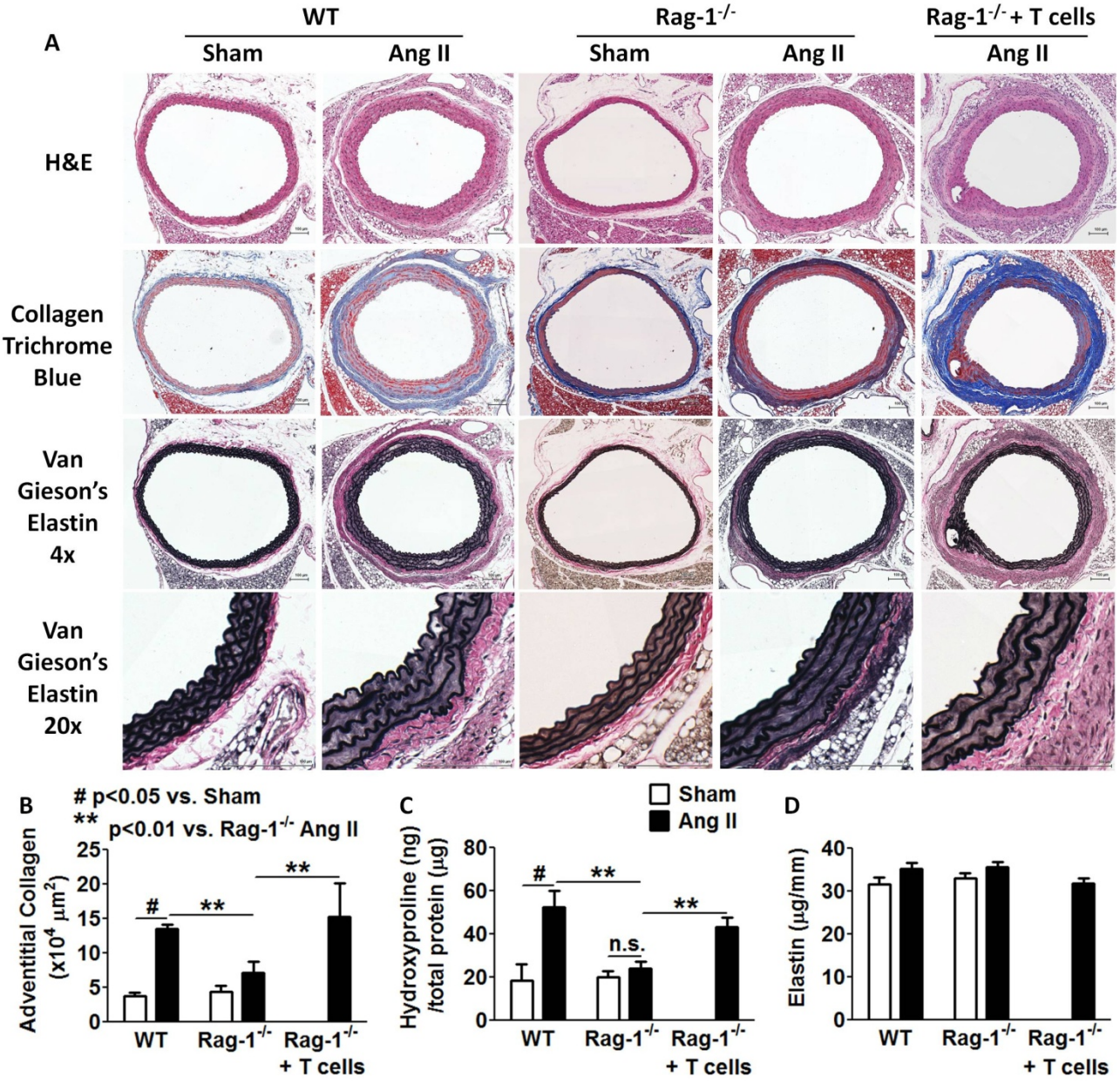

Figure 1 Role of T cells in aortic collagen deposition in hypertension. A) Effects of angiotensin II-induced hypertension on vascular collagen and elastin in WT and RAG-1$^{-/-}$ mice. Perfusion-fixed sections of the thoracic aortas were sectioned (6 mm) and stained with Hematoxylin and Eosin, Masson's trichome and Van Gieson's Elastica staining to highlight collagen (blue) and elastin (black). Scale bar indicates 100 μm. B) Adventitial collagen area was quantified by planimetry. C) Aortic collagen quantification by hydroxyproline assay. Isolated thoracic aortas were digested in 6 N HCl at 105 ˚C for 48 hours before hydroxyproline was quantified. D) Elastin was quantified biochemically by initial separation in 0.1 N NaOH at 90 ˚C for 30 min and subsequently by ninhydrin assay. Data were analyzed using two-way ANOVA (n=6-9).

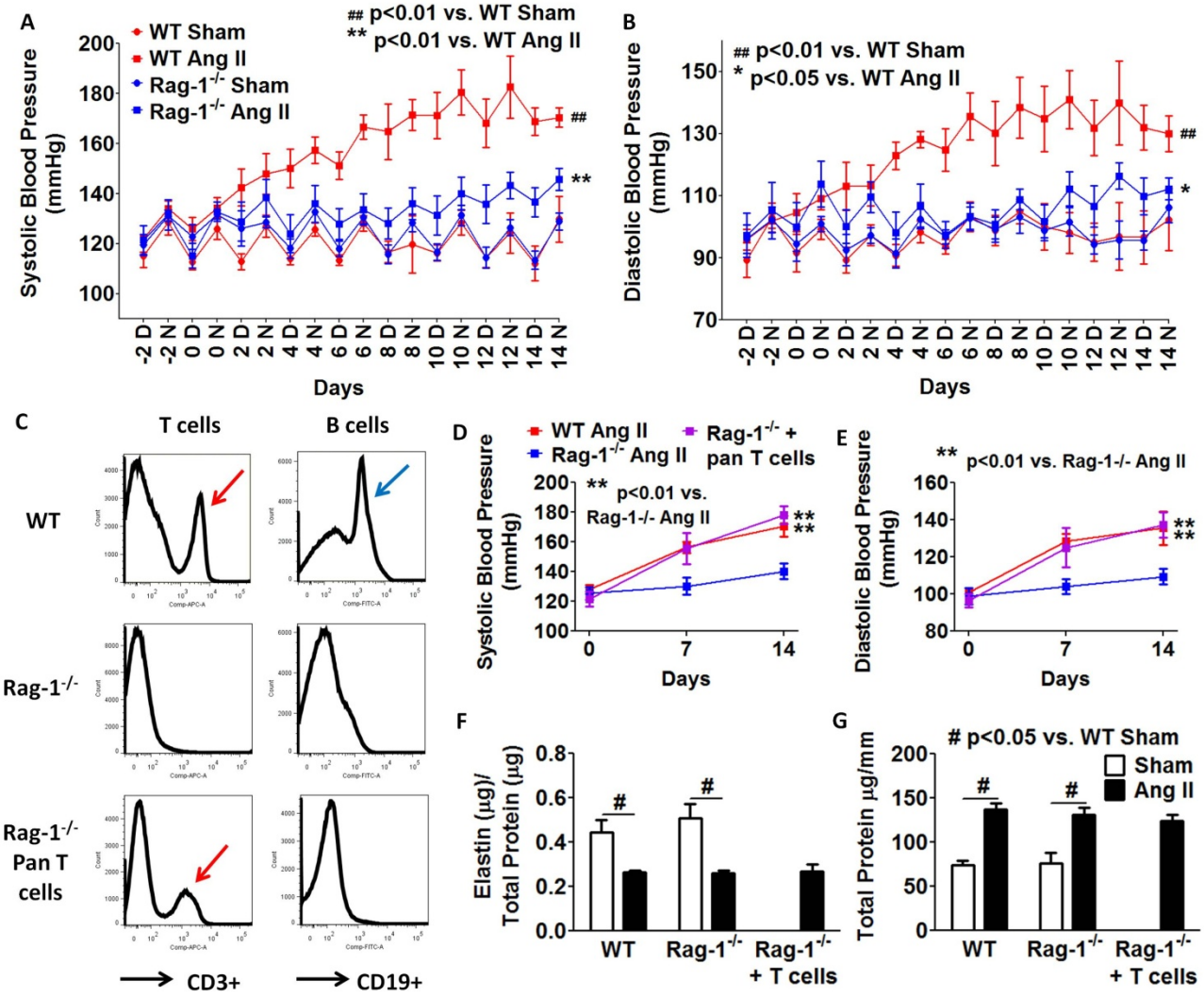

Figure 2 T cells mediate angiotensin II-induced hypertension.A and B) Telemetry recordings of blood pressure in WT and Rag-1$^{-/-}$ mice receiving either sham or angiotensin II (490 ng/kg/min) infusions by osmotic minipump for 2 weeks. D, day time; N, night time. C) Flow cytometry confirming reconstitution of T cells in Rag-1$^{-/-}$ mice. Pan T cells were isolated from age-matched C57Bl/6 mice and transfered into Rag-1$^{-/-}$ mice via tail vein injection. Angiotensin II was administered three weeks after adoptive transfer of T cells. D and E) Hypertensive response to angiotensin II in Rag-1$^{-/-}$ mice after adoptive transfer of T cells. Data analyzed with one-way ANOVA with repeated measurements (n=7-9). F)Elastin was quantified biochemically by initial separation in 0.1 N NaOH at 90 ˚C for 30 min and subsequently by ninhydrin assay. G) Total protein was determined as the total of elastin and all other proteins. Ang II, angiotensin II.Data analyzed using two-way ANOVA (n=6-9).

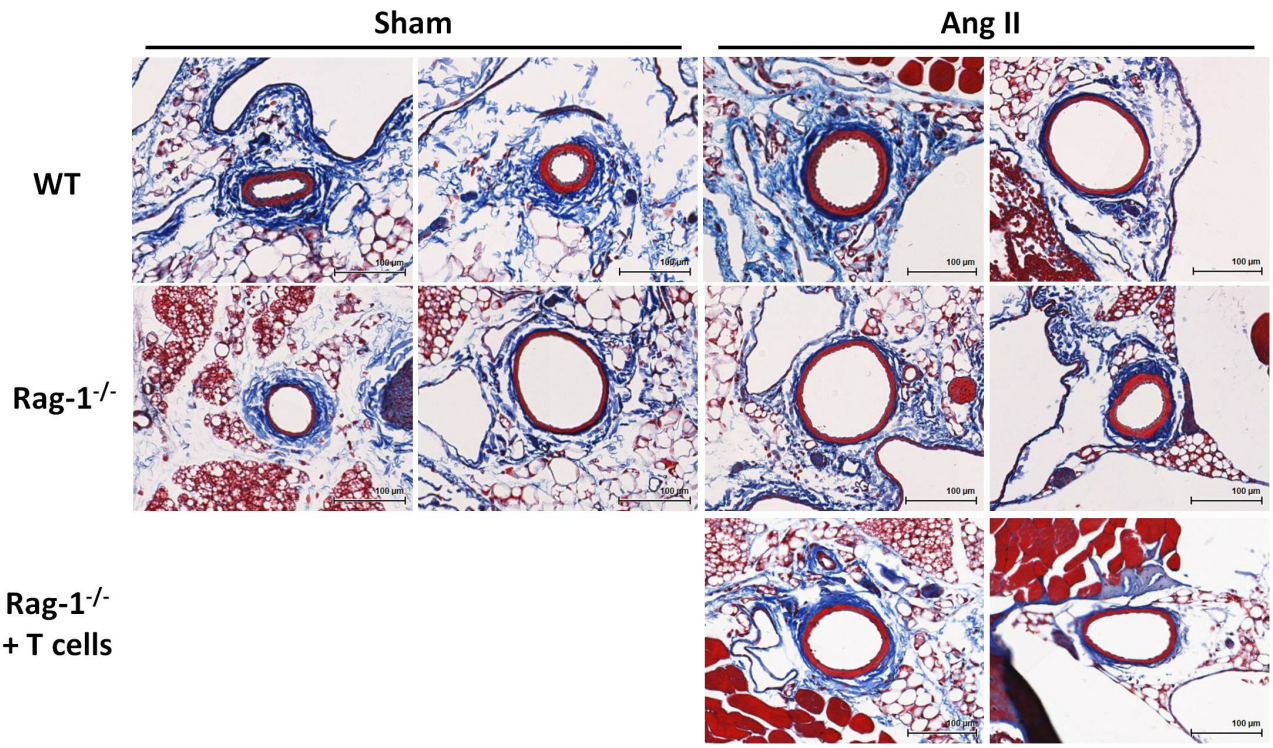

Figure 3 Role of T cells in collagen deposition in mesenteric arteries in angiotensin II-induced hypertension. Perfusion-fixed sections of the mesenteric arteries were sectioned (6 mm) and stained with Masson's trichome staining to highlight collagen (blue). Mesenteric arteries with diameters less than 100 µm were examined. Pan T cells were isolated from age-matched C57Bl/6 mice and transfered into Rag-1$^{-/-}$ mice via tail vein injection. Angiotensin II was administered three weeks after adoptive transfer of T cells. Scale bar indicates 100 µm. Ang II, angiotensin II.

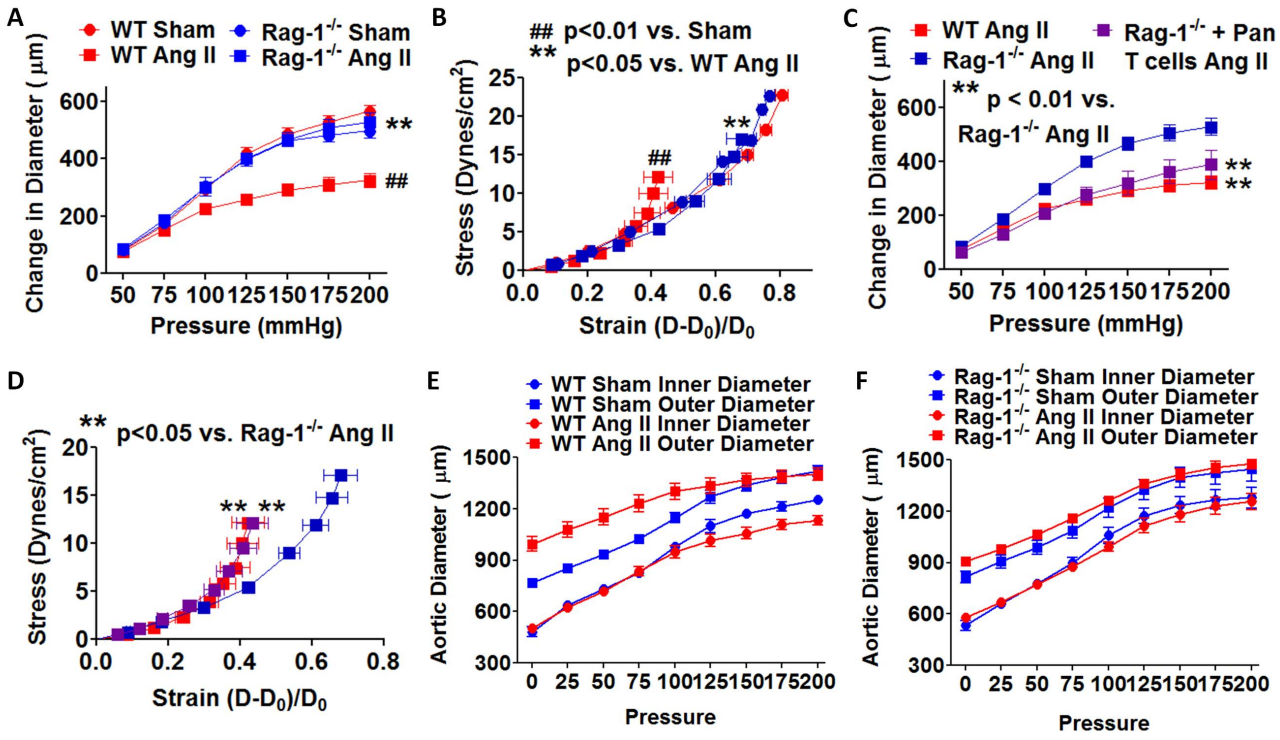

Figure 4 T cells mediate angiotensin II-induced aortic stiffening. Freshly-isolated aortas were mounted on a myograph system in Ca^{2+}-free buffer to determine pressure-diameter relationships. A-D) Compliance curves and stress-strain relationships were constructed from inner diameter and outer diameter. E and F) Inner and outer diameter of WT and RAG-$1^{-/-}$ mice measured at 25 mmHg step changes in pressure from 0-200 mmHg. Data were analyzed using one-way ANOVA with repeated measures (n=6-9).

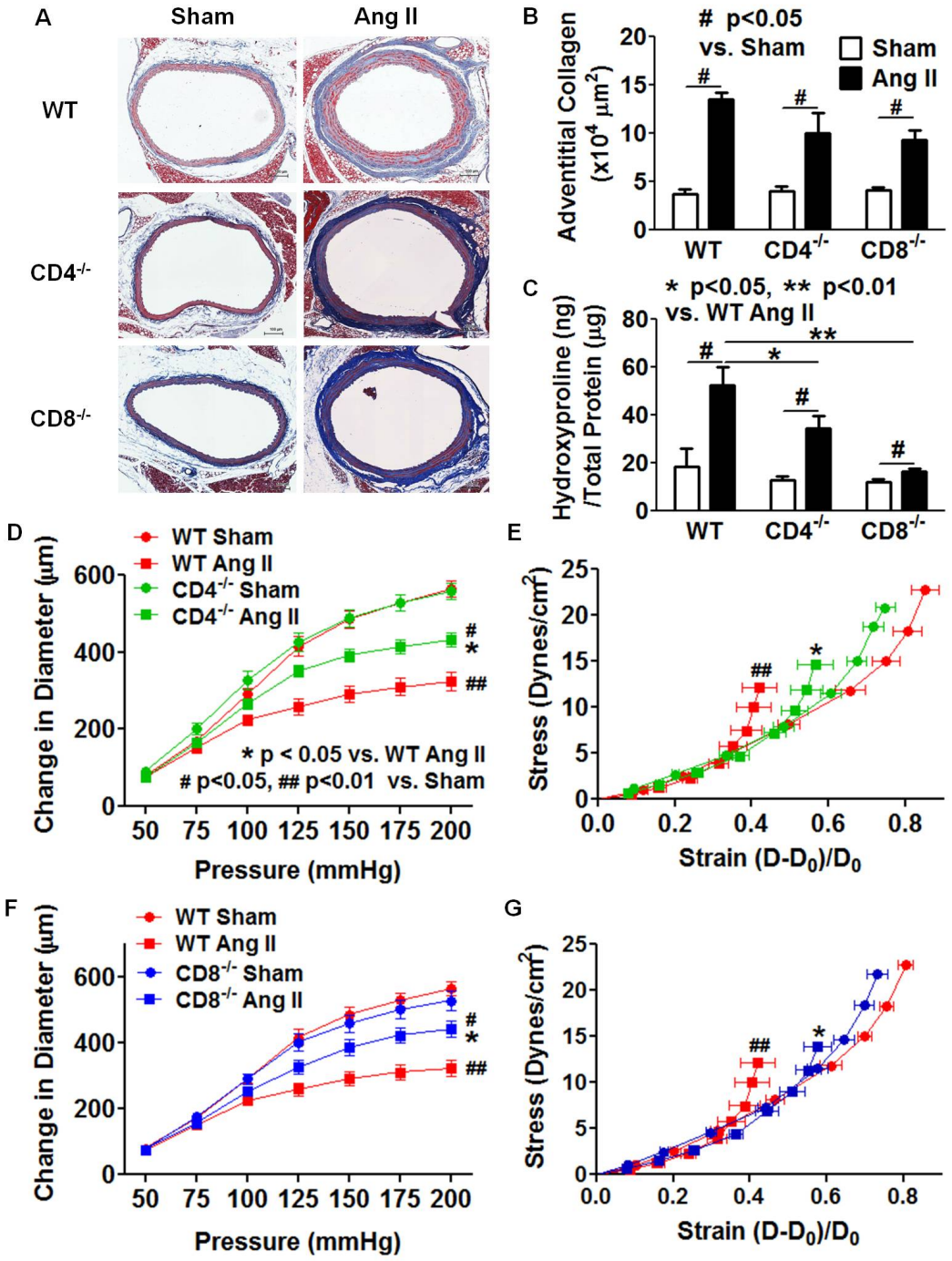

Figure 5 Role of CD4$^+$ and CD8$^+$ T cells in aortic stiffening.CD4+ deficient and CD8+ deficient mice were infused with chronic angiotensin II (490 ng/kg/min) for 14 days. A) Masson's trichrome staining. Scale bar indicates 100 μm. B) Adventitial collagen area determined by planimetry and C) hydroxyproline quantifcation. Data analyzed using two-way ANOVA. D and E) Compliance curves and stress-strain relationship for CD4$^{-/-}$ mice. F and G) Compliance curves and stress-strain curves for CD8$^{-/-}$ mice. Data were analyzed using one-way ANOVA with repeated measures (n=6-8).

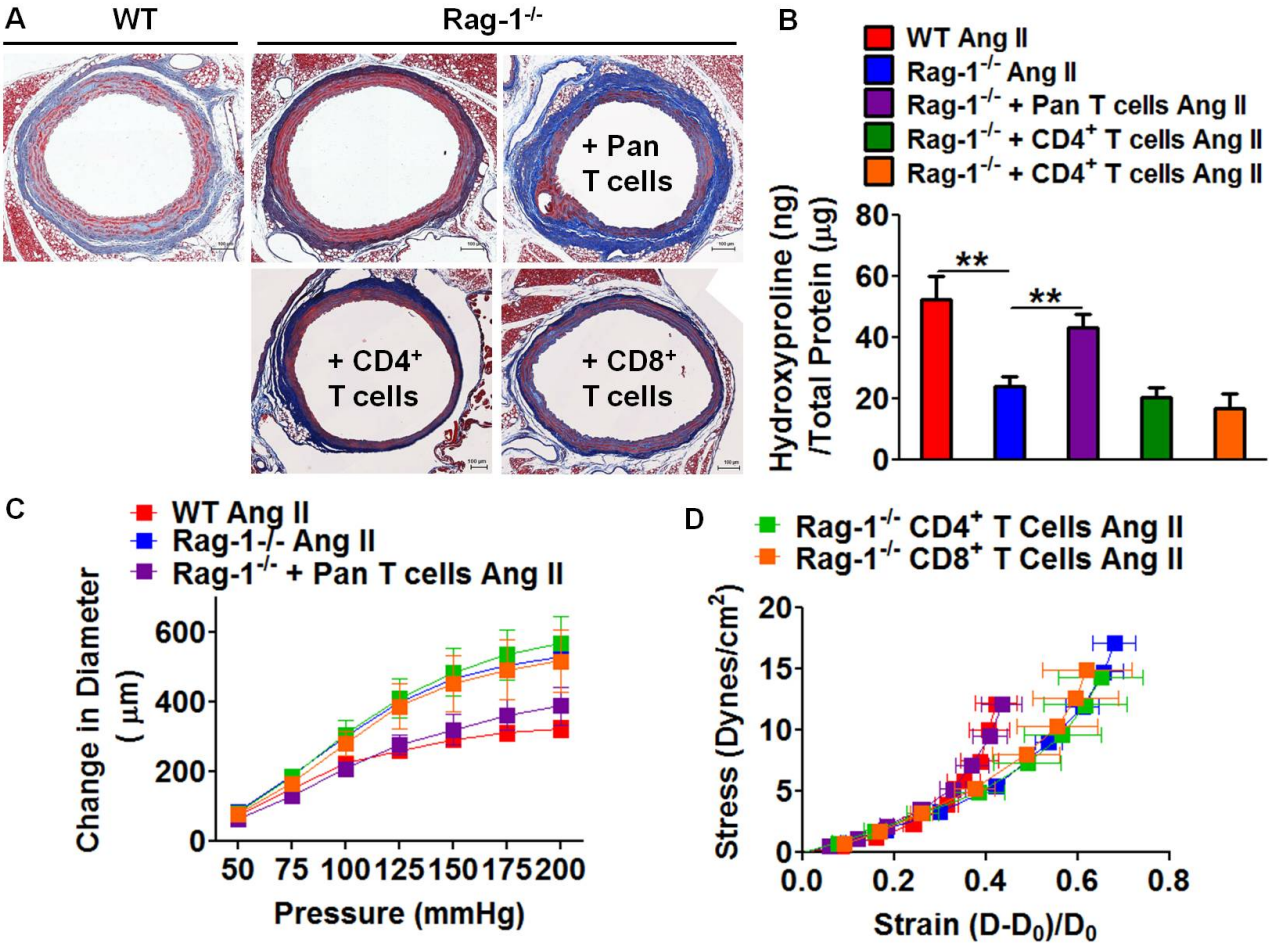

Figure 6 The effect of T cell subsets in angiotensin II-induced collagen deposition and aortic stiffening. Pan T cells, $CD4^+$ T cells and $CD8^+$ T cells were isolated from age-matched C57Bl/6 mice and transfered into Rag-$1^{-/-}$ mice via tail vein injection. Angiotensin II was administered three weeks after adoptive transfer of T cells. The effect of T cell sub-populations on collagen depostion (A and B) and aortic stiffening (C and D) are shown. Scale bar indicates 100 µm. Data for aortic stiffness were analyzed using one-way ANOVA with repeated measurements (n=5-7). Collagen deposition was analyzed using one-way ANOVA (n=5-7). Ang II, angiotensin II.

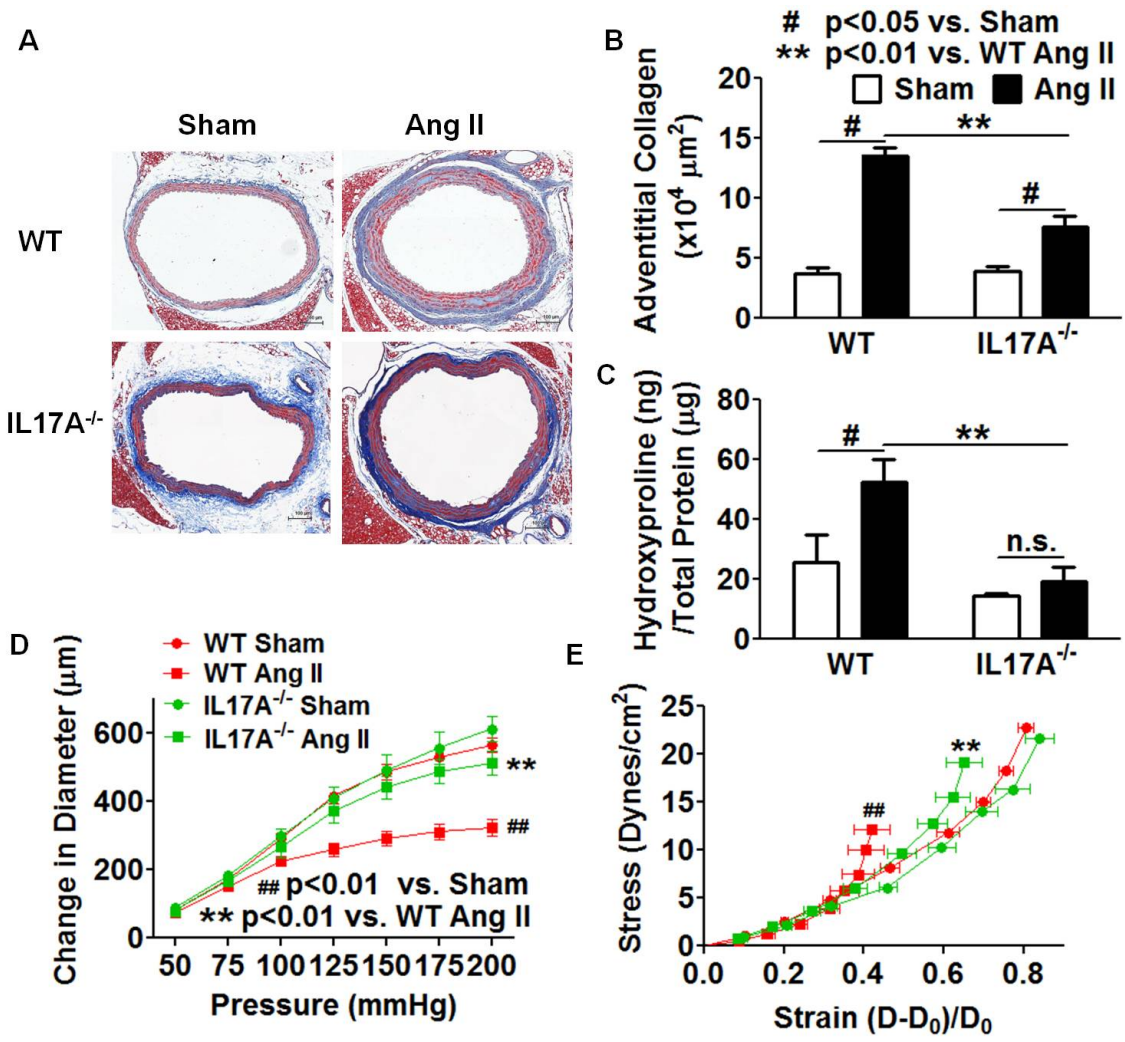

Figure 7 Role of IL-17a in aortic stiffening. IL-17a deficient mice were infused with chronic angiotensin II (490ng/kg/min) for 14 days. A and B)The thoracic aortas were fix-perfused for Masson's trichrome staining and quantified for adventitia collagen staining. Scale bar indicates 100 μm. C) Segments of the thoracic aorta were digested in 6N HCl at 105 ˚C for 48 hours and measured for hydroxyproline concentration. Data analyzed using two-way ANOVA. D and E) Compliance curves and stress-strain curves for IL-17a$^{-/-}$ mice. Data analyzed using one-way ANOVA with repeated measures(n=6-8).

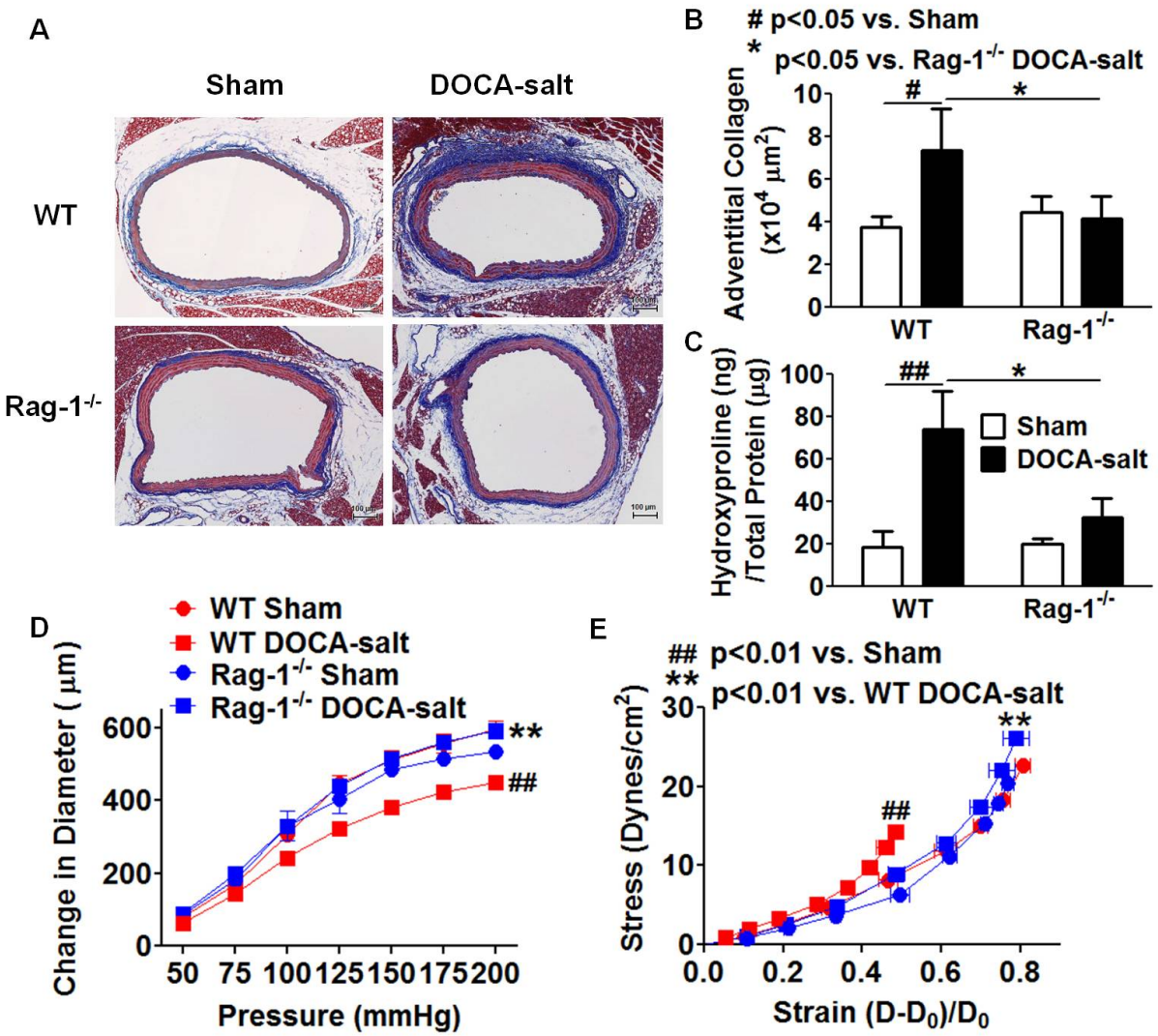

Figure 8 The effect of lymphocytes in DOCA-salt-induced aortic stiffening and collagen deposition. Mice were subjected to sham or deoxycorticosterone acetate (DOCA)-salt procedure for 3 weeks. In DOCA-salt mice, 100 mg deoxycorticosterone acetate pellet were implanted subcutaneously following uninephrectomy. These mice were maintained on drinking water with 0.9% NaCl throughout the experiment. A-C)The effect of lymphocytes on adventitial collagen depostion. D-E)The effect of lymphocytes on DOCA-salt-induced aortic stiffening. Scale bar indicates 100 μm. Ang II, angiotensin II. Data for aortic stiffness were analyzed using one-way ANOVA with repeated measurements (n=5-7). Collagen deposition was analyzed using one-way ANOVA (n=5-7).

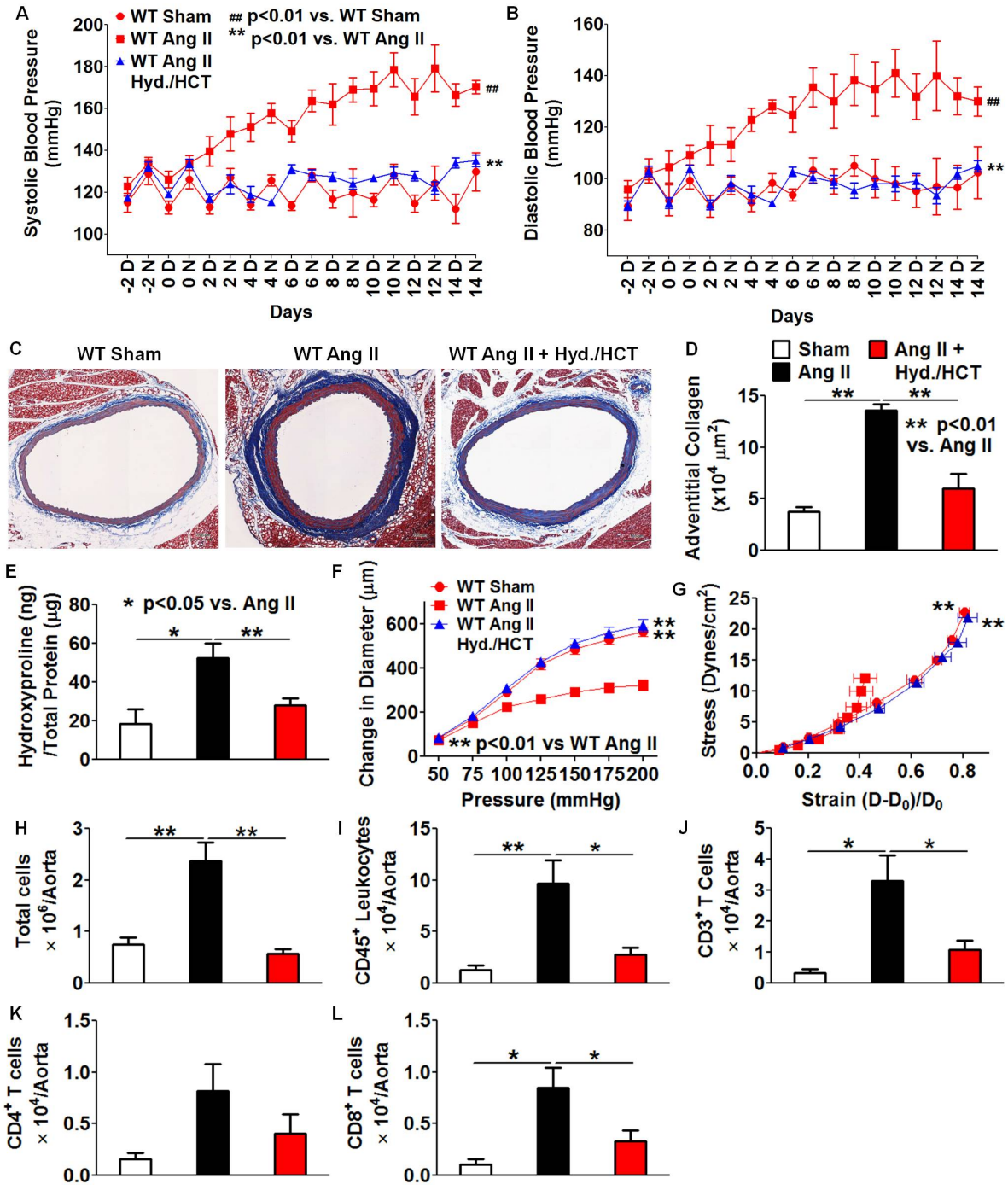

Figure 9 Antihypertensive treatment (antiHBP) prevents collagen deposition, aortic stiffening and T cell infiltration. Mice were treated with hydralazine and hydrochlorothiazide (320 mg/L and 60 mg/L in the drinking water) concurrently with angiotensin II infusion. Hyd., Hydralazine, HCT, hydrochlorothiazide. A and B) Telemetry recording of blood pressures. D, day; N, night. The effects of blood pressure normalization on collagen depostion (C-E), aortic stiffening (F and G) and aortic inflammatory cell infiltration (H-L) are shown. Scale bar indicates 100 µm. Data for blood pressure and aortic stiffness were analyzed using one-way ANOVA with repeated measurements (n=8). Collagen deposition and flow cytometry were analyzed using one-way ANOVA (n=8).

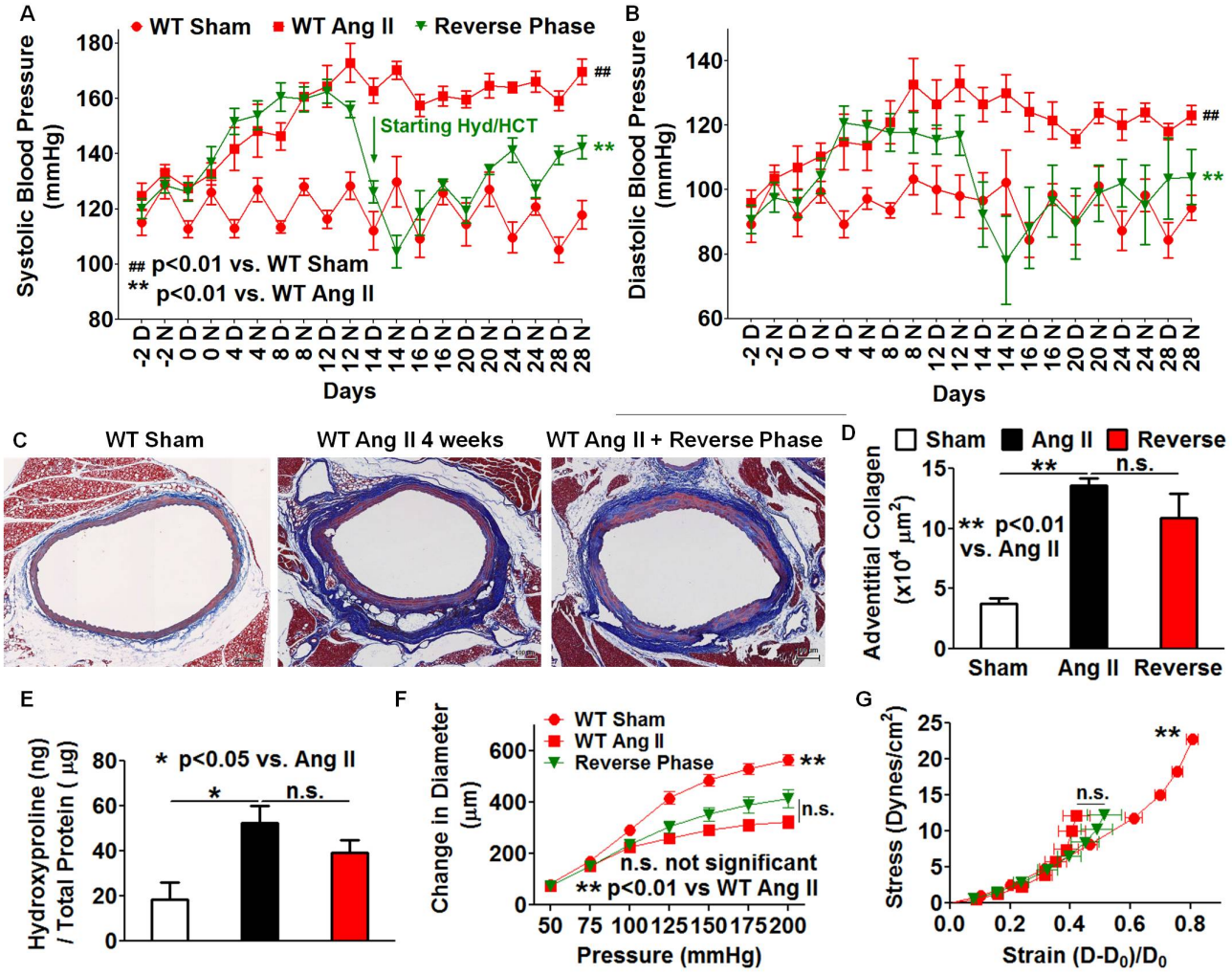

Figure 10 Normalization of blood pressure in established hypertension and aortic stiffening: the effects on collagen deposition and aortic stiffening. Mice were treated with sham or angiotensin II via osmotic minipump for 4 weeks (490 ng/kg/min). Reverse phase, blood pressure was normalized in the last two weeks of the 4 week angiotensin II infusion by hydralazine and hydrochlorothiazide given in drinking water (320 mg/L and 60 mg/L). A and B) Telemetry recording of blood pressures. The effects of blood pressure normalization on collagen depostion (C-E) and aortic stiffening (F and G) are shown. Scale bar indicates 100 μm. Ang II, angiotensin II. Data for blood pressure and aortic stiffness were analyzed using one-way ANOVA with repeated measurements (n=5-8). Collagen deposition was analyzed using one-way ANOVA (n=5-8).

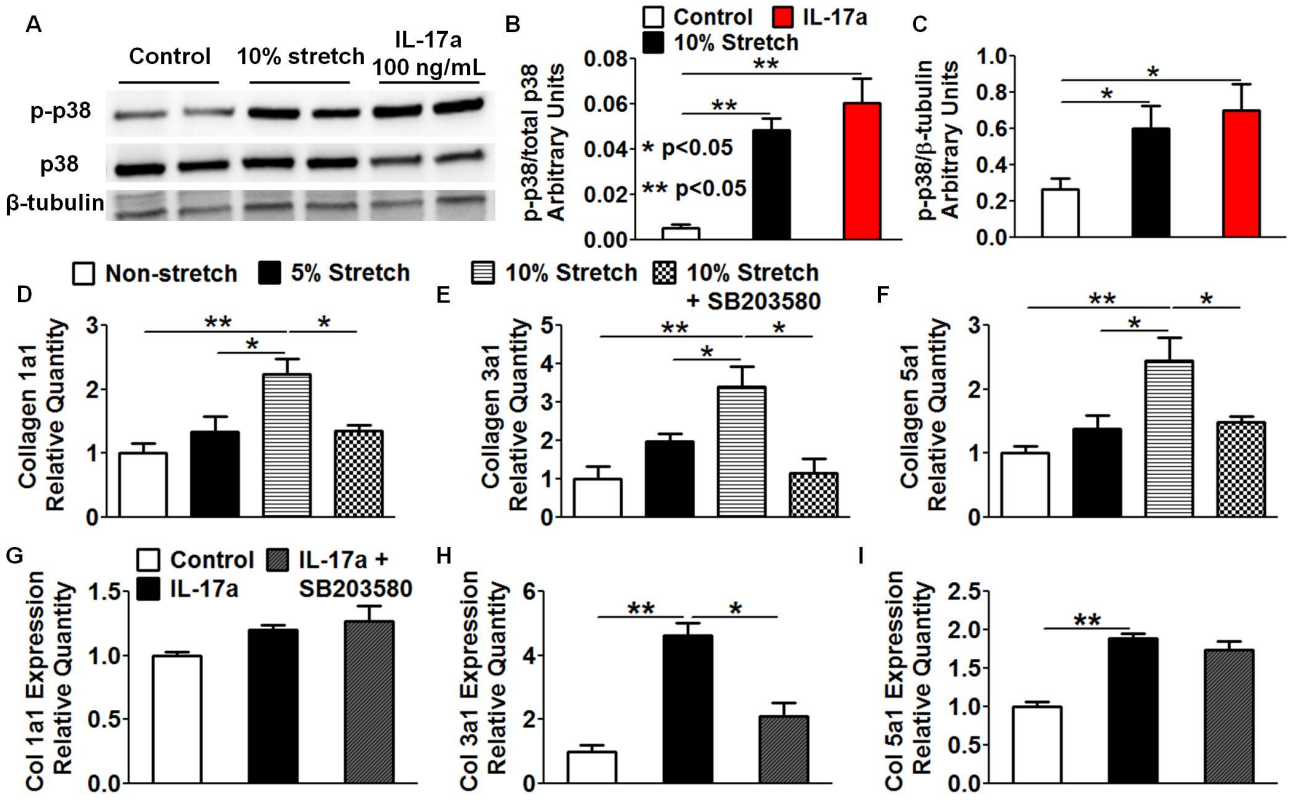

Figure 11 Effect of cyclical stretch and IL-17a on aortic fibroblasts and role of p38 MAP kinase. Mouse aortic fibrobasts were exposed to various degrees of cyclical stretch or the T cell cytokine IL-17a (100 ng/mL) in culture for 36 hours. A-C) Both hypertensive mechanical stretch and IL-17a activated p38 MAPK in cultured mouse aortic fibroblasts. D-F) The effects of p38 inhibitor SB203580 (10 ng/mL) on mechanical stretch-induced expression of collagen subtypes in fibroblasts. G-I) The effects of p38 inhibition on IL-17a-induced collagen expression. Data analyzed using one-way ANOVA(n=3-6).

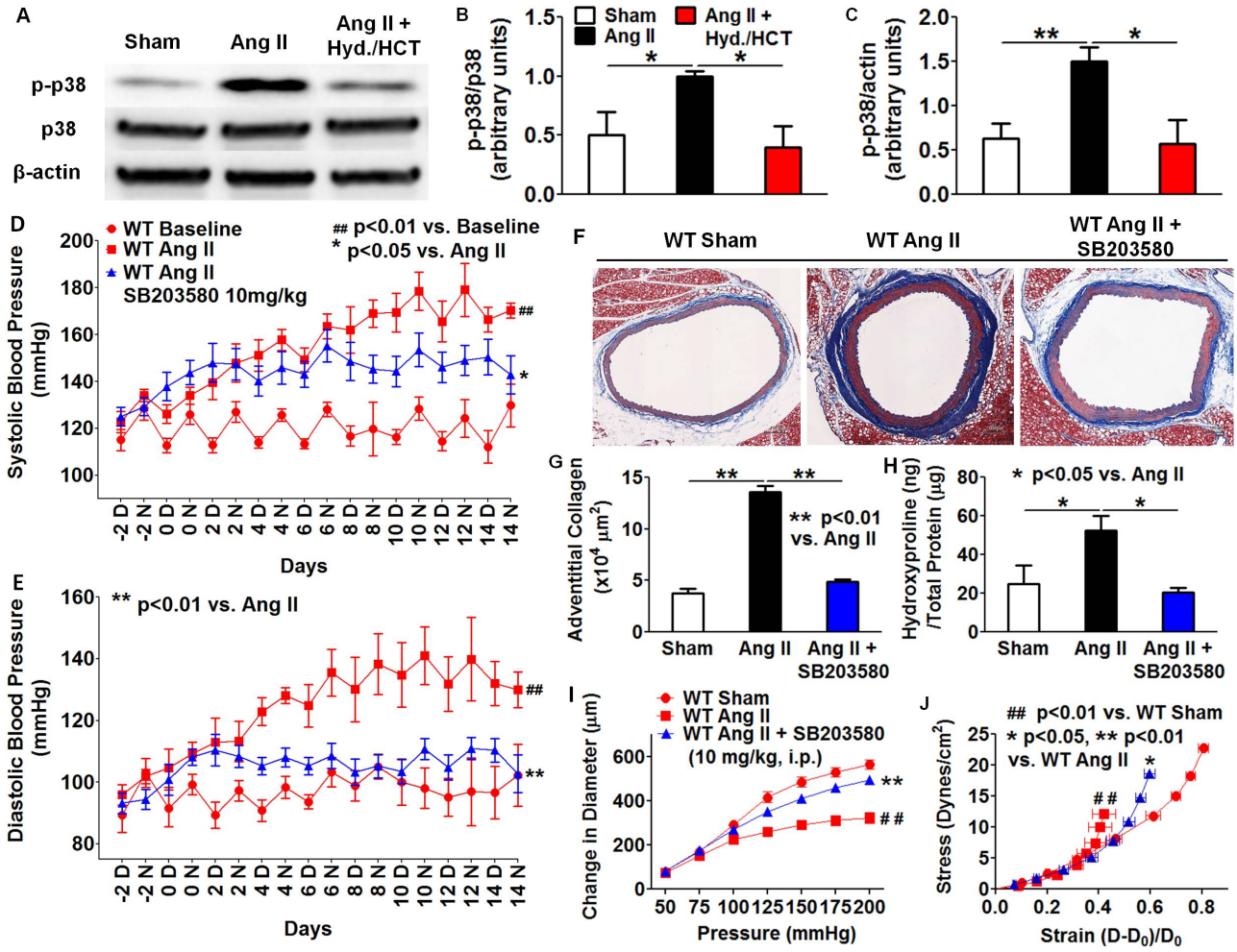

Figure 12 P38 MAP kinase mediates collagen deposition and aortic stiffening in angiotensin II-induced hypertension. A-C) Normalization of blood pressure prevented the activation of p38 MAP kinase in angiotensin II-infused mouse aortas. Data analyzed with one-way ANOVA (n=4-6). D and E) Effect of SB203580 on blood pressure. D, day; N, night. F-H) Effect of SB203580 on aortic collagen deposition. Data analyzed using one-way ANOVA (n=6-8). Mice received intraperitoneal injections of SB203580 (10 mg/kg/day) during angiotensin II infusion. Scale bar indicates 100 μm. I and J) Effect of SB203580 on aortic stiffening. Blood pressure and aortic stiffness were analyzed using one-way ANOVA with repeated measures (n=6-8).

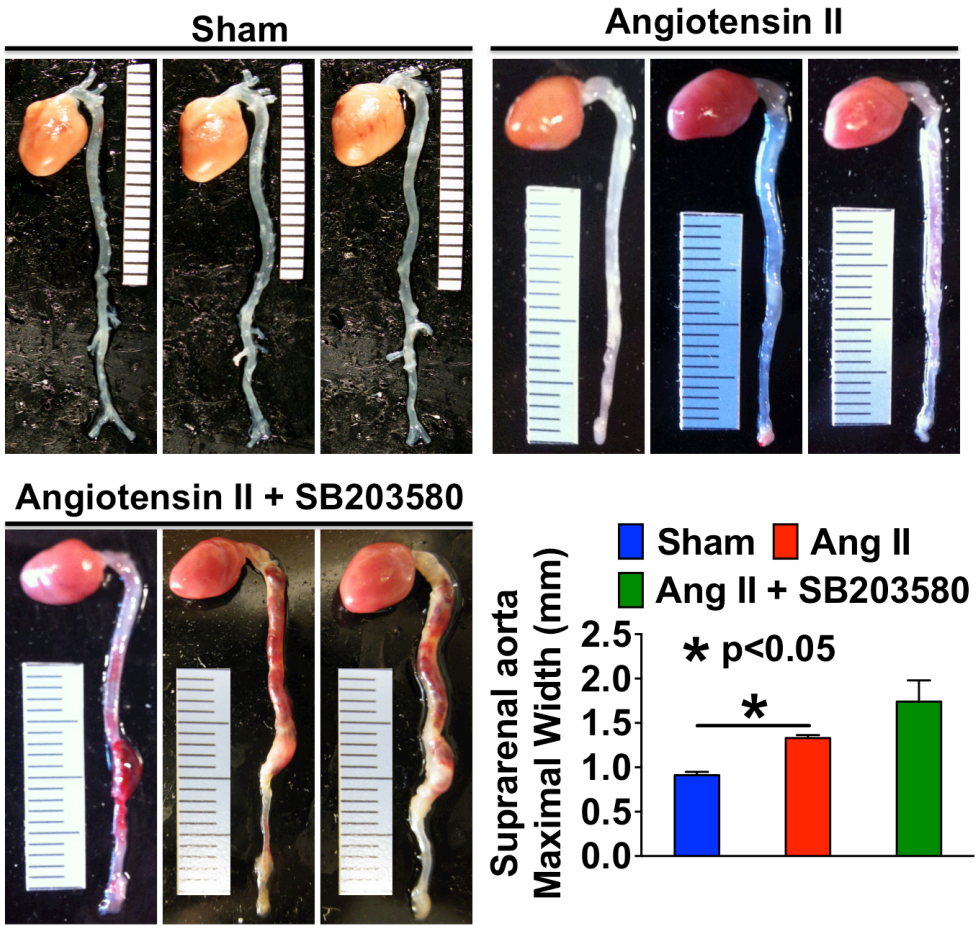

Figure 13 Inhibition of p38 MAP kinase induced aneurysm formation in angitoensin II-infused mice. Mice received intraperitoneal injection of SB203580 (10 mg/kg/day) during angiotension II infusion. Maximal suprarenal aorta width was measured ex vivo. One-way ANOVA was performed for mean data (n=5).

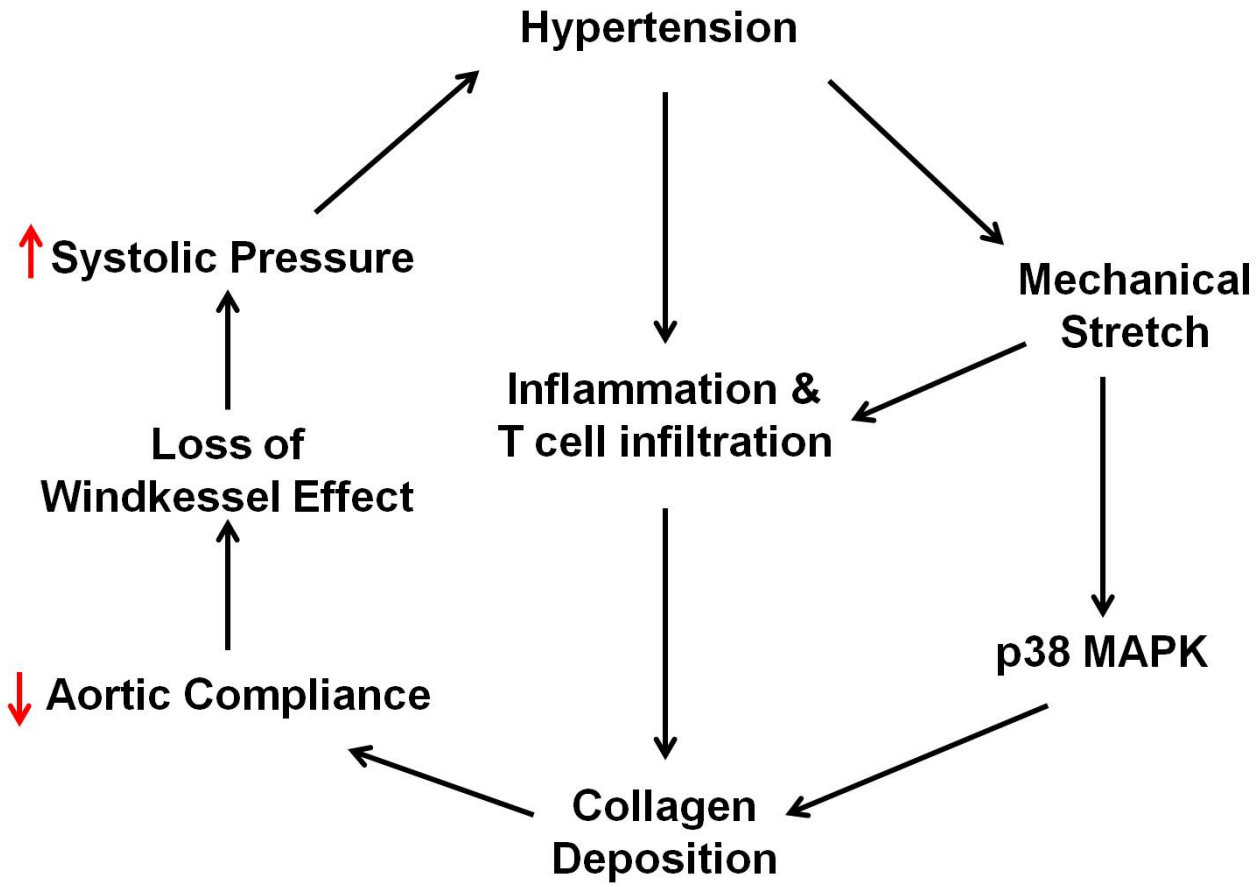

Figure 14 Pathway showing interactions of mechanical stretch and inflammation in aortic stiffening. Increased mechanical stretch promotes perivascular T cell infiltration and activates p38 MAP kinase, leading to adventitial collagen deposition. This reduces aortic compliance and ultimately leads to loss of windkessel effect in large capacitance arteries such as the aorta. Aortic stiffening increases systolic pressure and promotes hypertension by positive feedback.

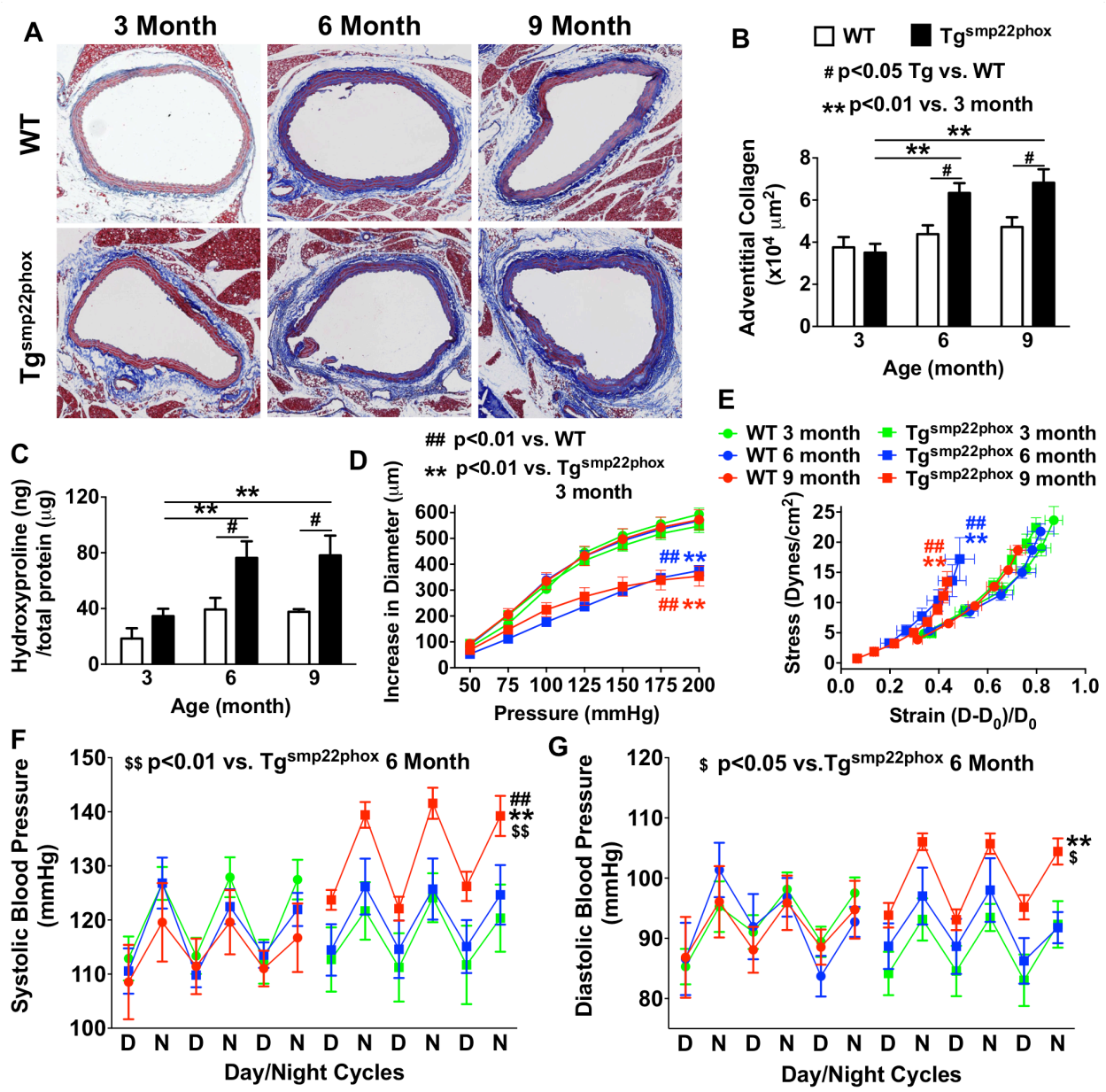

Figure 15 Tg^{smp22phox} mice develop age-related aortic stiffening and hypertension. A) Effects of aging on vascular collagen deposition in WT and Tg^{smp22phox} mice. Perfusion-fixed sections of the thoracic aortas were sectioned (6 μm) and stained with Masson's trichome to highlight collagen (blue). Scale bar indicates 100 μm. B) Adventitial collagen area was quantified by planimetry. C) Aortic collagen quantification by hydroxyproline assay. D and E)Freshly-isolated aortas were mounted on a myograph system in Ca^{2+}-free buffer to determine pressure-diameter relationships. Stress-strain relationships were constructed from inner diameter and outer diameter. Inner and outer diameter of WT and Tg^{smp22phox} mice measured at 25 mmHg step changes in pressure from 0-200 mmHg. F and G) Telemetry blood pressure of WT and tg^{smp22phox} mice at 3, 6 and 9 month of age. Data were analyzed using two-way ANOVA(n=6-9).

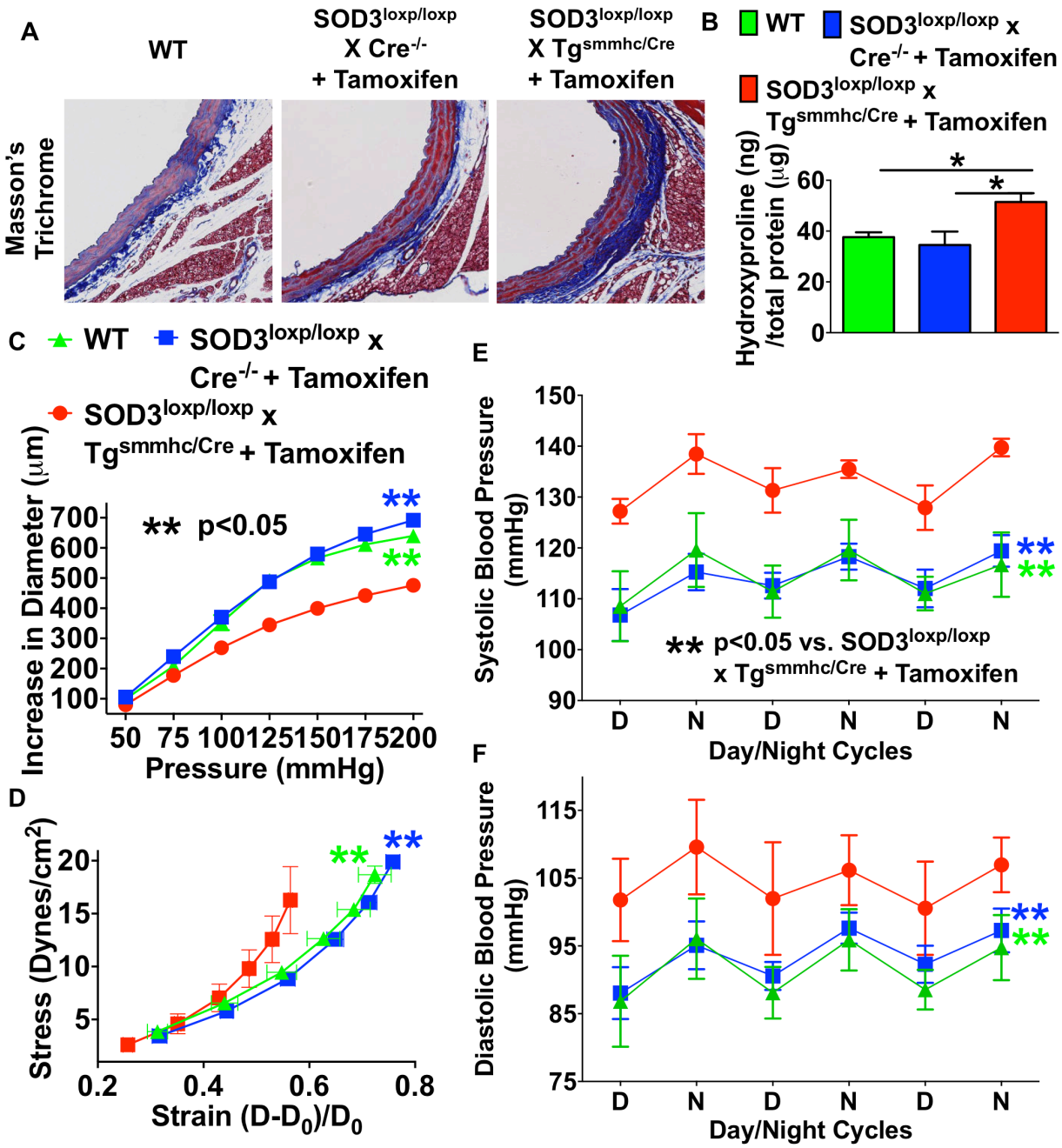

Figure 16 Vascular oxidative stress induced by deletion of smooth muscle SOD3 also promotes aortic stiffening and hypertension. A) Masson's trichrome blue staining and isoketal staining in 9 month-old WT, SOD3$^{loxp/loxp}$ x Cre-/- and SOD3$^{loxp/loxp}$ x Tg$^{smmhc/Cre}$ mice. Tamoxifen were administered at 3 mg/20 kg in corn oil via intraperitoneal injection at 3 month of age. B) Hydroxyproline assay. C-D) Pressure diameter relationship and stress-strain relationship. E-F) Blood pressure measured by radio telemetry (n=6).

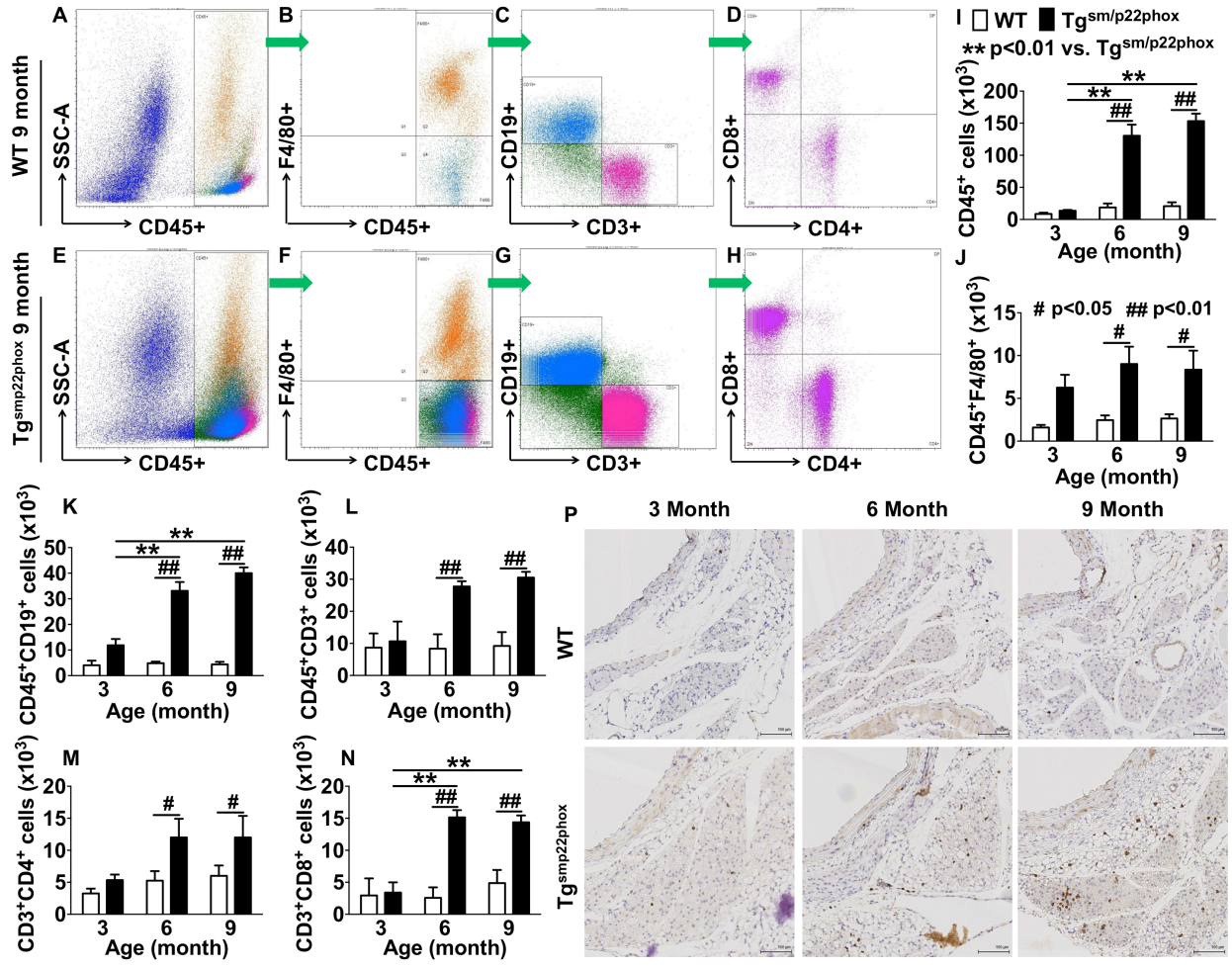

Figure 17 Flow cytometry analysis of inflammatory cells in the aorta of WT and Tg^{smp22phox} mice. Single cell suspension was prepared with freshly isolated mouse aortas via enzymatic digestion and mechanical dissociation. Only live cells and singlets were analyzed for vascular inflammatory cells. CD45+ Total leukocytes, F4/80+ macrophages, CD19+ B lymphocytes, CD3+ T lymphocytes and CD4+/CD8+T cell subsets were identified in the aorta of 9 month-old WT (A-D) and Tg^{smp22phox} mice (E-H). I-N) Quantification of infiltating leukocyte subsets usintwo-way ANOVA (n=6-8). P)Thoracic aortas were fixed with 4% formalin, sliced into 6 µm sections and stained for CD3 to highlight T lymphocytes (dark brown). Scale bar indicates 100 µm.

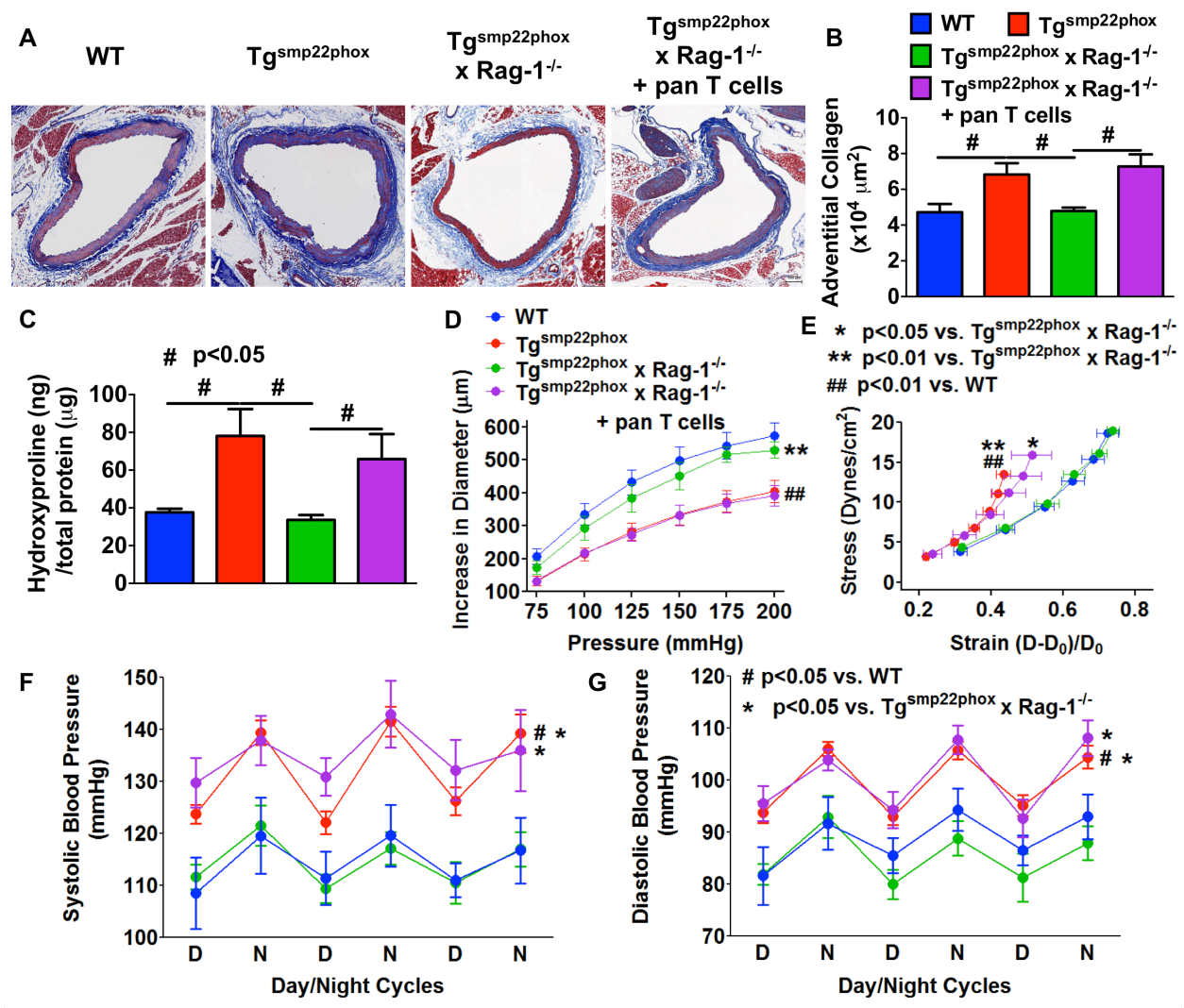

Figure 18 T cells mediate age-related aortic collagen deposition, aortic stiffening and elevation of blood pressure in Tg^{smp22phox} mice. A-C) The effects of T lymphocyte deficiency and restoration on vascular oxidative stress-induced collagen deposition. Pan T cells were isolated from the spleen of 3 month-old WT mice and adoptively transferred to age-matched Tg^{smp22phox} x Rag-1$^{-/-}$ mice to re-constitute T cell population. Mice were kept till 9 month of age after adoptive transfer procedure. D and E) Role of T cells in the development of age-related aortic stiffening in Tg^{smp22phox} mice. F and G) T cells are required for the elevation of blood pressure in aged Tg^{smp22phox} mice. Collagen deposition was quantified using one-way ANOVA. Aortic stiffness and blood pressure were analyzed with one-way ANOVA with repeated measurements (n=6-8).

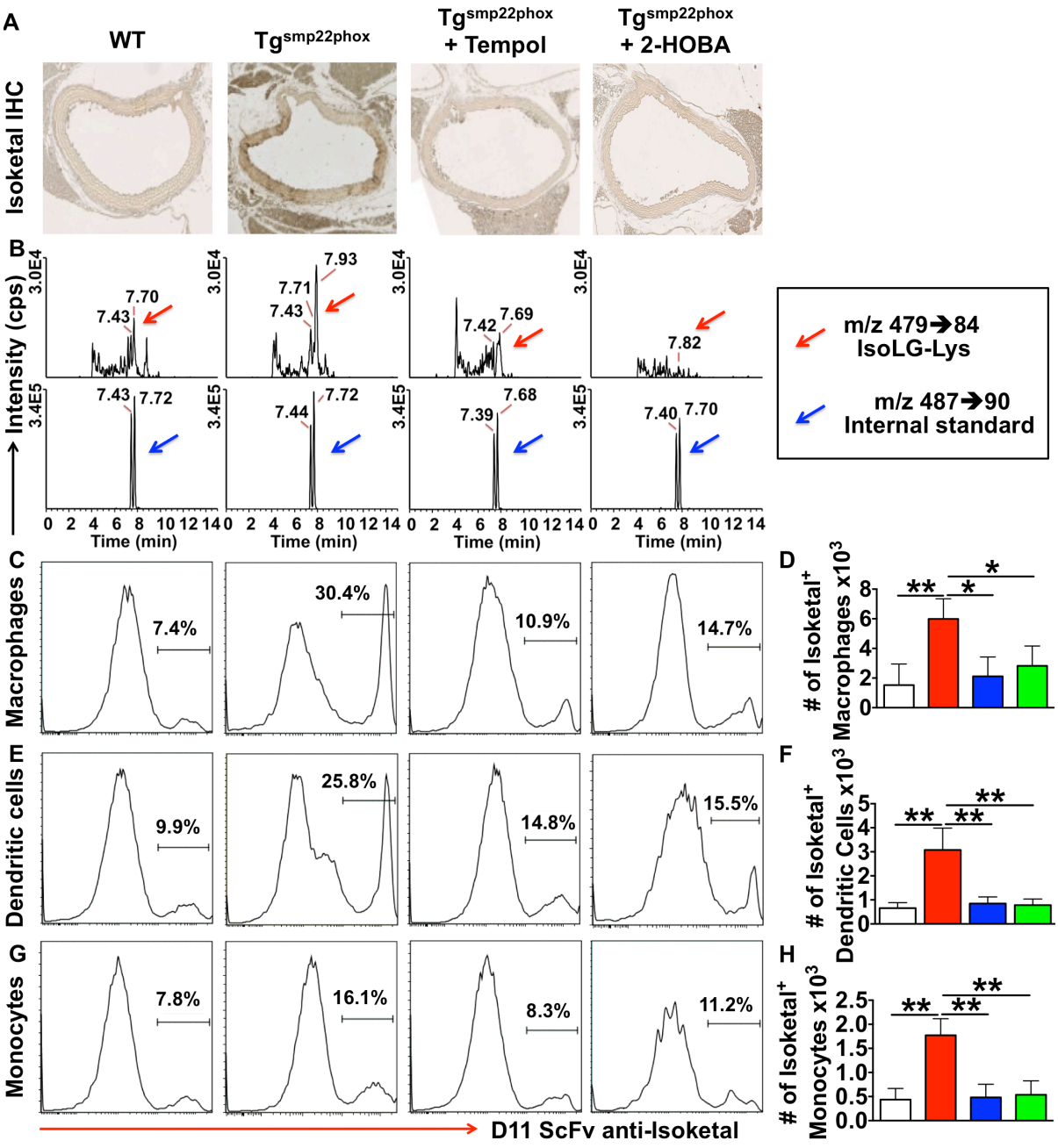

Figure 19 Tempol and 2-HOBA prevents the accumulation of isoketals in the aorta and antigen presenting cells in Tg^{smp22phox} mice. A) Fix-perfused mouse aortas were embedded in paraffin and subjected immunihistochemistry for isoketal staining. B) Stable isotope dilution multiple reactions monitoring mass spectrometry analysis of isoketal-lysine-lactam adduct in aortas. Representative LC/MS chromatographs from pooled samples for each group are shown. The top row shows multiple reactions monitoring m/z 479➔84 chromatographs for isoketal-lysine-lactam (IsoK-Lys) in sample, while the bottom row shows multiple reactions monitoring m/z 487➔90chromatograph for [$^{13}C_6{}^{15}N_2$] internal standard for same samples. These are performed by William Zackert in Dr. L. Jackson Roberts' laboratory and Dr. Sean S. Davies in the Department of Pharmacology. C-H) Intracellular staining for isoketals in spleen macrophages (C and D), dendritic cells (E and F) and monocytes (G and H) are shown. These data are analyzed using one-way ANOVA (n=6).

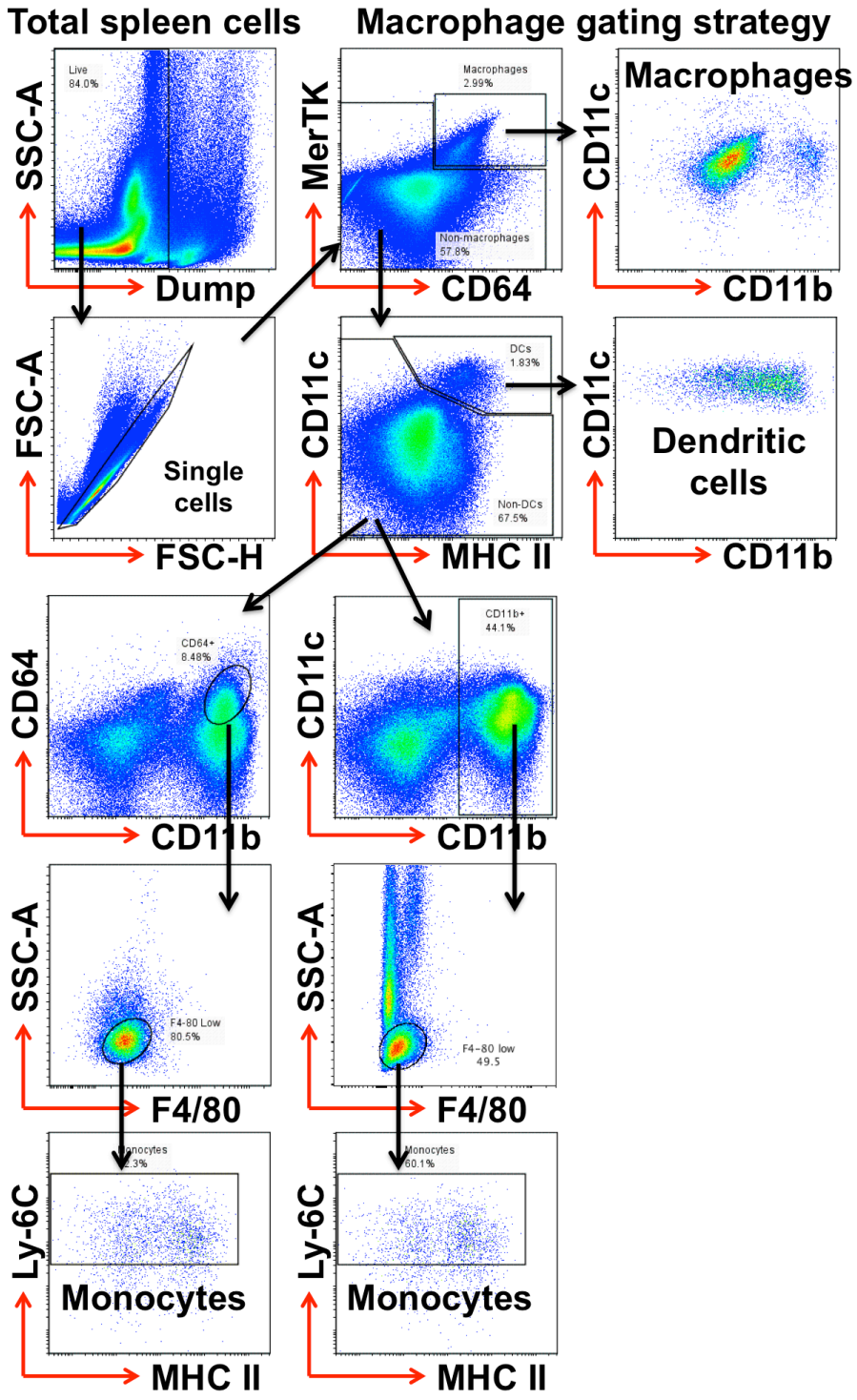

Figure 20 Gating strategy for macrophages, dendritic cells and monocytes in the spleen. Single cells suspension was prepared by mechanical dissociation and enzymatic digestion of mouse spleens. Dump chanel was set up to exclude dead cells, CD3+ T cells and CD19+ B cells.

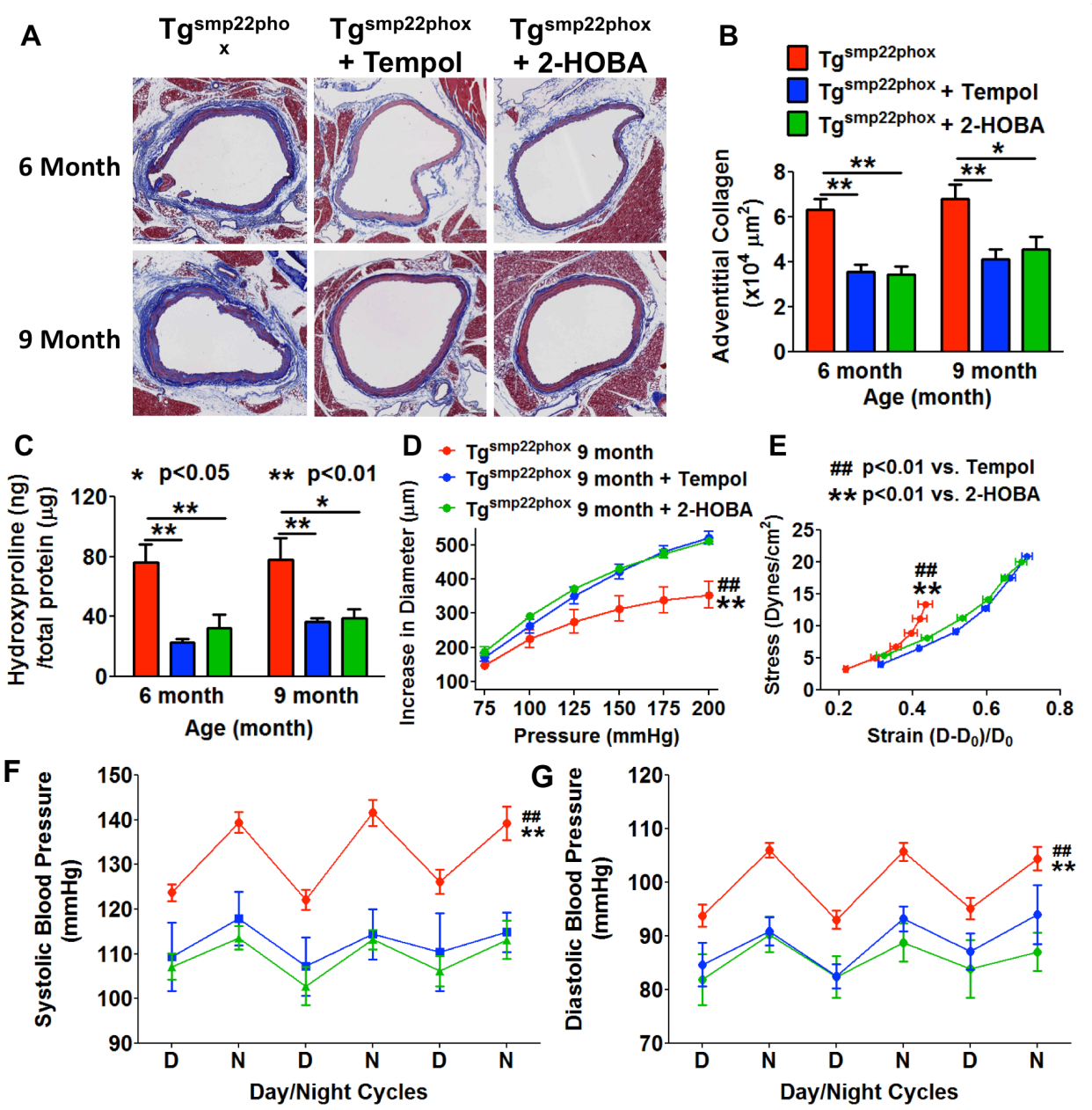

Figure 21 Antioxidant treatment prevents age-related aortic collagen deposition, aortic stiffening and elevation of blood pressure in Tg^{smp22phox} mice. A-C)Scavenging superoxide and isoketals prevents vascular oxidative stress-induced collagen deposition over aging. Tempol and 2-hydroxybenzylamine (2-HOBA) were adminstered in drinking water from 3-9 month of age. D and E) Role of reactive oxygen species in the development of age-related aortic stiffening in Tg^{smp22phox} mice. F and G) Antioxidant treatment prevents the elevation of blood pressure in aged Tg^{smp22phox} mice. Collagen deposition was quantified using one-way ANOVA. Aortic stiffness and blood pressure were analyzed with one-way ANOVA with repeated measurements (n=6-8).

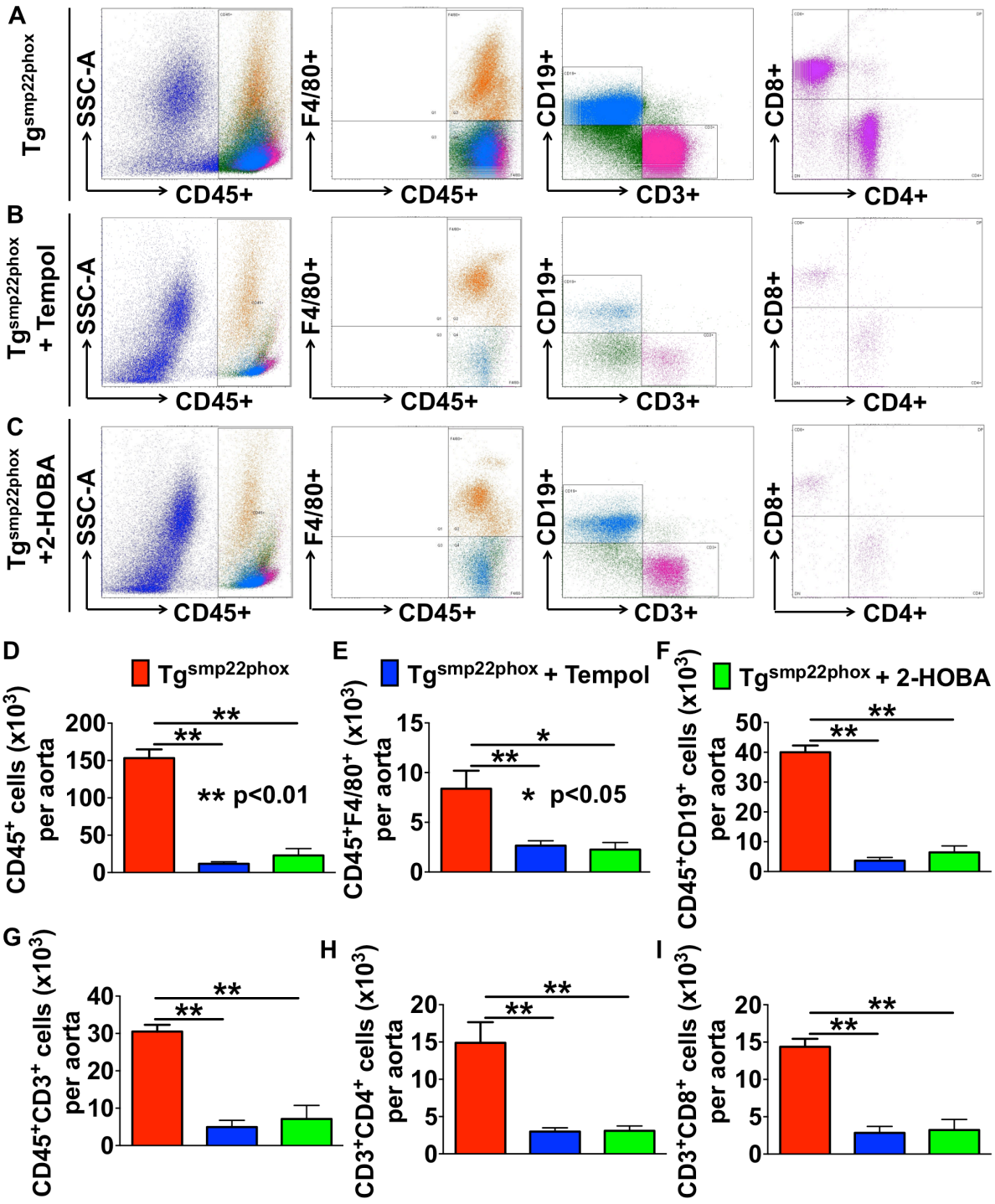

Figure 22 Antioxidant treatment prevents vascular inflammation in Tg^{smp22phox} mice. Tg^{smp22phox} mice were treated with tempol or 2-hydroxybenzylamine (2-HOBA) from 4 month of age until sacrifice at the end of 9 month. A-C)CD45+ total leukocytes, F4/80+ macrophages, CD19+ B lymphocytes, CD3+ T lymphocytes and CD4+/CD8+T cell subsets were identified in the aorta of these mice. D-I) Quantification of infiltating leukocyte subsets using one-way ANOVA (n=6-8).

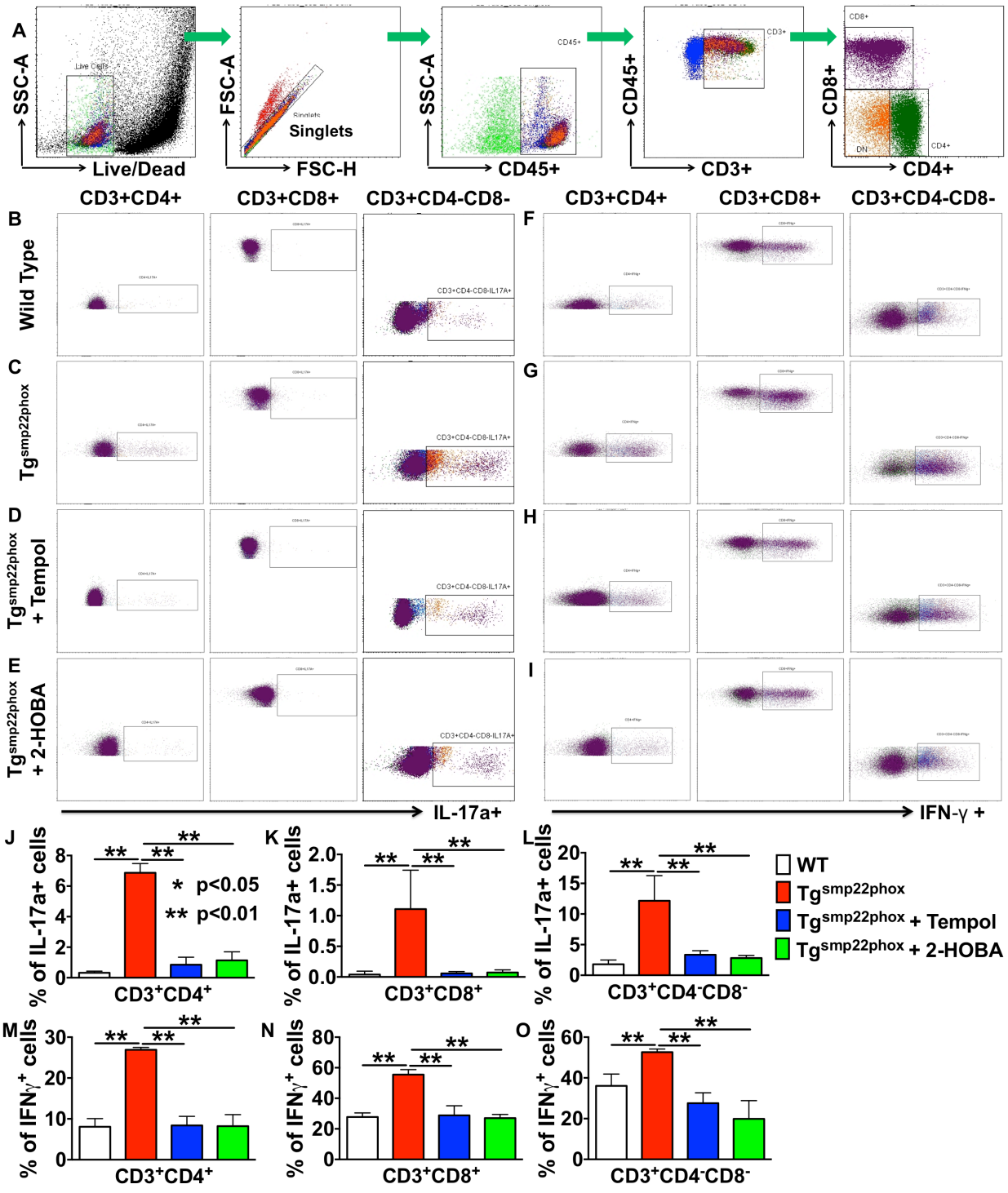

Figure 23 Cytokine production of T cells in the spleen of 9 month-old WT and Tg^{smp22phox} mice. A)Gating strategy for isolation of T cell population from total spleenocytes. Single cell suspension was prepared with freshly isolated mouse spleens via enzymatic digestion and mechanical dissociation. Intracellular staining indicating IL-17A (B-E) and IFN-γ (F-I) production in T cell subsets in WT and Tg^{smp22phox} mice. J-O) Quantification of IL-17A and IFN-γ in T cell sub-populations. Bar graphs analyzed using one-way ANOVA (n=5-7). My colleague Dr. Mohamed A. Saleh performed these experiments for me.

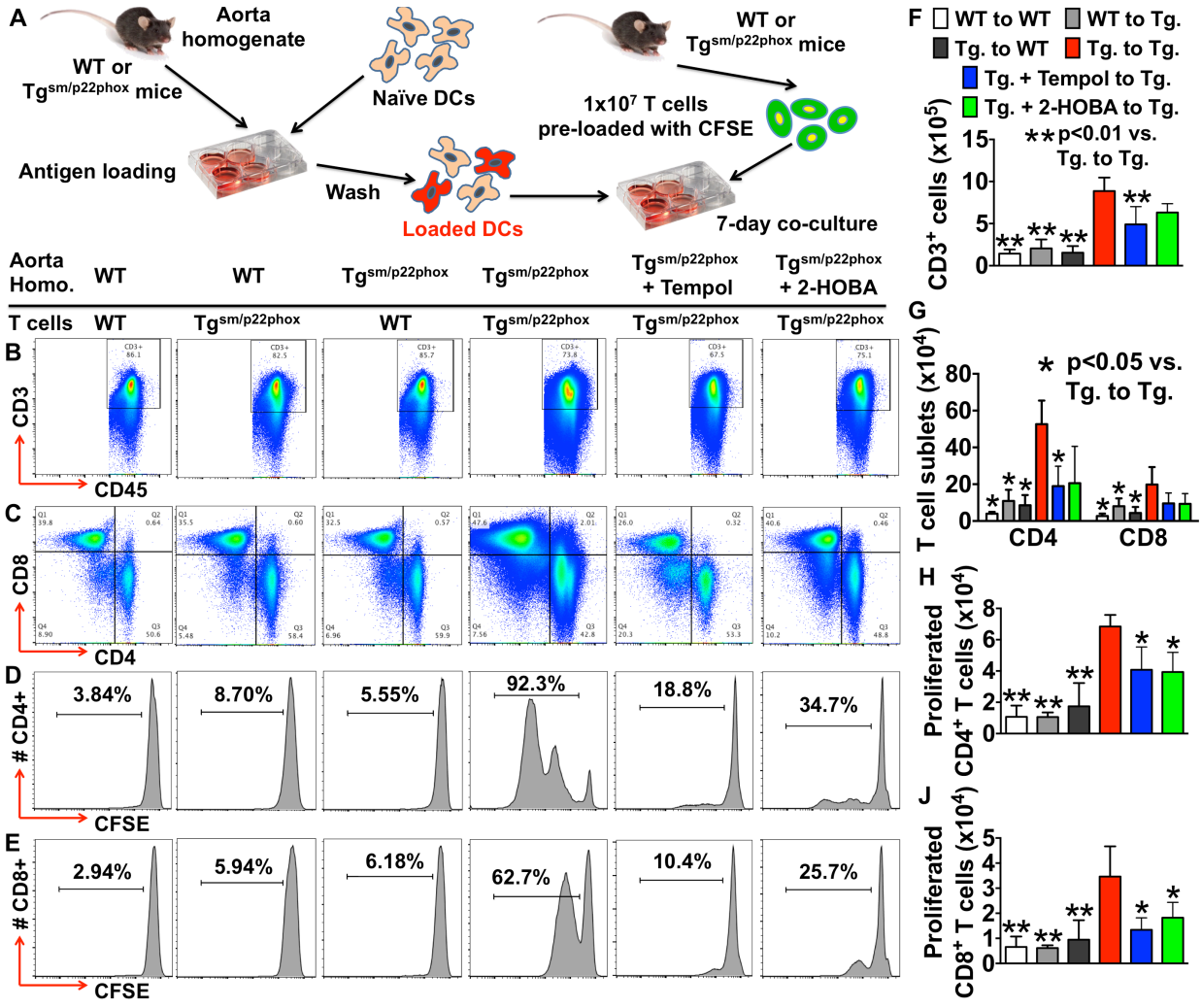

Figure 24 DCs exposed to isoketals promote T cells proliferation and cytokine production. A) Experimental design was depicted. B and C and F and G, Flow cytometry was used to determine the number of live CD3+ T cells and CD4+/CD8+ T cell subsets. D and E and H-J) Representative flow cytometry profiles and bar graph showing percentages and numbers of proliferated (D and H) CD4+ T cells and (E and J) CD8+ T cells, as reflected by CSFE dilution assays (n= 6, *P < 0.05, **P < 0.01, one-way ANOVA). Tg. stands for tg$^{sm/p22phox}$ mice. Homo. stands for homogenate.

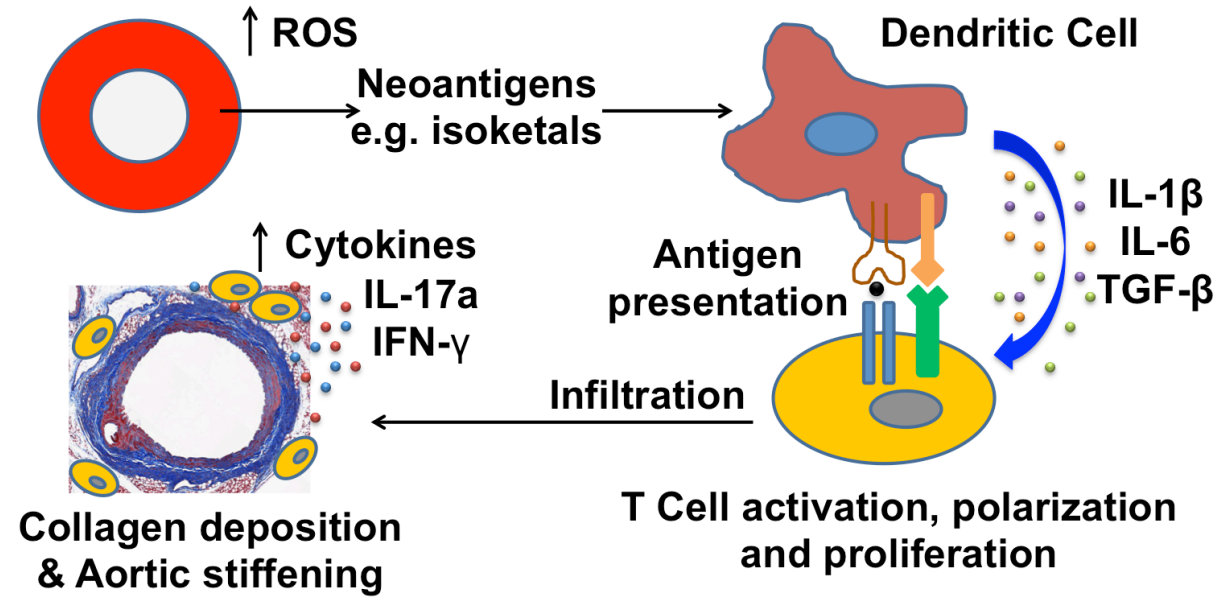

Figure 25 Proposed mechanisms for DC-T cell activation in aged related hypertension.

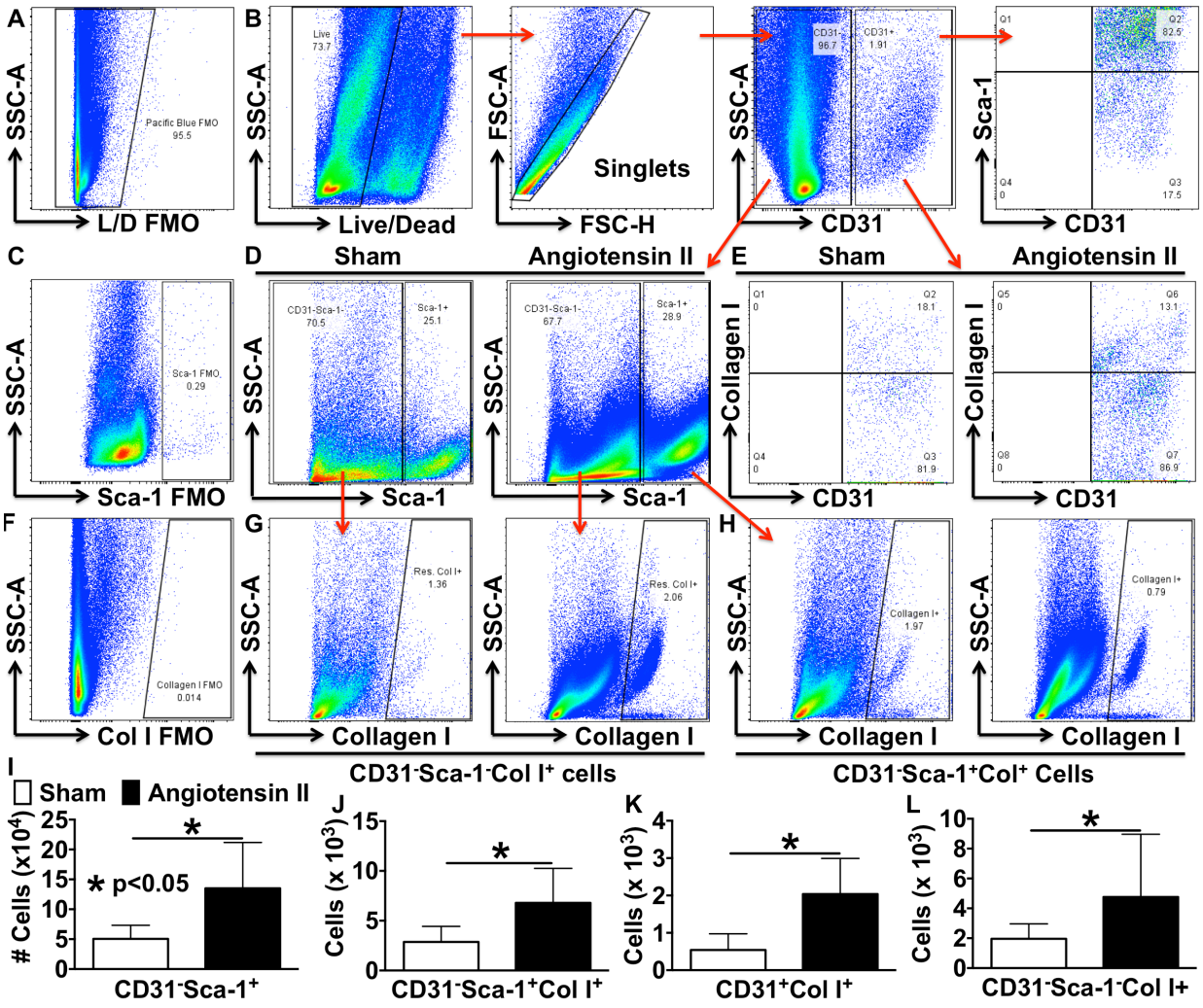

Figure 26 Hypertension increased the number of collagen I$^+$ cells in the aorta. Flow cytometry analysis of whole aortas of mice receiving 14-day angiotensin II or sham treatment. A and B) Gating strategy showing that live single cells were analyzed. C and D) Sca-1$^+$ cells identified in CD31$^-$ cells. E-H) Collagen I intracellular staining in CD31$^+$, CD31$^-$Sca-1$^+$ and CD31$^-$Sca-1$^-$ cells. I-L) Quantification of CD31$^-$Sca-1$^+$ cells and collagen I$^+$ cells. Student's t test was performed where significance is indicated (n=6-8).

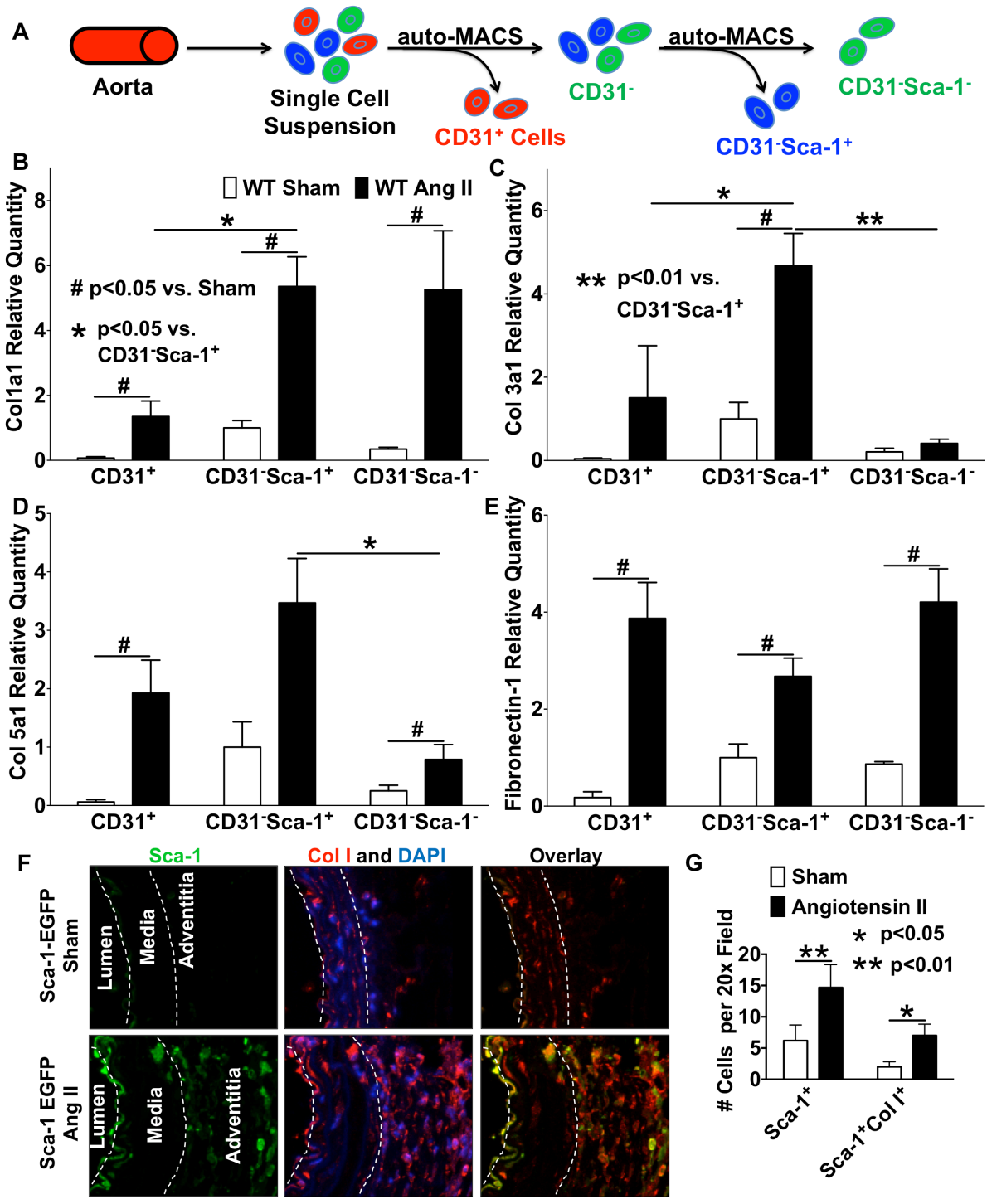

Figure 27 Aortic cells become fibroblast-like in hypertension. A) CD31$^+$, CD31$^-$Sca-1$^+$ and CD31$^-$ Sca-1$^-$ cells were isolated using magnet-activated cell sorting. B-E) Real-time PCR analysis of expression of collagen 1a1, 3a1, 5a1 and fibronectin-1 in cells fractions isolated from the aorta of sham and angiotensin II-treated mice (n=6). F and G) Immunofluorescence showing co-localization of Sca-1 and collagen I in the aorta adventitia.

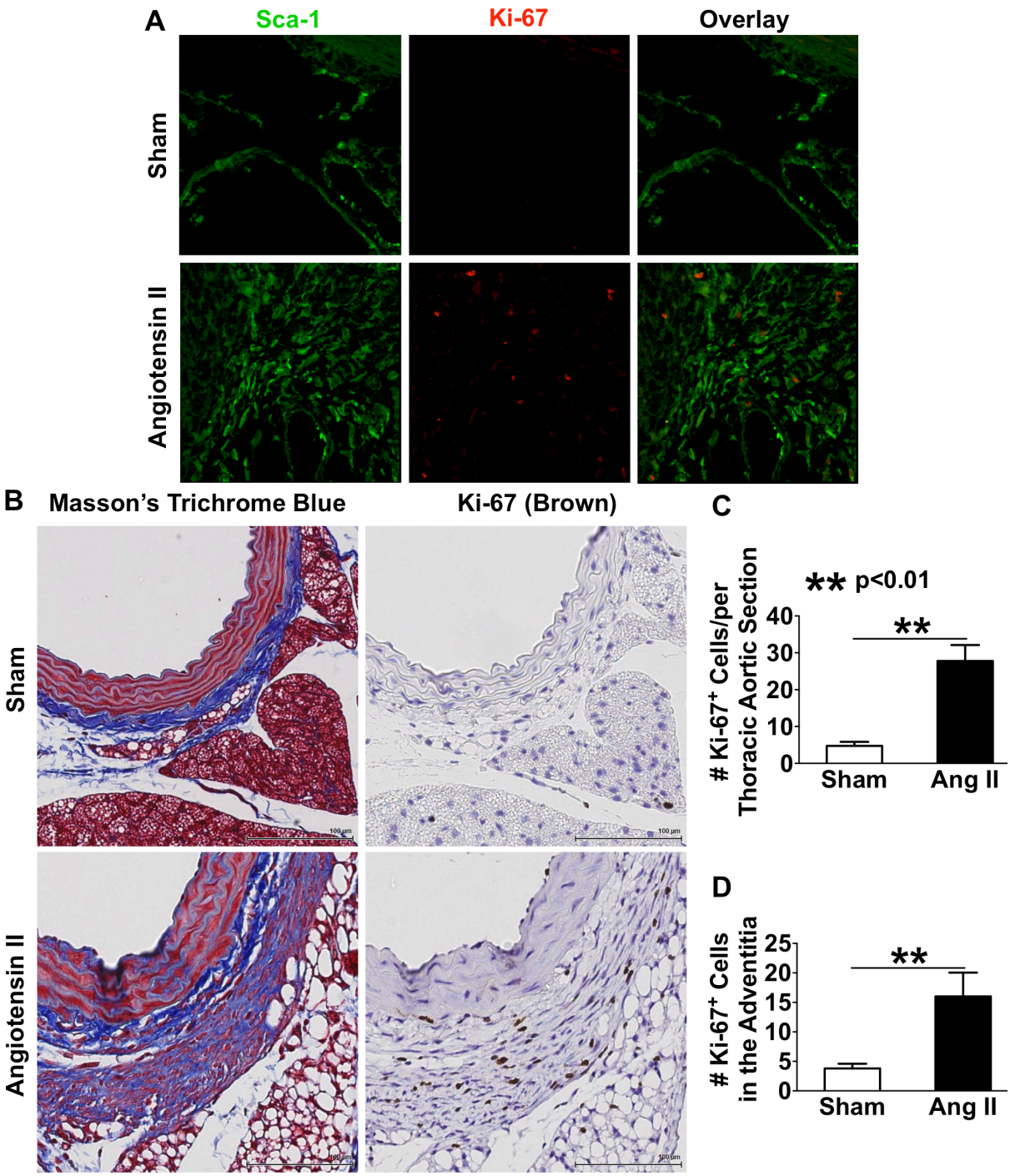

Figure 28 Aortic adventitial Sca-1$^+$ cells proliferate in hypertension. A) Co-localization of Sca-1$^+$ cells with proliferation marker Ki-67 in the adventitial of hypertensive mice. B) Ki-67$^+$ cells were identified in the areas of collagen deposition in the aortic adventitia (n=6). C and D) Quantification of Ki-67$^+$ cells in the aortic wall of sham and angiotensin II-infused mice.

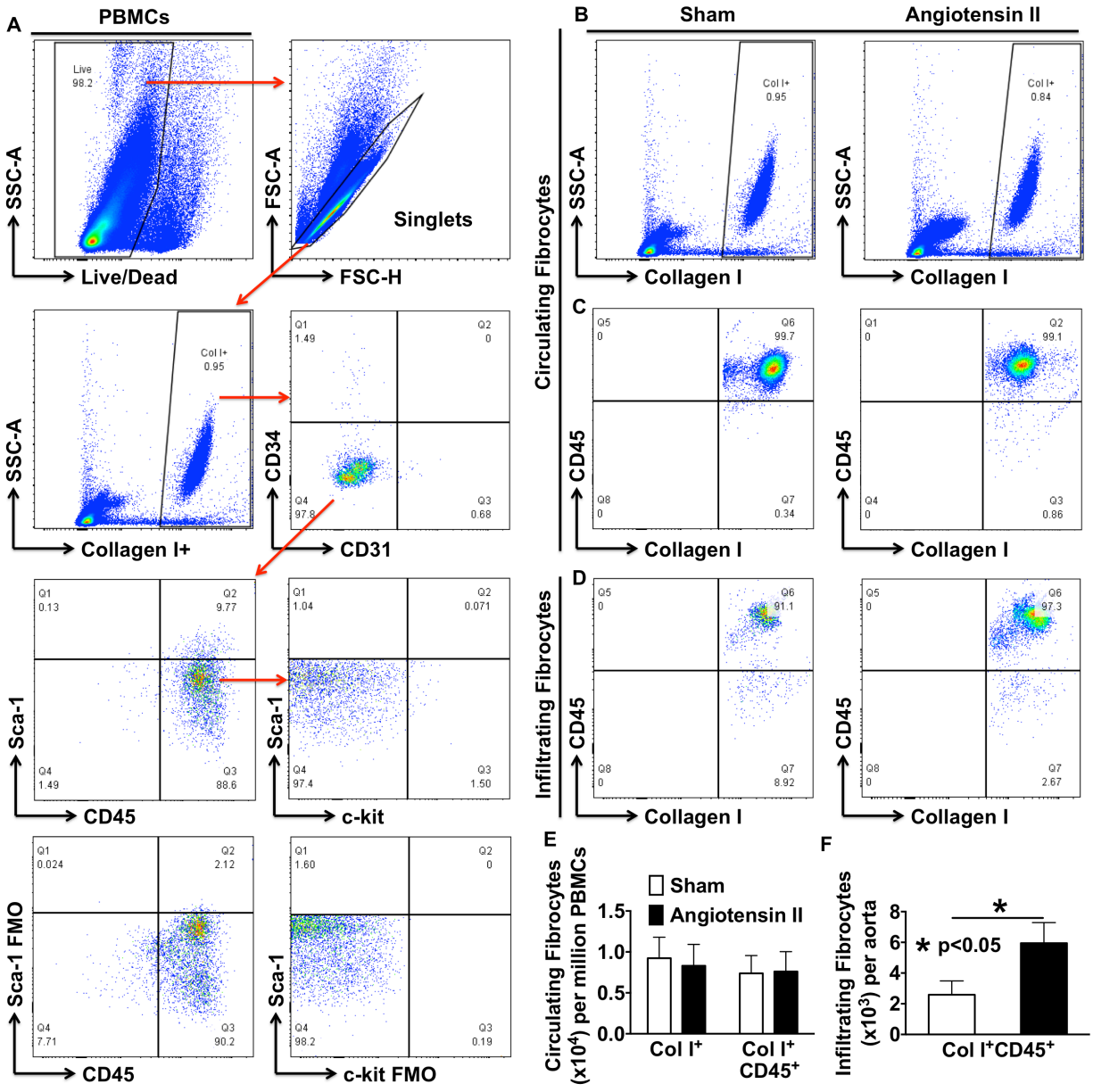

Figure 29 Col I^{+}CD45^{+} circulating fibrocytes migrate to hypertensive aortas. A) Gating strategy identifying circulating fibrocytes in the peripheral blood mononuclear cells (PBMCs). All col I+ cells were selected from live single cells, which were subsequently analyzed for CD34, CD31, CD45, Sca-1 and c-kit. B and C) PBMCs positive for Col I or Col I/CD45 were found in the blood of sham and angiotensin II infused mice. D) Col I+CD45+ fibrocytes found in the aorta. E-F) Quantification of fibrocytes in the peripheral blood and in the aorta.

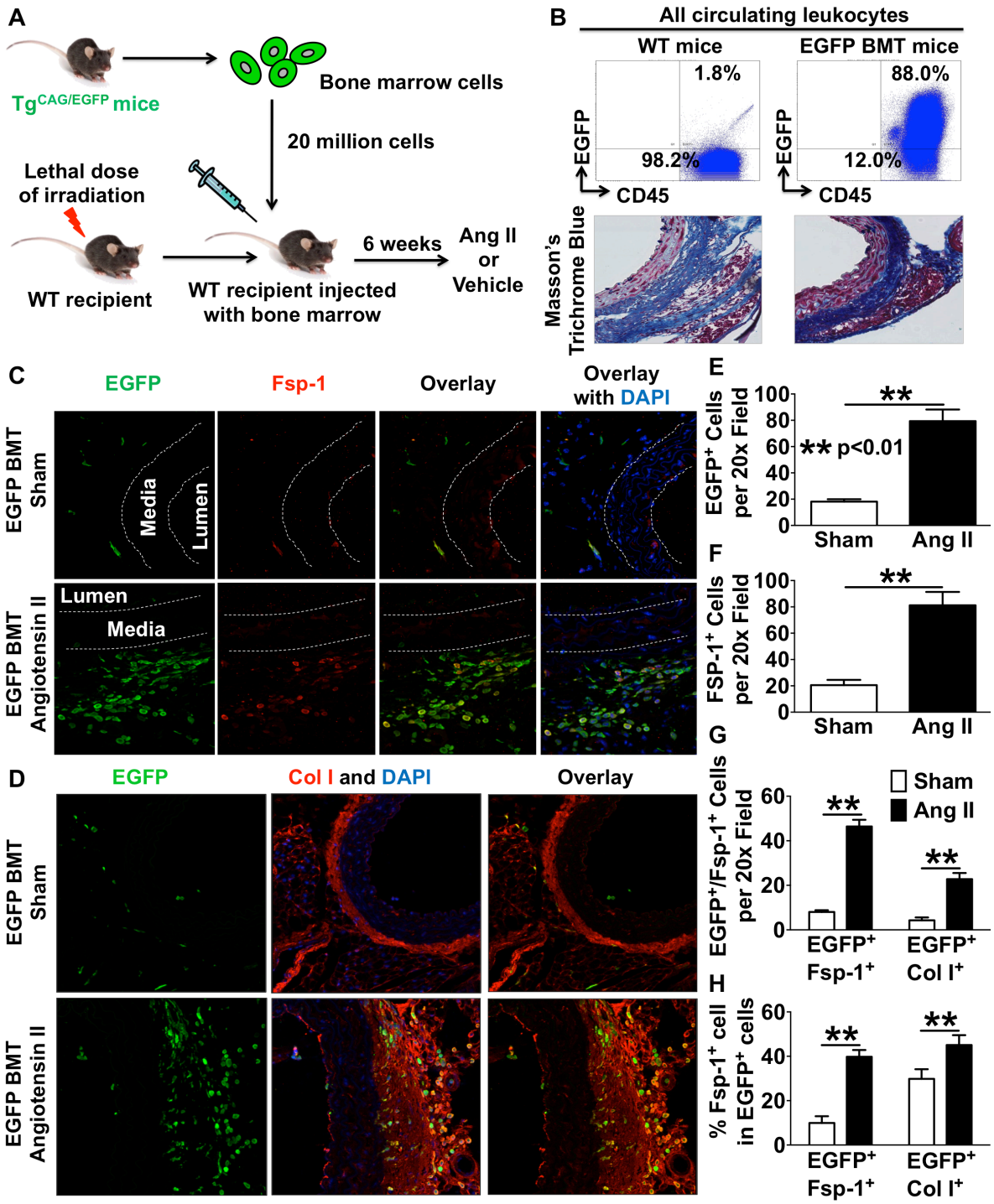

Figure 30 Bone marrow-derived cells express collagen I in the aortic adventitial of hypertensive mice. A) Scheme showing bone marrow transplantation technique. B) Circulating leukocytes were $EGFP^+$ in WT mice receiving EGFP transgenic bone marrow and these mice develop similar degree of aortic collagen deposition to WT mice in hypertension. C-H) Bone marrow-derived cells migrate to aortic adventitia and acquire fibroblast markers.

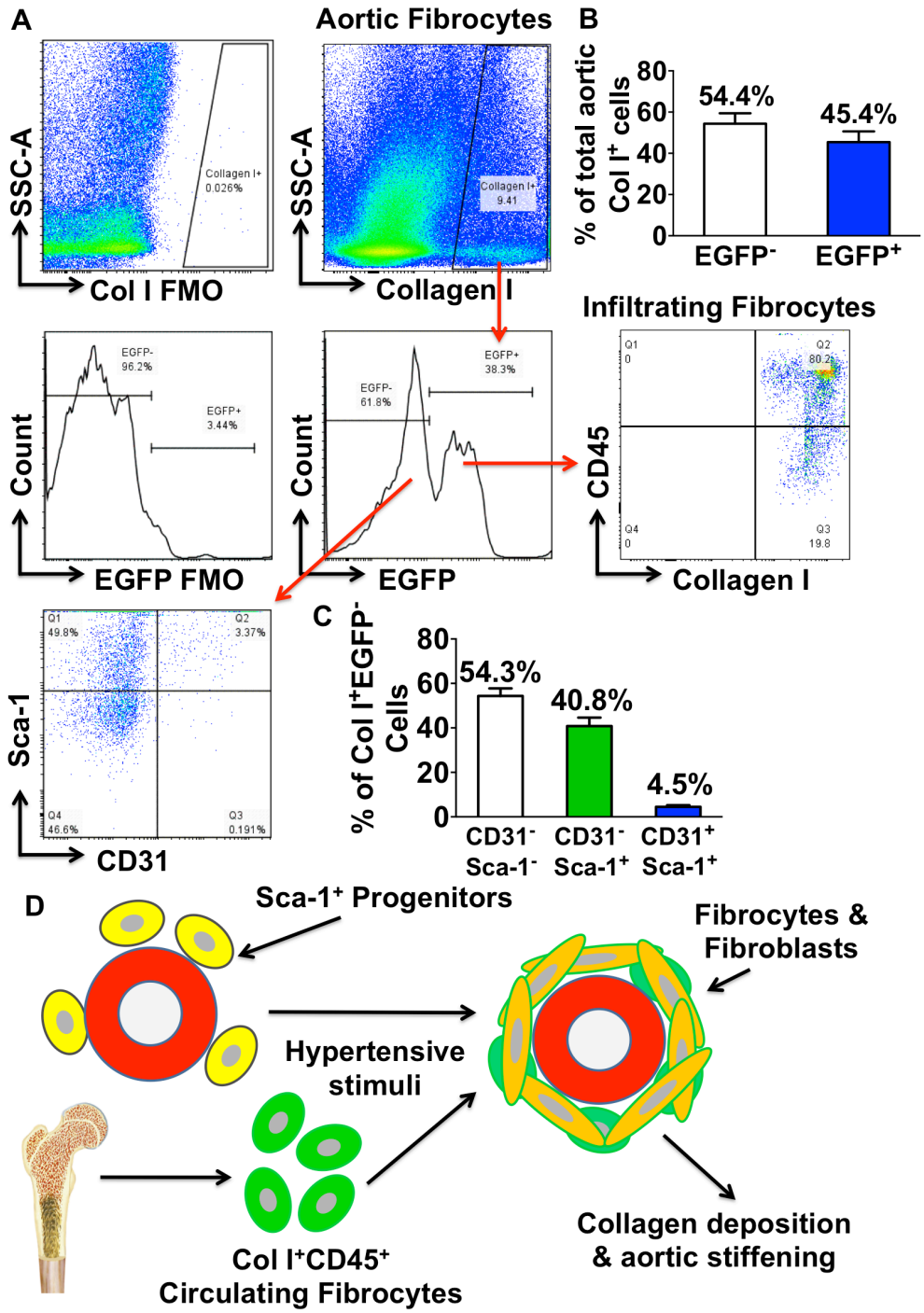

Figure 31 Vascular fibroblasts and bone marrow derived-fibrocytes equally contribute to aortic fibrosis. A) Gating strategy showing Col I^{+}EGFP^{+}CD45^{+} fibrocytes in the aorta. B) The proportions of EGFP^{+} and EGFP^{-} cells in the total aortic Col I^{+} cells. C) Relative contribution of fibroblast-like cells derived from vascular origins. D) Working hypothesis showing that the roles of arterial Sca-1+ progenitors and circulating fibrocytes in fibrosis and stiffening of the aorta in hypertension.

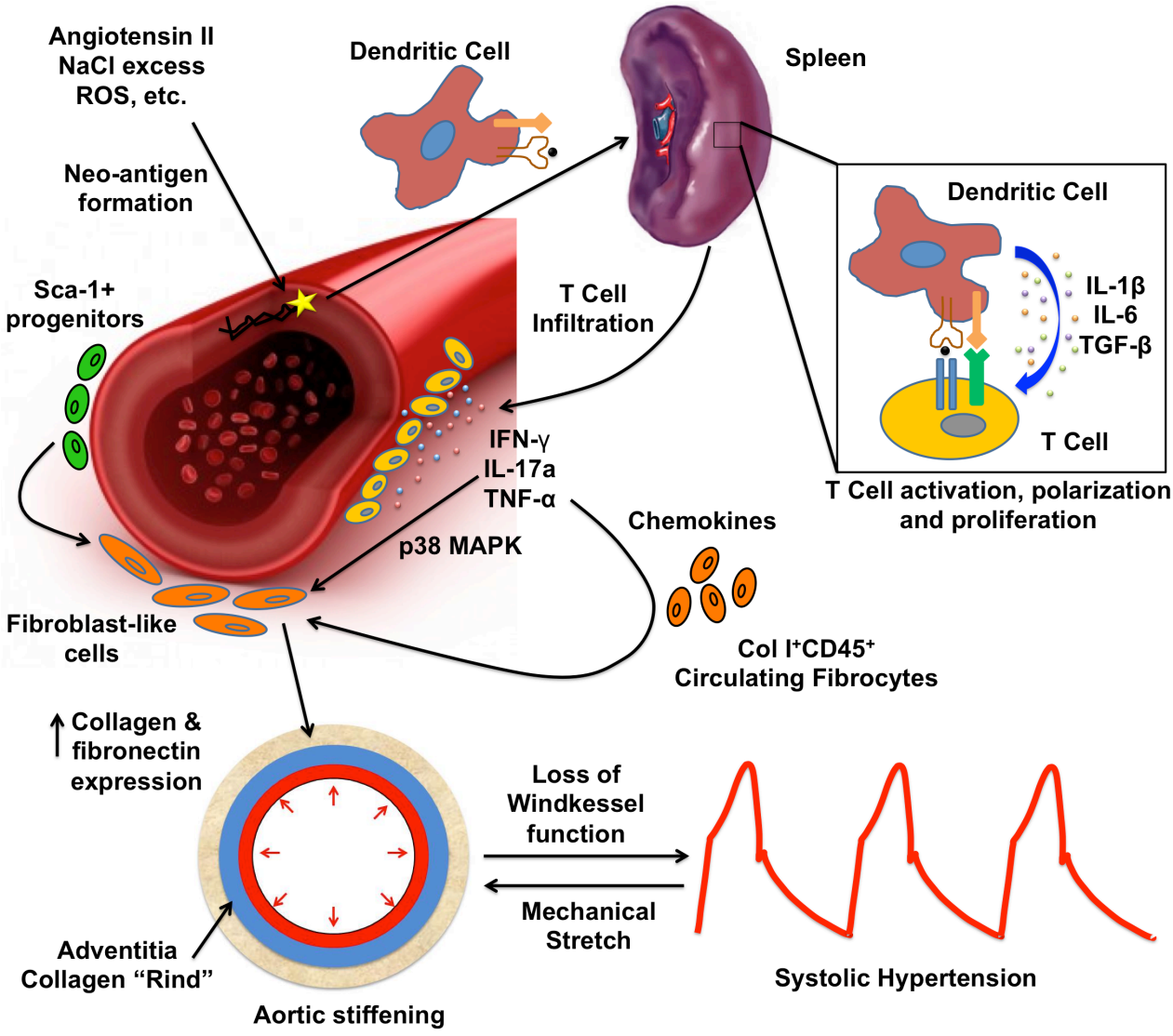

Figure 32 Working hypothesis summarizing findings of my dissertation research. This diagram depicts the interplay between oxidative stress, inflammtion and adaptive immunity the development of aortic stiffening and hypertension.

REFERENCES

1. Qureshi AI, Suri MF, Kirmani JF, Divani AA. Prevalence and trends of prehypertension and hypertension in united states: National health and nutrition examination surveys 1976 to 2000. *Medical science monitor : international medical journal of experimental and clinical research*. 2005;11:CR403-409

2. Narayan KM, Ali MK, Koplan JP. Global noncommunicable diseases--where worlds meet. *The New England journal of medicine*. 2010;363:1196-1198

3. Howard G, Prineas R, Moy C, Cushman M, Kellum M, Temple E, Graham A, Howard V. Racial and geographic differences in awareness, treatment, and control of hypertension: The reasons for geographic and racial differences in stroke study. *Stroke; a journal of cerebral circulation*. 2006;37:1171-1178

4. Chobanian AV, Bakris GL, Black HR, Cushman WC, Green LA, Izzo JL, Jr., Jones DW, Materson BJ, Oparil S, Wright JT, Jr., Roccella EJ, National Heart L, Blood Institute Joint National Committee on Prevention DE, Treatment of High Blood P, National High Blood Pressure Education Program Coordinating C. The seventh report of the joint national committee on prevention, detection, evaluation, and treatment of high blood pressure: The jnc 7 report. *Jama*. 2003;289:2560-2572

5. Tanira MO, Al Balushi KA. Genetic variations related to hypertension: A review. *J Hum Hypertens*. 2005;19:7-19

6. Luft FC. Mendelian forms of human hypertension and mechanisms of disease. *Clinical medicine & research*. 2003;1:291-300

7. Kobayashi N, DeLano FA, Schmid-Schonbein GW. Oxidative stress promotes endothelial cell apoptosis and loss of microvessels in the spontaneously hypertensive rats. *Arterioscler Thromb Vasc Biol*. 2005;25:2114-2121

8. Abboud FM, Huston JH. Measurement of arterial aging in hypertensive patients. *J Clin Invest*. 1961;40:1915-1921

9. Weisbrod RM, Shiang T, Al Sayah L, Fry JL, Bajpai S, Reinhart-King CA, Lob HE, Santhanam L, Mitchell G, Cohen RA, Seta F. Arterial stiffening precedes systolic hypertension in diet-induced obesity. *Hypertension*. 2013;62:1105-1110

10. Kaess BM, Rong J, Larson MG, Hamburg NM, Vita JA, Levy D, Benjamin EJ, Vasan RS, Mitchell GF. Aortic stiffness, blood pressure progression, and incident hypertension. *Jama*. 2012;308:875-881

11. Selvin E, Najjar SS, Cornish TC, Halushka MK. A comprehensive histopathological evaluation of vascular medial fibrosis: Insights into the pathophysiology of arterial stiffening. *Atherosclerosis*. 2010;208:69-74

12. Mihout F, Shweke N, Bige N, Jouanneau C, Dussaule JC, Ronco P, Chatziantoniou C, Boffa JJ. Asymmetric dimethylarginine (adma) induces chronic kidney disease through a mechanism involving collagen and tgf-beta1 synthesis. *The Journal of pathology*. 2011;223:37-45

13. Qiu H, Depre C, Ghosh K, Resuello RG, Natividad FF, Rossi F, Peppas A, Shen YT, Vatner DE, Vatner SF. Mechanism of gender-specific differences in aortic stiffness with aging in nonhuman primates. *Circulation*. 2007;116:669-676

14. Faury G, Pezet M, Knutsen RH, Boyle WA, Heximer SP, McLean SE, Minkes RK, Blumer KJ, Kovacs A, Kelly DP, Li DY, Starcher B, Mecham RP. Developmental adaptation of the mouse cardiovascular system to elastin haploinsufficiency. *J Clin Invest*. 2003;112:1419-1428

15. Sies H. Oxidative stress: From basic research to clinical application. *Am J Med*. 1991;91:31S-38S

16. Nakazono K, Watanabe N, Matsuno K, Sasaki J, Sato T, Inoue M. Does superoxide underlie the pathogenesis of hypertension? *Proc Natl Acad Sci U S A*. 1991;88:10045-10048

17. Fukui T, Ishizaka N, Rajagopalan S, Laursen JB, Capers Qt, Taylor WR, Harrison DG, de Leon H, Wilcox JN, Griendling KK. P22phox mrna expression and nadph oxidase activity are increased in aortas from hypertensive rats. *Circ Res*. 1997;80:45-51

18. Rajagopalan S, Kurz S, Munzel T, Tarpey M, Freeman BA, Griendling KK, Harrison DG. Angiotensin ii-mediated hypertension in the rat increases vascular superoxide production via membrane nadh/nadph oxidase activation. Contribution to alterations of vasomotor tone. *J Clin Invest*. 1996;97:1916-1923

19. Laursen JB, Rajagopalan S, Galis Z, Tarpey M, Freeman BA, Harrison DG. Role of superoxide in angiotensin ii-induced but not catecholamine-induced hypertension. *Circulation*. 1997;95:588-593

20. Somers MJ, Mavromatis K, Galis ZS, Harrison DG. Vascular superoxide production and vasomotor function in hypertension induced by deoxycorticosterone acetate-salt. *Circulation*. 2000;101:1722-1728

21. Myung SK, Ju W, Cho B, Oh SW, Park SM, Koo BK, Park BJ, Korean Meta-Analysis Study G. Efficacy of vitamin and antioxidant supplements in prevention of cardiovascular disease: Systematic review and meta-analysis of randomised controlled trials. *Bmj*. 2013;346:f10

22. Bjelakovic G, Nikolova D, Gluud LL, Simonetti RG, Gluud C. Mortality in randomized trials of antioxidant supplements for primary and secondary prevention: Systematic review and meta-analysis. *JAMA*. 2007;297:842-857

23. Philips N, Samuel P, Parakandi H, Gopal S, Siomyk H, Ministro A, Thompson T, Borkow G. Beneficial regulation of fibrillar collagens, heat shock protein-47, elastin fiber components, transforming growth factor-beta1, vascular endothelial growth factor and oxidative stress effects by copper in dermal fibroblasts. *Connective tissue research*. 2012;53:373-378

24. Rajagopalan S, Meng XP, Ramasamy S, Harrison DG, Galis ZS. Reactive oxygen species produced by macrophage-derived foam cells regulate the activity of vascular matrix metalloproteinases in vitro. Implications for atherosclerotic plaque stability. *J Clin Invest*. 1996;98:2572-2579

25. Valentin F, Bueb JL, Kieffer P, Tschirhart E, Atkinson J. Oxidative stress activates mmp-2 in cultured human coronary smooth muscle cells. *Fundamental & clinical pharmacology*. 2005;19:661-667

26. Soskel NT, Watanabe S, Sandberg LB. Mechanisms of lung injury in the copper-deficient hamster model of emphysema. *Chest*. 1984;85:70S-73S

27. Foronjy RF, Mirochnitchenko O, Propokenko O, Lemaitre V, Jia Y, Inouye M, Okada Y, D'Armiento JM. Superoxide dismutase expression attenuates cigarette smoke- or elastase-generated emphysema in mice. *American journal of respiratory and critical care medicine*. 2006;173:623-631

28. Chandrakasan G, Bhatnagar RS. Stimulation of collagen synthesis in fibroblast cultures by superoxide. *Cell Mol Biol*. 1991;37:751-755

29. Hecker L, Vittal R, Jones T, Jagirdar R, Luckhardt TR, Horowitz JC, Pennathur S, Martinez FJ, Thannickal VJ. Nadph oxidase-4 mediates myofibroblast activation and fibrogenic responses to lung injury. *Nature medicine*. 2009;15:1077-1081

30. Kass DA, Shapiro EP, Kawaguchi M, Capriotti AR, Scuteri A, deGroof RC, Lakatta EG. Improved arterial compliance by a novel advanced glycation end-product crosslink breaker. *Circulation*. 2001;104:1464-1470

31. Yao D, Brownlee M. Hyperglycemia-induced reactive oxygen species increase expression of the receptor for advanced glycation end products (rage) and rage ligands. *Diabetes*. 2010;59:249-255

32. Wolffenbuttel BH, Boulanger CM, Crijns FR, Huijberts MS, Poitevin P, Swennen GN, Vasan S, Egan JJ, Ulrich P, Cerami A, Levy BI. Breakers of advanced glycation end products restore large artery properties in experimental diabetes. *Proceedings of the National Academy of Sciences of the United States of America*. 1998;95:4630-4634

33. Guzik TJ, Hoch NE, Brown KA, McCann LA, Rahman A, Dikalov S, Goronzy J, Weyand C, Harrison DG. Role of the t cell in the genesis of angiotensin ii induced hypertension and vascular dysfunction. *J Exp Med*. 2007;204:2449-2460

34. Madhur MS, Funt SA, Li L, Vinh A, Chen W, Lob HE, Iwakura Y, Blinder Y, Rahman A, Quyyumi AA, Harrison DG. Role of interleukin 17 in inflammation, atherosclerosis, and vascular function in apolipoprotein e-deficient mice. *Arterioscler Thromb Vasc Biol*. 2011;31:1565-1572

35. Hildreth KL, Kohrt WM, Moreau KL. Oxidative stress contributes to large elastic arterial stiffening across the stages of the menopausal transition. *Menopause*. 2013

36. Wang DS, Proffit D, Tsao PS. Mechanotransduction of endothelial oxidative stress induced by cyclic strain. *Endothelium : journal of endothelial cell research*. 2001;8:283-291

37. Hishikawa K, Oemar BS, Yang Z, Luscher TF. Pulsatile stretch stimulates superoxide production and activates nuclear factor-kappa b in human coronary smooth muscle. *Circ Res*. 1997;81:797-803

38. Sakai N, Wada T, Yokoyama H, Lipp M, Ueha S, Matsushima K, Kaneko S. Secondary lymphoid tissue chemokine (slc/ccl21)/ccr7 signaling regulates fibrocytes in renal fibrosis. *Proc Natl Acad Sci U S A*. 2006;103:14098-14103

39. Madhur MS, Lob HE, McCann LA, Iwakura Y, Blinder Y, Guzik TJ, Harrison DG. Interleukin 17 promotes angiotensin ii-induced hypertension and vascular dysfunction. *Hypertension*. 2010;55:500-507

40. Fan LM, Douglas G, Bendall JK, McNeill E, Crabtree MJ, Hale AB, Mai A, Li JM, McAteer MA, Schneider JE, Choudhury RP, Channon KM. Endothelial cell-specific reactive oxygen species production increases susceptibility to aortic dissection. *Circulation*. 2014;129:2661-2672

41. Inauen W, Payne DK, Kvietys PR, Granger DN. Hypoxia/reoxygenation increases the permeability of endothelial cell monolayers: Role of oxygen radicals. *Free Radic Biol Med*. 1990;9:219-223

42. Marko L, Kvakan H, Park JK, Qadri F, Spallek B, Binger KJ, Bowman EP, Kleinewietfeld M, Fokuhl V, Dechend R, Muller DN. Interferon-gamma signaling inhibition ameliorates angiotensin ii-induced cardiac damage. *Hypertension*. 2012;60:1430-1436

43. Svendsen UG. Evidence for an initial, thymus independent and a chronic, thymus dependent phase of doca and salt hypertension in mice. *Acta pathologica et microbiologica Scandinavica. Section A, Pathology*. 1976;84:523-528

44. Mahmoud F, Omu A, Abul H, El-Rayes S, Haines D. Lymphocyte subpopulations in pregnancy complicated by hypertension. *Journal of obstetrics and gynaecology : the journal of the Institute of Obstetrics and Gynaecology*. 2003;23:20-26

45. Seaberg EC, Munoz A, Lu M, Detels R, Margolick JB, Riddler SA, Williams CM, Phair JP, Multicenter ACS. Association between highly active antiretroviral therapy and hypertension in a large cohort of men followed from 1984 to 2003. *Aids*. 2005;19:953-960

46. Marvar PJ, Thabet SR, Guzik TJ, Lob HE, McCann LA, Weyand C, Gordon FJ, Harrison DG. Central and peripheral mechanisms of t-lymphocyte activation and vascular inflammation produced by angiotensin ii-induced hypertension. *Circ Res*. 2010;107:263-270

47. Kirabo A, Fontana V, de Faria AP, Loperena R, Galindo CL, Wu J, Bikineyeva AT, Dikalov S, Xiao L, Chen W, Saleh MA, Trott DW, Itani HA, Vinh A, Amarnath V, Amarnath K, Guzik TJ, Bernstein KE, Shen XZ, Shyr Y, Chen SC, Mernaugh RL, Laffer CL, Elijovich F, Davies SS, Moreno LH, Madhur MS, Roberts J, 2nd, Harrison DG. Dc isoketal-modified proteins activate t cells and promote hypertension. *J Clin Invest*. 2014

48. Lob HE, Schultz D, Marvar PJ, Davisson RL, Harrison DG. Role of the nadph oxidases in the subfornical organ in angiotensin ii-induced hypertension. *Hypertension*. 2013;61:382-387

49. Trott DW, Thabet SR, Kirabo A, Saleh MA, Itani H, Norlander AE, Wu J, Goldstein A, Arendshorst WJ, Madhur MS, Chen W, Li CI, Shyr Y, Harrison DG. Oligoclonal cd8+ t cells play a critical role in the development of hypertension. *Hypertension*. 2014;64:1108-1115

50. Landmesser U, Cai H, Dikalov S, McCann L, Hwang J, Jo H, Holland SM, Harrison DG. Role of p47(phox) in vascular oxidative stress and hypertension caused by angiotensin ii. *Hypertension*. 2002;40:511-515

51. O'Rourke MF. Arterial aging: Pathophysiological principles. *Vasc Med*. 2007;12:329-341

52. Mitchell GF, Guo CY, Benjamin EJ, Larson MG, Keyes MJ, Vita JA, Vasan RS, Levy D. Cross-sectional correlates of increased aortic stiffness in the community: The framingham heart study. *Circulation*. 2007;115:2628-2636

53. Dietrich T, Schaefer-Graf U, Fleck E, Graf K. Aortic stiffness, impaired fasting glucose, and aging. *Hypertension*. 2010;55:18-20

54. Payne RA, Wilkinson IB, Webb DJ. Arterial stiffness and hypertension: Emerging concepts. *Hypertension*. 2010;55:9-14

55. Mitchell GF, DeStefano AL, Larson MG, Benjamin EJ, Chen MH, Vasan RS, Vita JA, Levy D. Heritability and a genome-wide linkage scan for arterial stiffness, wave reflection, and mean arterial pressure: The framingham heart study. *Circulation*. 2005;112:194-199

56. Mattace-Raso FU, van der Cammen TJ, Hofman A, van Popele NM, Bos ML, Schalekamp MA, Asmar R, Reneman RS, Hoeks AP, Breteler MM, Witteman JC. Arterial stiffness and risk of coronary heart disease and stroke: The rotterdam study. *Circulation*. 2006;113:657-663

57. Laurent S, Katsahian S, Fassot C, Tropeano AI, Gautier I, Laloux B, Boutouyrie P. Aortic stiffness is an independent predictor of fatal stroke in essential hypertension. *Stroke; a journal of cerebral circulation*. 2003;34:1203-1206

58. Abramson JL, Weintraub WS, Vaccarino V. Association between pulse pressure and c-reactive protein among apparently healthy us adults. *Hypertension*. 2002;39:197-202

59. Yasmin, McEniery CM, Wallace S, Mackenzie IS, Cockcroft JR, Wilkinson IB. C-reactive protein is associated with arterial stiffness in apparently healthy individuals. *Arterioscler Thromb Vasc Biol*. 2004;24:969-974

60. Nakhai-Pour HR, Grobbee DE, Bots ML, Muller M, van der Schouw YT. C-reactive protein and aortic stiffness and wave reflection in middle-aged and elderly men from the community. *J Hum Hypertens*. 2007;21:949-955

61. Tsioufis C, Dimitriadis K, Selima M, Thomopoulos C, Mihas C, Skiadas I, Tousoulis D, Stefanadis C, Kallikazaros I. Low-grade inflammation and hypoadiponectinaemia have an additive detrimental effect on aortic stiffness in essential hypertensive patients. *Eur Heart J*. 2007;28:1162-1169

62. Selzer F, Sutton-Tyrrell K, Fitzgerald S, Tracy R, Kuller L, Manzi S. Vascular stiffness in women with systemic lupus erythematosus. *Hypertension*. 2001;37:1075-1082

63. Wallberg-Jonsson S, Caidahl K, Klintland N, Nyberg G, Rantapaa-Dahlqvist S. Increased arterial stiffness and indication of endothelial dysfunction in long-standing rheumatoid arthritis. *Scand J Rheumatol*. 2008;37:1-5

64. Gisondi P, Fantin F, Del Giglio M, Valbusa F, Marino F, Zamboni M, Girolomoni G. Chronic plaque psoriasis is associated with increased arterial stiffness. *Dermatology*. 2009;218:110-113

65. Mattson DL, Lund H, Guo C, Rudemiller N, Geurts AM, Jacob H. Genetic mutation of recombination activating gene 1 in dahl salt-sensitive rats attenuates hypertension and renal damage. *Am J Physiol Regul Integr Comp Physiol*. 2013;304:R407-414

66. Schrader LI, Kinzenbaw DA, Johnson AW, Faraci FM, Didion SP. Il-6 deficiency protects against angiotensin ii induced endothelial dysfunction and hypertrophy. *Arterioscler Thromb Vasc Biol*. 2007;27:2576-2581

67. Nguyen H, Chiasson VL, Chatterjee P, Kopriva SE, Young KJ, Mitchell BM. Interleukin-17 causes rho-kinase-mediated endothelial dysfunction and hypertension. *Cardiovasc Res*. 2013;97:696-704

68. Kurasawa K, Hirose K, Sano H, Endo H, Shinkai H, Nawata Y, Takabayashi K, Iwamoto I. Increased interleukin-17 production in patients with systemic sclerosis. *Arthritis Rheum*. 2000;43:2455-2463

69. Molet SM, Hamid QA, Hamilos DL. Il-11 and il-17 expression in nasal polyps: Relationship to collagen deposition and suppression by intranasal fluticasone propionate. *Laryngoscope*. 2003;113:1803-1812

70. Feng W, Li W, Liu W, Wang F, Li Y, Yan W. Il-17 induces myocardial fibrosis and enhances rankl/opg and mmp/timp signaling in isoproterenol-induced heart failure. *Exp Mol Pathol*. 2009;87:212-218

71. Baumbach GL, Siems JE, Heistad DD. Effects of local reduction in pressure on distensibility and composition of cerebral arterioles. *Circ Res*. 1991;68:338-351

72. Hofman K, Hall B, Cleaver H, Marshall S. High-throughput quantification of hydroxyproline for determination of collagen. *Anal Biochem*. 2011;417:289-291

73. Mecham RP. Methods in elastic tissue biology: Elastin isolation and purification. *Methods*. 2008;45:32-41

74. Starcher B. A ninhydrin-based assay to quantitate the total protein content of tissue samples. *Anal Biochem*. 2001;292:125-129

75. Liang Q, Elson AC, Gerdes AM. P38 map kinase activity is correlated with angiotensin ii type 1 receptor blocker-induced left ventricular reverse remodeling in spontaneously hypertensive heart failure rats. *Journal of cardiac failure*. 2006;12:479-486

76. Park JK, Fischer R, Dechend R, Shagdarsuren E, Gapeljuk A, Wellner M, Meiners S, Gratze P, Al-Saadi N, Feldt S, Fiebeler A, Madwed JB, Schirdewan A, Haller H, Luft FC, Muller DN. P38 mitogen-activated protein kinase inhibition ameliorates angiotensin ii-induced target organ damage. *Hypertension*. 2007;49:481-489

77. Wang D, Warner GM, Yin P, Knudsen BE, Cheng J, Butters KA, Lien KR, Gray CE, Garovic VD, Lerman LO, Textor SC, Nath KA, Simari RD, Grande JP. Inhibition of p38 mapk attenuates renal atrophy and fibrosis in a murine renal artery stenosis model. *American journal of physiology. Renal physiology*. 2013;304:F938-947

78. Paravicini TM, Montezano AC, Yusuf H, Touyz RM. Activation of vascular p38mapk by mechanical stretch is independent of c-src and nadph oxidase: Influence of hypertension and angiotensin ii. *J Am Soc Hypertens*. 2012;6:169-178

79. Maki-Petaja KM, Elkhawad M, Cheriyan J, Joshi FR, Ostor AJ, Hall FC, Rudd JH, Wilkinson IB. Anti-tumor necrosis factor-alpha therapy reduces aortic inflammation and stiffness in patients with rheumatoid arthritis. *Circulation*. 2012;126:2473-2480

80. Galarraga B, Khan F, Kumar P, Pullar T, Belch JJ. Etanercept improves inflammation-associated arterial stiffness in rheumatoid arthritis. *Rheumatology (Oxford)*. 2009;48:1418-1423

81. Ortega C, Fernandez AS, Carrillo JM, Romero P, Molina IJ, Moreno JC, Santamaria M. Il-17-producing cd8+ t lymphocytes from psoriasis skin plaques are cytotoxic effector cells that secrete th17-related cytokines. *J Leukoc Biol*. 2009;86:435-443

82. He D, Wu L, Kim HK, Li H, Elmets CA, Xu H. Cd8+ il-17-producing t cells are important in effector functions for the elicitation of contact hypersensitivity responses. *J Immunol*. 2006;177:6852-6858

83. Matsushita H, Lee KH, Tsao PS. Cyclic strain induces reactive oxygen species production via an endothelial nad(p)h oxidase. *Journal of cellular biochemistry. Supplement*. 2001;Suppl 36:99-106

84. Cheng JJ, Wung BS, Chao YJ, Wang DL. Cyclic strain enhances adhesion of monocytes to endothelial cells by increasing intercellular adhesion molecule-1 expression. *Hypertension*. 1996;28:386-391

85. Hyytiainen M, Penttinen C, Keski-Oja J. Latent tgf-beta binding proteins: Extracellular matrix association and roles in tgf-beta activation. *Critical reviews in clinical laboratory sciences*. 2004;41:233-264

86. Crawford SE, Stellmach V, Murphy-Ullrich JE, Ribeiro SM, Lawler J, Hynes RO, Boivin GP, Bouck N. Thrombospondin-1 is a major activator of tgf-beta1 in vivo. *Cell*. 1998;93:1159-1170

87. Perdiguero E, Sousa-Victor P, Ruiz-Bonilla V, Jardi M, Caelles C, Serrano AL, Munoz-Canoves P. P38/mkp-1-regulated akt coordinates macrophage transitions and resolution of inflammation during tissue repair. *The Journal of cell biology*. 2011;195:307-322

88. Wang G, Kwan BC, Lai FM, Chow KM, Li PK, Szeto CC. Urinary mir-21, mir-29, and mir-93: Novel biomarkers of fibrosis. *American journal of nephrology*. 2012;36:412-418

89. Wang J, Gao Y, Ma M, Li M, Zou D, Yang J, Zhu Z, Zhao X. Effect of mir-21 on renal fibrosis by regulating mmp-9 and timp1 in kk-ay diabetic nephropathy mice. *Cell biochemistry and biophysics*. 2013

90. Villar AV, Garcia R, Merino D, Llano M, Cobo M, Montalvo C, Martin-Duran R, Hurle MA, Nistal JF. Myocardial and circulating levels of microrna-21 reflect left ventricular fibrosis in aortic stenosis patients. *Int J Cardiol*. 2012

91. Zhu H, Luo H, Li Y, Zhou Y, Jiang Y, Chai J, Xiao X, You Y, Zuo X. Microrna-21 in scleroderma fibrosis and its function in tgf-beta- regulated fibrosis-related genes expression. *Journal of clinical immunology*. 2013

92. Kaess BM, Rong J, Larson MG, Hamburg NM, Vita JA, Levy D, Benjamin EJ, Vasan RS, Mitchell GF. Aortic stiffness, blood pressure progression, and incident hypertension. *Jama*. 2012;308:875-881

93. Chen J, Wu J, Li L, Zou YZ, Zhu DL, Gao PJ. Effect of an acute mechanical stimulus on aortic structure in the transverse aortic constriction mouse model. *Clin Exp Pharmacol Physiol*. 2011;38:570-576

94. Meaume S, Benetos A, Henry OF, Rudnichi A, Safar ME. Aortic pulse wave velocity predicts cardiovascular mortality in subjects >70 years of age. *Arterioscler Thromb Vasc Biol*. 2001;21:2046-2050

95. Kals J, Kampus P, Kals M, Pulges A, Teesalu R, Zilmer K, Kullisaar T, Salum T, Eha J, Zilmer M. Inflammation and oxidative stress are associated differently with endothelial function and arterial stiffness in healthy subjects and in patients with atherosclerosis. *Scand J Clin Lab Invest*. 2008;68:594-601

96. Stephen EA, Venkatasubramaniam A, Good TA, Topoleski LD. The effect of oxidation on the mechanical response and microstructure of porcine aortas. *J Biomed Mater Res A*. 2013

97. Kume K, Amano K, Yamada S, Hatta K, Ohta H, Kuwaba N. Tocilizumab monotherapy reduces arterial stiffness as effectively as etanercept or adalimumab monotherapy in rheumatoid arthritis: An open-label randomized controlled trial. *J Rheumatol*. 2011;38:2169-2171

98. Angel K, Provan SA, Gulseth HL, Mowinckel P, Kvien TK, Atar D. Tumor necrosis factor-alpha antagonists improve aortic stiffness in patients with inflammatory arthropathies: A controlled study. *Hypertension*. 2010;55:333-338

99. Wu J, Thabet SR, Kirabo A, Trott DW, Saleh MA, Xiao L, Madhur MS, Chen W, Harrison DG. Inflammation and mechanical stretch promote aortic stiffening in hypertension through activation of p38 mitogen-activated protein kinase. *Circ Res*. 2014;114:616-625

100. Davies SS, Amarnath V, Brame CJ, Boutaud O, Roberts LJ, 2nd. Measurement of chronic oxidative and inflammatory stress by quantification of isoketal/levuglandin gamma-ketoaldehyde protein adducts using liquid chromatography tandem mass spectrometry. *Nature protocols*. 2007;2:2079-2091

101. Miyashita H, Chikazawa M, Otaki N, Hioki Y, Shimozu Y, Nakashima F, Shibata T, Hagihara Y, Maruyama S, Matsumi N, Uchida K. Lysine pyrrolation is a naturally-occurring covalent modification involved in the production of DNA mimic proteins. *Sci Rep*. 2014;4:5343

102. Vinh A, Chen W, Blinder Y, Weiss D, Taylor WR, Goronzy JJ, Weyand CM, Harrison DG, Guzik TJ. Inhibition and genetic ablation of the b7/cd28 t-cell costimulation axis prevents experimental hypertension. *Circulation*. 2010;122:2529-2537

103. Lob HE, Vinh A, Li L, Blinder Y, Offermanns S, Harrison DG. Role of vascular extracellular superoxide dismutase in hypertension. *Hypertension*. 2011;58:232-239

104. Jakubzick C, Gautier EL, Gibbings SL, Sojka DK, Schlitzer A, Johnson TE, Ivanov S, Duan Q, Bala S, Condon T, van Rooijen N, Grainger JR, Belkaid Y, Ma'ayan A, Riches DW, Yokoyama WM, Ginhoux F, Henson PM, Randolph GJ. Minimal differentiation of classical monocytes as they survey steady-state tissues and transport antigen to lymph nodes. *Immunity*. 2013;39:599-610

105. Davies SS, Talati M, Wang X, Mernaugh RL, Amarnath V, Fessel J, Meyrick BO, Sheller J, Roberts LJ, 2nd. Localization of isoketal adducts in vivo using a single-chain antibody. *Free Radic Biol Med*. 2004;36:1163-1174

106. Laude K, Cai H, Fink B, Hoch N, Weber DS, McCann L, Kojda G, Fukai T, Schmidt HH, Dikalov S, Ramasamy S, Gamez G, Griendling KK, Harrison DG. Hemodynamic and biochemical adaptations to vascular smooth muscle overexpression of p22phox in mice. *Am J Physiol Heart Circ Physiol*. 2005;288:H7-12

107. Nguyen H, Chiasson VL, Chatterjee P, Kopriva SE, Young KJ, Mitchell BM. Interleukin-17 causes rho-kinase-mediated endothelial dysfunction and hypertension. *Cardiovasc Res*. 2013;97:696-704

108. Mitchell GF, Parise H, Benjamin EJ, Larson MG, Keyes MJ, Vita JA, Vasan RS, Levy D. Changes in arterial stiffness and wave reflection with advancing age in healthy men and women: The framingham heart study. *Hypertension*. 2004;43:1239-1245

109. Smit AJ, Lutgers HL. The clinical relevance of advanced glycation endproducts (age) and recent developments in pharmaceutics to reduce age accumulation. *Current medicinal chemistry*. 2004;11:2767-2784

110. Sajithlal GB, Chithra P, Chandrakasan G. Advanced glycation end products induce crosslinking of collagen in vitro. *Biochimica et biophysica acta*. 1998;1407:215-224

111. Urios P, Grigorova-Borsos AM, Sternberg M. Aspirin inhibits the formation of pentosidine, a cross-linking advanced glycation end product, in collagen. *Diabetes research and clinical practice*. 2007;77:337-340

112. Valente AJ, Yoshida T, Gardner JD, Somanna N, Delafontaine P, Chandrasekar B. Interleukin-17a stimulates cardiac fibroblast proliferation and migration via negative regulation of the dual-specificity phosphatase mkp-1/dusp-1. *Cell Signal*. 2012;24:560-568

113. Trott DW, Thabet SR, Kirabo A, Saleh M, Itani H, Norlander AE, Wu J, Goldstein A, Arendshorst WJ, Li CL, Shyr Y, Chen W, Madhur MS, Harrison DG. Oligoclonal cd8+ t cells play a critical role in the development of hypertension. *Hypertension*. 2014;In Press

114. Orabona C, Grohmann U, Belladonna ML, Fallarino F, Vacca C, Bianchi R, Bozza S, Volpi C, Salomon BL, Fioretti MC, Romani L, Puccetti P. Cd28 induces immunostimulatory signals in dendritic cells via cd80 and cd86. *Nat Immunol*. 2004;5:1134-1142

115. Czernichow S, Bertrais S, Blacher J, Galan P, Briancon S, Favier A, Safar M, Hercberg S. Effect of supplementation with antioxidants upon long-term risk of hypertension in the su.Vi.Max study: Association with plasma antioxidant levels. *J Hypertens*. 2005;23:2013-2018

116. Matoba T, Shimokawa H, Kubota H, Morikawa K, Fujiki T, Kunihiro I, Mukai Y, Hirakawa Y, Takeshita A. Hydrogen peroxide is an endothelium-derived hyperpolarizing factor in human mesenteric arteries. *Biochem Biophys Res Commun*. 2002;290:909-913

117. Arnold RS, Shi J, Murad E, Whalen AM, Sun CQ, Polavarapu R, Parthasarathy S, Petros JA, Lambeth JD. Hydrogen peroxide mediates the cell growth and transformation caused by the mitogenic oxidase nox1. *Proc Natl Acad Sci U S A*. 2001;98:5550-5555

118. Liu L, Wise DR, Diehl JA, Simon MC. Hypoxic reactive oxygen species regulate the integrated stress response and cell survival. *J Biol Chem*. 2008;283:31153-31162

119. Roberts LJ, 2nd, Oates JA, Linton MF, Fazio S, Meador BP, Gross MD, Shyr Y, Morrow JD. The relationship between dose of vitamin e and suppression of oxidative stress in humans. *Free Radic Biol Med*. 2007;43:1388-1393

120. Majesky MW, Dong XR, Hoglund V, Mahoney WM, Jr., Daum G. The adventitia: A dynamic interface containing resident progenitor cells. *Arterioscler Thromb Vasc Biol*. 2011;31:1530-1539

121. Passman JN, Dong XR, Wu SP, Maguire CT, Hogan KA, Bautch VL, Majesky MW. A sonic hedgehog signaling domain in the arterial adventitia supports resident sca1+ smooth muscle progenitor cells. *Proc Natl Acad Sci U S A*. 2008;105:9349-9354

122. Hu Y, Zhang Z, Torsney E, Afzal AR, Davison F, Metzler B, Xu Q. Abundant progenitor cells in the adventitia contribute to atherosclerosis of vein grafts in apoe-deficient mice. *J Clin Invest*. 2004;113:1258-1265

123. Psaltis PJ, Harbuzariu A, Delacroix S, Witt TA, Holroyd EW, Spoon DB, Hoffman SJ, Pan S, Kleppe LS, Mueske CS, Gulati R, Sandhu GS, Simari RD. Identification of a monocyte-predisposed hierarchy of hematopoietic progenitor cells in the adventitia of postnatal murine aorta. *Circulation*. 2012;125:592-603

124. Sainz J, Al Haj Zen A, Caligiuri G, Demerens C, Urbain D, Lemitre M, Lafont A. Isolation of "side population" progenitor cells from healthy arteries of adult mice. *Arterioscler Thromb Vasc Biol*. 2006;26:281-286

125. Xia Y, Jin X, Yan J, Entman ML, Wang Y. Cxcr6 plays a critical role in angiotensin ii-induced renal injury and fibrosis. *Arterioscler Thromb Vasc Biol*. 2014;34:1422-1428

126. Rosin NL, Sopel M, Falkenham A, Myers TL, Legare JF. Myocardial migration by fibroblast progenitor cells is blood pressure dependent in a model of angii myocardial fibrosis. *Hypertension research : official journal of the Japanese Society of Hypertension*. 2012;35:449-456

127. Bucala R, Spiegel LA, Chesney J, Hogan M, Cerami A. Circulating fibrocytes define a new leukocyte subpopulation that mediates tissue repair. *Molecular medicine*. 1994;1:71-81

128. Campbell JJ, Bowman EP, Murphy K, Youngman KR, Siani MA, Thompson DA, Wu L, Zlotnik A, Butcher EC. 6-c-kine (slc), a lymphocyte adhesion-triggering chemokine expressed by high endothelium, is an agonist for the mip-3beta receptor ccr7. *The Journal of cell biology*. 1998;141:1053-1059

129. Riol-Blanco L, Sanchez-Sanchez N, Torres A, Tejedor A, Narumiya S, Corbi AL, Sanchez-Mateos P, Rodriguez-Fernandez JL. The chemokine receptor ccr7 activates in dendritic cells two signaling modules that independently regulate chemotaxis and migratory speed. *J Immunol*. 2005;174:4070-4080

130. LeBleu VS, Taduri G, O'Connell J, Teng Y, Cooke VG, Woda C, Sugimoto H, Kalluri R. Origin and function of myofibroblasts in kidney fibrosis. *Nat Med*. 2013;19:1047-1053

131. Ma X, Robin C, Ottersbach K, Dzierzak E. The ly-6a (sca-1) gfp transgene is expressed in all adult mouse hematopoietic stem cells. *Stem cells*. 2002;20:514-521

132. Boisset JC, van Cappellen W, Andrieu-Soler C, Galjart N, Dzierzak E, Robin C. In vivo imaging of haematopoietic cells emerging from the mouse aortic endothelium. *Nature*. 2010;464:116-120

133. Schober A, Knarren S, Lietz M, Lin EA, Weber C. Crucial role of stromal cell-derived factor-1alpha in neointima formation after vascular injury in apolipoprotein e-deficient mice. *Circulation*. 2003;108:2491-2497

134. Torsney E, Xu Q. Resident vascular progenitor cells. *J Mol Cell Cardiol*. 2011;50:304-311

135. Psaltis PJ, Harbuzariu A, Delacroix S, Holroyd EW, Simari RD. Resident vascular progenitor cells--diverse origins, phenotype, and function. *Journal of cardiovascular translational research*. 2011;4:161-176

136. Hidestrand M, Richards-Malcolm S, Gurley CM, Nolen G, Grimes B, Waterstrat A, Zant GV, Peterson CA. Sca-1-expressing nonmyogenic cells contribute to fibrosis in aged skeletal muscle. *The journals of gerontology. Series A, Biological sciences and medical sciences*. 2008;63:566-579

137. Zeisberg EM, Tarnavski O, Zeisberg M, Dorfman AL, McMullen JR, Gustafsson E, Chandraker A, Yuan X, Pu WT, Roberts AB, Neilson EG, Sayegh MH, Izumo S, Kalluri R. Endothelial-to-mesenchymal transition contributes to cardiac fibrosis. *Nat Med*. 2007;13:952-961

138. Zeisberg EM, Potenta SE, Sugimoto H, Zeisberg M, Kalluri R. Fibroblasts in kidney fibrosis emerge via endothelial-to-mesenchymal transition. *J Am Soc Nephrol*. 2008;19:2282-2287

139. Kitao A, Sato Y, Sawada-Kitamura S, Harada K, Sasaki M, Morikawa H, Shiomi S, Honda M, Matsui O, Nakanuma Y. Endothelial to mesenchymal transition via transforming growth factor-beta1/smad activation is associated with portal venous stenosis in idiopathic portal hypertension. *Am J Pathol*. 2009;175:616-626

140. Nataraj D, Ernst A, Kalluri R. Idiopathic pulmonary fibrosis is associated with endothelial to mesenchymal transition. *American journal of respiratory cell and molecular biology*. 2010;43:129-130

141. Chen PY, Qin L, Barnes C, Charisse K, Yi T, Zhang X, Ali R, Medina PP, Yu J, Slack FJ, Anderson DG, Kotelianski V, Wang F, Tellides G, Simons M. Fgf regulates tgf-beta signaling and endothelial-to-mesenchymal transition via control of let-7 mirna expression. *Cell reports*. 2012;2:1684-1696

142. Liu Y. Cellular and molecular mechanisms of renal fibrosis. *Nature reviews. Nephrology*. 2011;7:684-696

143. Prokopowicz ZM, Arce F, Biedron R, Chiang CL, Ciszek M, Katz DR, Nowakowska M, Zapotoczny S, Marcinkiewicz J, Chain BM. Hypochlorous acid: A natural adjuvant that facilitates antigen processing, cross-priming, and the induction of adaptive immunity. *J Immunol*. 2010;184:824-835

144. Xia Y, Entman ML, Wang Y. Critical role of cxcl16 in hypertensive kidney injury and fibrosis. *Hypertension*. 2013;62:1129-1137

145. Wang Y, Ait-Oufella H, Herbin O, Bonnin P, Ramkhelawon B, Taleb S, Huang J, Offenstadt G, Combadiere C, Renia L, Johnson JL, Tharaux PL, Tedgui A, Mallat Z. Tgf-beta activity protects against inflammatory aortic aneurysm progression and complications in angiotensin ii-infused mice. *J Clin Invest*. 2010;120:422-432

146. Romain M, Taleb S, Dalloz M, Ponnuswamy P, Esposito B, Perez N, Wang Y, Yoshimura A, Tedgui A, Mallat Z. Overexpression of socs3 in t lymphocytes leads to impaired interleukin-17 production and severe aortic aneurysm formation in mice--brief report. *Arterioscler Thromb Vasc Biol*. 2013;33:581-584

147. Shin S, Cho YP, Jun H, Park H, Hong HN, Kwon TW. Transglutaminase type 2 in human abdominal aortic aneurysm is a potential factor in the stabilization of extracellular matrix. *Journal of vascular surgery*. 2013;57:1362-1370